



**CHALMERS**  
UNIVERSITY OF TECHNOLOGY



# A study of electrical efficiency improvements in Waste CHP plants

Master's thesis in Sustainable Energy Systems

MAX TAPIA MOLANDER

DEPARTMENT OF SPACE, EARTH AND ENVIRONMENT

---

CHALMERS UNIVERSITY OF TECHNOLOGY  
Gothenburg, Sweden 2023  
[www.chalmers.se](http://www.chalmers.se)



MASTER'S THESIS 2023

**A study of electrical efficiency  
improvements in Waste CHP plants**

MAX TAPIA MOLANDER



**CHALMERS**  
UNIVERSITY OF TECHNOLOGY

Department of Space, Earth and Environment  
*Division of Energy Technology*  
High Temperature Processes group  
CHALMERS UNIVERSITY OF TECHNOLOGY  
Gothenburg, Sweden 2023

A study of electrical efficiency improvements in Waste CHP plants  
MAX TAPIA MOLANDER

© MAX TAPIA MOLANDER, 2023.

Supervisor: Dr. Thomas Allgurén, Allguren Energy Engineering Consulting  
Examiner: Dr. Klas Andersson, Division of Energy Technology

Master's Thesis 2023  
Department of Space, Earth and Environment  
Division of Energy Technology  
High temperature research group  
Chalmers University of Technology  
SE-412 96 Gothenburg  
Telephone +46 31 772 1000

Typeset in L<sup>A</sup>T<sub>E</sub>X  
Printed by Chalmers Reproservice  
Gothenburg, Sweden 2023

A study of electrical efficiency improvements in Waste CHP plants  
MAX TAPIA MOLANDER  
Department of Space, Earth and Environment  
Chalmers University of Technology

## Abstract

By 2045, Sweden aims to achieve climate neutrality and to achieve such a goal work in each sector is of importance. One way to achieve such a goal is through the strategy of waste and biomass incineration to phase out fossile fuels, and in particular through combined heat and power, CHP, systems where the fuel can be used as efficiently as possible. For this thesis, the work is aimed towards that of waste fired CHP plants, and the ways of increasing the electrical efficiency, such that the generation of electricity to the grid is increased without increasing carbon emissions.

Due to the nature of municipal solid waste, MSW, being combusted in such plants, being high in chlorine and alkali metals such as Na and K, the steam data is typically lowered to reduce problems with deposition and high temperature corrosion, HTC. This work examines the potential of increasing the electrical efficiency in existing plants through experimental work at a reference plant, and through alterations or future plant designs using modelling.

In the modelling work, two primary models representing the reference plant were constructed for the two seasonal extremes: winter and summer, during which the operation of the plant differs the most from one another. Through these primary models, the effects of increased temperature and pressure could be examined. From there, larger changes were modelled such as the addition of a reheat cycle, the effects of changing the MSW to biomass, and in a final case also the impact of co-firing, both indirectly and in parallel. These models showed that there exists great potential to increase the electrical efficiency in a variety of ways. For the cases where biomass was used in modelling, a method was developed to roughly estimate which steam temperature would be applicable for each fuel through comparison of the fuel and ash composition and simulations of ash melt fractions.

Through examining the alkali content and if there exists margins in the S/Cl ratio, one could determine if the steam data is set to cautiously and thus the possibility for increasing said values. Such margins were looked at both on a day-to-day basis through on site data collection, and through long term evaluation of data from the reference plant *Lillesjöverket*. For the existing plant, it was determined that both on a day-to-day basis and in the long term, there were no peaks large enough to support such an increase at present conditions without better precision in alkali measurements.

Keywords: Process modelling, Simulations, Ebsilon, Ash, HTC, Sulphation, Electrical efficiency



A study of electrical efficiency improvements in Waste CHP plants  
MAX TAPIA MOLANDER  
Department of Space, Earth and Environment  
Chalmers University of Technology

## Sammanfattning

År 2045 siktar Sverige på klimatneutralitet, ett mål vars syfte kräver förbättring i alla sektorer. Ett sätt som Sverige arbetar med detta mål är dess användning av avfall och biomassa för att fasa ut förbänningen av fosila bränslen, speciellt inom kraftvärmesektorn där bränslet kan användas så effektivt som möjligt. Huvudsyftet med detta arbete är riktat mot avfallseldade kraftvärmeverk och hur elverkningsgraden i dessa kan ökas, sådant att produktionen till elnätet kan öka utan ökade utsläpp.

På grund av sammansättningen av avfall som förbränns i dessa kraftvärmeverk, med höga halter av klor och alkali metaller som Na och K, behöver ångdatan ofta sänkas för att inte stöta på ökade problem med högttemperaturskorrosion, HTC, och depositioner. Detta i sin tur sänker elverkningsgraden i dessa verk, vilket blir huvudsyftet i detta arbete: att undersöka hur elverkningsgraden kan ökas. Detta undersöks genom experimentellt arbete på ett referensverk, samt modelleringsarbete där potentiella förändringar och nya designidéer tas up.

I modelleringsarbetet gjordes först två primära basmodeller som representerar referensanläggningen under de två säsongsextremerna: vinter och sommar, där produktionen på anläggningen skiljer sig mest från varandra. Från basmodellerna kunde sedan effekterna av ökad temperatur och tryck undersökas. Därefter kunde större förändringar undersökas såsom tillägget av en återuppvärmningscykel, utbyte av avfall mot biomassa, samt en kombination av de tidigare nämnda genom antingen indirekt eller parallel sameldning. Dessa modellerna visade att det fanns stor potential att öka elverkningsgraden på flera olika sätt med varierande komplexitet. I fallen där biomassa användes för modelleringen utvecklades en rudimentär metod för att uppskatta vilken ångdata som skulle vara möjlig för vardera bränsle genom att undersöka bränslet och dess askas sammansättning samt simulering av asksmältorna.

Genom att undersöka omfånget av alkali i systemet, samt ifall det finns några nämnbara marginaler i förhållandet av S/Cl, kan det avgöras om ångdatan har sänkts med onödig försiktighet och därmed om det skulle finnas möjlighet att öka temperaturen. Dessa marginaler undersöktes både på tidsskalan av dag-till-dag genom provtagning och längre skalor genom analys av långtidsdata från referensverket *Lillesjö*. Från dessa analyser framkom att det verket i nuvarande form inte bör öka temperaturen baserat på förhållandet av S/Cl utan bättre precision i alkali mätningarna.

Nyckelord: Processmodellering, Simuleringar, Epsilon, Aska, Högtemperaturskorrosion, Sulfatering, Elverkningsgrad



## Acknowledgements

For this work I would like to express my thanks to my supervisor Thomas, who even though being on a parental leave for a large portion of the project and working at both Chalmers and as a consultant for Lillesjö had time to supervise and guide me through this project. Thanks also to Klas, who will be grading this thesis, for taking a part in the project in ways that far exceeds what could be expected of an examiner.

Great thanks to the workers at Lillesjö for allowing us to conduct our measurements on site and for providing access to data that helped make the arguments put forth in this thesis. Thanks especially to Pawel for helping navigate the data collection system and arranging access, and to Göran and Jack for the valuable input on the work.

Thanks also to Jakob and Ivan for taking the time to join us during the measurement campaign at Lillesjö, without your help with setting up for the measurements and for your help in performing the gas composition and SID measurements. Klas, Thomas and I would have been stuck there far longer.

A big thanks also goes out to the entire research group for the support on the project over the year, for giving me insight into the academic world, and allowing me to listen in and learn from everyone's work.

I would also like to express my gratitude towards my partner for the many evenings she has had to endure discussions of this thesis and for the support she has shown during the writing process. Without her external perspective, input and aid in creating figures this thesis would not have been visually appealing.

Max Tapia Molander, Gothenburg, 2023



# List of Acronyms

Below is the list of acronyms that have been used throughout this thesis listed in alphabetical order:

BECCS	Bio Energy Carbon Capture and Storage
CCS	Carbon Capture and Storage
CHP	Combined Heat and Power
DLPI	Dekati Low Pressure Impactor
ESP	Electrostatic Precipitator
FFT	Fast Fourier Transform
FGC	Flue Gas Condenser
FTIR	Fourier-transform infrared
HHV	Higher Heating Value
HOP	Heat only Plant
HTC	High Temperature Corrosion
IACM	In-situ Alkali-Chloride Measurement
LHV	Lower Heating Value
LP	Low Pressure
MP	Medium Pressure
MSS	Municipal Sewage Sludge
MSW	Municipal Solid Waste
NCV	Net Calorific Value
SCR	Selective Catalytic Reduction
SID	Surface Ionization Detector
TOC	Total Organic Carbon
WtE	Waste to Energy



# Contents

<b>List of Acronyms</b>	<b>vii</b>
<b>List of Figures</b>	<b>xi</b>
<b>List of Tables</b>	<b>xv</b>
<b>1 Introduction</b>	<b>1</b>
<b>2 Theory</b>	<b>5</b>
2.1 Combustion . . . . .	5
2.2 Fuel types . . . . .	7
2.3 HTC and depositions . . . . .	9
2.4 Waste Fired CHP . . . . .	10
2.5 Sulphur Recirculation . . . . .	11
2.6 Co-combustion technologies . . . . .	12
2.7 Surface Ionization Detection - SID . . . . .	13
2.8 Fourier-transform infrared spectroscopy - FTIR . . . . .	13
<b>3 A reference plant - Lillesjö</b>	<b>15</b>
3.1 Boiler . . . . .	15
3.2 Fluegas cleaning . . . . .	17
<b>4 Methods</b>	<b>21</b>
4.1 Introductory Epsilon Modelling . . . . .	21
4.1.1 Base operation cases . . . . .	22
4.1.2 Temperature-Pressure study . . . . .	25
4.1.3 Case 1 - Addition of Reheat . . . . .	25
4.1.4 Case 2 - Impact of fuel variation . . . . .	26
4.1.5 Case 3 - Co-combustion with Biomass . . . . .	27
4.2 Experimental setup - Lillesjöverket . . . . .	29
4.2.1 Deposition Rate . . . . .	32
4.2.2 Temperature . . . . .	33
4.2.3 Gas composition . . . . .	33
4.2.4 Aerosols . . . . .	35
4.2.5 Alkali . . . . .	36
4.3 Fuel classification . . . . .	37
4.3.1 Steam temperature estimation . . . . .	37

4.3.2	FactSage . . . . .	38
<b>5</b>	<b>Results and Discussion</b>	<b>41</b>
5.1	Data collection - Lillesjöverket . . . . .	41
5.1.1	Deposition Rate . . . . .	41
5.1.2	Temperature . . . . .	43
5.1.3	Gas Composition . . . . .	44
5.1.3.1	Comparison to process data . . . . .	47
5.1.4	Aerosols . . . . .	49
5.1.5	Alkali . . . . .	52
5.1.6	Comparison to other MSW plants . . . . .	54
5.2	Introductory Modelling cases . . . . .	55
5.2.1	Base operation cases . . . . .	55
5.2.2	Temperature-Pressure study . . . . .	56
5.2.3	Case 1 - Addition of Reheat . . . . .	58
5.2.4	Case 2 - Impact of fuel variation . . . . .	59
5.2.5	Case 3 - Co-combustion with Biomass . . . . .	61
5.2.5.1	Indirect co-firing . . . . .	61
5.2.5.2	Parallel co-firing . . . . .	62
5.3	Fuel classification . . . . .	65
5.3.1	Steam temperature estimation . . . . .	65
5.3.2	FactSage . . . . .	66
5.4	Summary . . . . .	67
<b>6</b>	<b>Conclusion</b>	<b>69</b>
6.1	Future Work . . . . .	70
	<b>Bibliography</b>	<b>71</b>
<b>A</b>	<b>Epsilon</b>	<b>I</b>
A.1	Component list . . . . .	I
A.2	Models . . . . .	XI
<b>B</b>	<b>Additional Data</b>	<b>XV</b>
B.1	Experimental Campaign . . . . .	XV
B.2	FactSage & Temperature Estimations . . . . .	XVIII

# List of Figures

2.1	Schematic illustration of the deposition locations in relation to the fluegas flow. A) Initial (inside) deposition, B) outer deposition, C) side depositions, D) backside (eddy) depositions. . . . .	9
2.2	Representation of a Waste CHP plant. Various colors signify: Red - superheated steam; Blue - condensate; Yellow & Orange - saturated steam. . . . .	11
2.3	Three most common technologies for co-firing as described by [41] . .	12
3.1	Representation of the Lillesjö moving grate boiler . . . . .	16
3.2	Representation of how an ESP works, inducing an electric charge on the particles passing through and pulling them from the gas . . . . .	18
4.1	Ebsilon Professional model of the summer operation case. . . . .	22
4.2	Ebsilon Professional model of the winter operation case. . . . .	22
4.3	Ebsilon Professional model of the winter operation case, accessible version . . . . .	24
4.4	Schematic representation of the Lillesjö boiler with all available points for measurements marked. Yellow - used points, Orange - ports interesting for future measurements, Blue - semi accessible ports . . . .	30
4.5	Schematic representation of the Lillesjö boiler with only the used points marked out in yellow and their respective names. 7.5(S) represents the port 7.5 available on the opposite side of the boiler. . . . .	31
4.6	Schematic of ring dimensions, showing the inner and outer diameters, $\phi_i$ and $\phi_o$ respectively, as well as the depth, $h$ , of the ring. . . . .	32
4.7	Schematic representation of the setup used to sample gases and determine composition. . . . .	34
4.8	Schematic representation of a DLPI used to sample and determine a fluegas particle size distribution . . . . .	35
5.1	Graphical representation of the deposition rates, $R_D$ measured. . . . .	42
5.2	Temperatures measurements from floor 5 through floor 8. . . . .	43
5.3	Changes in average gas concentration between ports, normalized for measurements conducted in ports A1. . . . .	45
5.4	Relation between $SO_2/HCl$ in ports B1, B2. Each figure shows the mean ratio for each respective measurement denoted with $A$ and the boiler load during the duration of the measurement, $L$ , as well as the overall mean ratio for all measurements in each respective port. . . .	47

5.5	Relation between SO <sub>2</sub> /HCl in ports B3 and BESP. Each figure shows the mean ratio for each respective measurement denoted with <i>A</i> and the boiler load during the duration of the measurement, <i>L</i> , as well as the overall mean ratio for all measurements in each respective port. . . . .	47
5.6	Ratio of SO <sub>2</sub> to HCl from continuous measurements 2019-2022 . . . . .	48
5.7	Compilation of experimental measurements compared with reference measurements from the same time period in vol % and mg/Nm <sup>3</sup> . . . . .	49
5.8	Trend of particle distribution from first DLPI measurement at port B1 on floor 8. . . . .	50
5.9	Trend of particle distribution from second DLPI measurement at port B1S on floor 8. . . . .	50
5.10	DLPI component showing excess material spilled over from measurements . . . . .	51
5.11	DLPI aluminum foil pieces from stages 1, 4, 7 and 10. . . . .	51
5.12	Compilation of SID measurement signal for KCl <sub>eq</sub> from floors 5-8 . . . . .	53
5.13	Plot of electrical efficiencies when altering temperature and pressure in the winter model from 350C and 30bar to 550C and 180bar. . . . .	57
5.14	Effects on the winter model production with varying fuels . . . . .	60
5.15	Effects on the winter model efficiencies with varying fuels . . . . .	60
5.16	Effects on the winter model production with varying fuels . . . . .	61
5.17	Effects on the winter model efficiencies with varying fuels . . . . .	62
5.18	Effects on the production with varying fuels using parallel co-firing alternative 1 . . . . .	63
5.19	Effects on the efficiencies with varying fuels using parallel co-firing alternative 1 . . . . .	63
5.20	Effects on the production with varying fuels using parallel co-firing alternative 2 . . . . .	64
5.21	Effects on the efficiencies with varying fuels using parallel co-firing alternative 2 . . . . .	64
5.22	Estimated temperatures of respective fuels when combusted separately or, if indicated, combusted as an in-going mixture . . . . .	65
5.23	FactSage simulations of ash melt tendencies of MSW and Coal as references, to estimate the tendencies of wood logs, pellets and cardboard. . . . .	66
A.1	Component 1 - Boundary Input Value: Boundary input where the composition and state of the stream can be specified. . . . .	I
A.2	Component 2 - Throttle: Used to model pressure drops in the system, can be specified externally or calculated by the model. . . . .	I
A.3	Component 4 - Splitter: Allows streams to be split into two separate streams. . . . .	II
A.4	Component 5 - Steam Generator: Component which simulates the economizing, evaporation and economizing of steam in one unit. May also include reheating. . . . .	II

A.5	Component 6 - Steam Turbine: Component used to expand streams of pressurised steam, has the option for two extractions in ports 3 and 4, for feed water heating. . . . .	II
A.6	Component 8 - Pump: Component used to simulate pump work in the system increasing or maintaining the pressure. . . . .	III
A.7	Component 9 - Deareator / Feedwater Heater: Open heat exchanger used for preheating the feedwater. . . . .	III
A.8	Component 10 - Feedwater Heater: Closed heat exchanger used for preheating the feedwater. . . . .	III
A.9	Component 11 - Generator: Component attached to Steam turbine simulating the electricity generation from work extracted by expanding steam. . . . .	IV
A.10	Component 12 - Controller (External): Allows to set control point between to streams based on an external input value . . . . .	IV
A.11	Component 21 - Combustion Chamber: Unit that simulates the combustion of one fuel input in port 4, with the option for a secondary fuel input in port 6. Uses air from port 1, and produces hot fluegases in port 2 for steam generation. . . . .	IV
A.12	Component 24 - Compressor: Used to simulate the pressurization of primary air inlets. . . . .	V
A.13	Component 25 - Air Preheater: Used to preheat the air intake to the combustion chamber, preheated using either fluegases or steam in ports 3 and 4. . . . .	V
A.14	Component 26 - Economizer/Evaporator/Superheater: Heat exchanger unit specialized for fluegas/water and fluegas/steam heat transfer. . .	V
A.15	Component 29 - Electric Motor: Provides pump and compressor components with the energy needed, also outputs the electricity demand of these components used for determining efficiencies. . . . .	VI
A.16	Component 31 - Power Summarizer: component used to summarize logic components indicating pumpwork, electricity demand and generation, as well as heat provided to DH network. . . . .	VI
A.17	Component 32 - Efficiency meter: Component that determines efficiency based on two given inputs, such as heat provided through fuel and electricity generated. . . . .	VI
A.18	Component 33 - Start Value: similar to component 1, but may be placed anywhere in the system where certain parameters would otherwise be unspecified. Can also set composition of stream. . . . .	VII
A.19	Component 35 - Heat Consumer: Used to simulate outgoing heat flows, such as heat provided to the district heating network, cooling or heat towards the pelletization plant. . . . .	VII
A.20	Component 37 - Simple Mixer: Component used to recombine two separate streams into one. . . . .	VII
A.21	Component 38 - Water Injection: Component used to simulate water being added to the system, used in the fluegas cleaning step where the fluegases are clean by direct contact with water. . . . .	VIII

A.22	Component 39 - Controller (Internal): Allows to set a control between two streams and an internal input value, such as controlling the temperature of one stream by limiting the mass flow of the other.	VIII
A.23	Component 54 - Drain: Component opposite of the water injection, used to drain condensate from fluegas streams post fluegas condensation.	VIII
A.24	Component 70 - Evaporator with Steam Drum: Component specialized for evaporation of steam and typically works in tandem with component 26.	IX
A.25	Component 85 - Electrostatic Precipitator: Cleaning unit that removes fly ash and particulate matter.	IX
A.26	Component 86 - Selective catalytic reduction unit: Unit whose primary assignment is to remove NOx from the fluegases.	IX
A.27	Component 99 - Separator: Used to simulate other fluegas cleaning components. In this case the removal of SOx and HF, HCl.	X
A.28	Component 169 - Gasifier: Component that simulates the gasification of the biomass fuels introduced in the indirect co-firing cases after gasification.	X
A.29	Ebsilon Professional model of the summer model with the accessible redesign.	XI
A.30	Ebsilon Professional model of the winter operating case with the addition of a reheat cycle and extra turbine.	XII
A.31	Ebsilon Professional model of an indirect co-firing plant	XIII
A.32	Ebsilon Professional model of the 1st version of parallel co-firing.	XIV
A.33	Ebsilon Professional model of the 2nd version of parallel co-firing.	XIV
B.1	Boiler load during the experimental campaign in terms of steam produced. Top figure showing the entire duration, and the bottom figure showing the load during individual gas measurement occasions.	XV
B.2	Differences in temperatures estimated per fuel depending on method of weighting. Alternative weighting using a softer 0.25 weight on several components instead of 0.5 that is used in the current method.	XVIII

# List of Tables

2.1	Overview of some natural and artificial fuels. (*) Although not created specifically for the use as a fuel it would for the purpose of this thesis be classified as artificial. . . . .	7
2.2	UBET classification of biofuel sources by different characteristics [26]. * The term "By-products" includes the improperly called solid, liquid and gaseous residues and wastes derived from biomass processing activities. . . . .	8
4.1	Fuel compositions and net calorific value (NCV) used for the Winter and Summer operational cases . . . . .	23
4.2	Primary steam, extraction and district heating data for Summer and Winter operational cases . . . . .	24
4.3	Primary steam, extraction and district heating data for Winter operation of Case 0 with lowered and increased steam data . . . . .	25
4.4	Primary steam, extraction and district heating data for Winter operation of Case 1 . . . . .	25
4.5	Fuels examined for co-firing with MSW separated into four categories: Untreated, Treated, Refined and Miscellaneous . . . . .	26
4.6	Primary steam data for an array of various fuels estimated in section 4.3 as well as MSW as a reference. . . . .	27
4.7	Primary steam, extraction and district heating data for Winter operation of Case 3 models. (†) 2.25 times the pressures presented in Table 4.6. (‡) same temperatures presented in Table 4.6 . . . . .	28
4.8	Summary of measurements conducted in each port, with roman numerals indicating the amount of measurements per position . . . . .	29
4.9	Initial weight and dimensions of deposition rings prior to usage, as well as the type of material used. . . . .	32
4.10	DLPI stage median particle diameter collection size . . . . .	36
4.11	Schematic illustrating the method for first estimation of steam temperatures for fuels by comparing compositions. Temperatures rounded to the closest 5°C. . . . .	38
5.1	Deposition rate measurements, in time inserted (t), added weight of depositions ( $m_d$ ), the deposition area ( $A_d$ ) and the amount of deposition per area . . . . .	41

5.2	Averaged volumetric concentrations of each respective species for each measurement ordered in the sequence they were performed. (.w) measured on a wet basis, (.d) measured on a dry basis. (‡) due to larger diameter of measuring port air diluted the sample, recalculated values available in Table B.2. (*) due to pressure fluctuations close to the boundary layer of where combustion ends, short bursts with increased levels of unburnt airborne material drive up the averages. . . . .	44
5.3	Summary of percentage difference between experimentally measured (CTH) values and reference values (UKAB) in gas composition . . . .	49
5.4	Results from SID measurements in ppm and $mg/Nm^3$ , averages for ports A1-A3 and B1-BESP also included. . . . .	52
5.5	Overview and comparison of Waste incineration plants from BAT [62] outlying typical parameters common for MSW plants with an 11% O <sub>2</sub> reference value and that of <i>Lillesjö</i> recalculated to the same oxygen content. . . . .	54
5.6	Fluegas composition post cleaning for Winter and Summer operational cases based on Epsilon models . . . . .	55
5.7	Results and comparison of base operation modelling (m) in operation parameters and efficiencies with reference values (r) for winter and summer. . . . .	56
5.8	Results of increasing temperature or pressure on efficiencies . . . . .	57
5.9	Influence on operation parameters with changes in T and P. . . . .	58
5.10	Influence on operation parameters with the addition of a reheat cycle. . . . .	58
5.11	Results from the addition of a reheat cycle on efficiencies. . . . .	59
B.1	Weighing protocol for the deposition rings, in milligrams (mg). . . . .	XVI
B.2	Recalculated concentrations of each respective species for measurements conducted before the ESP to compensated for increased air dilution. . . . .	XVI
B.3	DLPI particle measurement: Sample 1 - port 7.5. Weighed three times, measurements in milligrams (mg). . . . .	XVI
B.4	DLPI particle measurement: Sample 2 - port 7.5S. Weighed three times, measurements in milligrams (mg). . . . .	XVII

# 1

## Introduction

### Background

As the climate becomes an altogether more pressing matter, industries and the average citizen alike become more aware of the problems of pollution and emissions [2]. Industries are working more and more to include green ideas and solutions, whilst the average citizen becomes better and better at sorting their trash, minimizing their emissions and reducing unnecessary or wasteful energy usages [3]. There are still a ways to go but as we are moving towards a more sustainable society, many processes and industries have to change their ordinary ways of operating. One such example, that will be the key focus point of this thesis, is the operation of combined heat and power, CHP, plants. CHP plants compared to heat only plants, HOP, or regular power plants, have the benefit of being able to generate both electricity and heat, and may shift the production depending on given demand [4]. Moreover, if connected to a fluegas condenser, the plants may reach efficiencies above 100% by drawing out as much energy from the fuel as possible with minimal losses [5]. The plants may operate with a wide array of fuels depending on construction but for this thesis, waste fired CHP plants will be in focus with *Lillesjöverket* as a reference plant.

Waste fired plants are constantly changing in their operation as they run on a fuel that is constantly changing . As household and industrial sorting becomes better, and better the fuel used by waste incineration plants change over time. More and more high moisture content fractions such as compostable materials are being sorted out, meaning that waste plant operators have to adapt their operation over time to a changing fuel [3, 6].

Moreover, this thesis will focus on the electricity production of these plants in Sweden. Due to the temperate climate in Sweden with cold winters, and low political incentives, many CHP plants have had a focus mainly on the heat production and seen the electricity as somewhat of a byproduct [7]. However, with changing climates, increasing strain on the electric grid and soaring electricity prices, there is an opportunity for CHP plants formerly focused on mainly producing heat to readjust and view their electricity production as an increasingly lucrative business. Thus, this thesis will look into opportunities of increasing said electricity production by exploring different alternatives to raise the electrical efficiency. Furthermore, the work conducted in this thesis is part of a project financed by the Swedish *Bio+* project that focuses on developing bio-based solutions as a way of contributing to

Swedens' energy and climate goals with the aim of becoming fossil free [8]. With that in mind, the thesis will focus on the potential of co-firing municipal solid waste, MSW, with various types of biomass. This will include the potential effects of implementing biomass and the benefits that may come with it.

Biomass in general is becoming a more and more sought after fuel for many industries due to its renewable nature. With increased interest in a specific fuel, more and more focus will be laid on developing more efficient versions of said fuel, and that is not an understatement with Biomass. Biomass may be found and used in a multitude of ways and forms from unprocessed rice husk to somewhat processed wooden shavings, or with more effort turned into a energy dense fuel after torrefaction or pelletization [9]. All of these come with their own benefits and potential drawbacks which makes biomass as a class of fuels very versatile. Unfortunately, as they become more sought after and they are being widely used in more industries the competition for the fuel rises, so it becomes a balancing job of implementing them at a rate such that it remains viable, both for economically and sustainably [10].

The reference plant *Lillesjöverket* is located in Uddevalla and operates on a mixture of municipal and industrial waste, but has at times had test runs with other types of fuel and their company Uddevalla Energi AB has an underlying interest in sourcing new materials for future use making them a perfect match for the project. Today the plant is operated continuously with high uptimes producing steam of 400°C and 40 bars of pressure and designed to produce about 10MW of electricity and 36MW of heat. The plant utilizes a fluegas condenser which allows them, when needed, to draw out and utilize energy that would otherwise be lost and when the fluegases are released in the chimney. This way the plant can operate with efficiencies above 100% during colder periods. The plant is also connected to pellet plant and cooling unit that operate mainly during the summer months when district heating, DH, is not in as high of a demand as it is during cold winter months. Most of that excess energy goes into the production of pellets but at times when too much heat is produced the leftovers need to be cooled of using the cooling unit [11].

The usage of MSW as a fuel is widely used in waste to energy, WtE, and CHP plants in Europe and are emerging more and more in industrializing countries as an alternative to landfills. In the EU alone the incineration of waste has grown from 30 to 62 million tonnes anually from 1995 to 2021, whilst landfilling has seen a decrease from 121 to 54 [12]. Sweden has long had a policy where plants who would take on waste for incineration are payed for the amount they take in and can take care of which is why Sweden today turns approximately 60% of its produced MSW into usable energy in the form of heat or electricity and sort, recycle and compost 38% [13]. This leaves approximately 2% to the Swedish landfills compared to the European average of 25%. This way Sweden can produce energy in a way that limits potential damage and pollution to the soil and groundwater due to landfill and provides a terminus for fossile components [14]. It does however bring its own challenges to the table. Since waste is so diverse, each scoop of waste that is added to the boiler

will have vastly different compositions which requires the boiler to have a durable interior to withstand the combustion environment. Furthermore due to the many metals, particles, and atmospherically harmful gases produced during the incineration process waste operated plants usually require more complex and developed flue gas cleaning systems compared to their fossil-based relatives [15]. *Lillesjöverket* is no exception, as it equipped with an effective array of cleaning units, reducing their  $\text{NO}_x$ ,  $\text{SO}_x$ , total organic carbon, TOC, particle, and heavy metal emissions well below the Swedish restrictions thanks to their relatively young and modern fluegas cleaning train.

## Aim and Scope

This thesis aims to provide alternatives that provide increased emphasis on the electrical efficiency of waste fired CHP plants - using *Lillesjö* as reference - both for existing plants and for future plant design ideas. This aim is to be achieved through modelling of potential cases using the process modelling software *Epsilon Professional* in combination with experimental work conducted at the reference plant, combustion simulations using *FactSage* and ash analyses.

Through experimental measurements conducted on site, there will be the opportunity of testing equipment on a modern waste CHP plant to map the internal conditions. With the experimental measurements in combination with long term data logging there is an aim that certain margins in the sulphur/chlorine ratios in the boiler environment can be identified. These will reveal if the process is currently run too modestly with larger safety margins than needed and thus that higher pressures or temperatures could be utilized to boost the electrical efficiency.

For the modelling of potential future improvements or additions, ideas such as the addition of a reheat cycle and a turbine for top production of electricity in times of need could then be examined. Some more extensive alternatives directed towards the potential benefits of implementing co-firing technologies, either as a way to circumvent or ease the HTC issues connected to using waste as a fuel, were explored.

The thesis will however not look into the economical aspects of these alternatives but focus mainly on the engineering, process and energy side of the study to find areas of potential improvements. This opens up for further economical feasibility studies later on if the results are worthwhile to investigate further and potentially determine whether the potential improvements are economically viable.



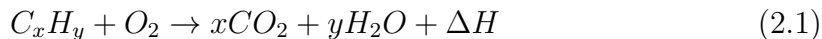
# 2

## Theory

This chapter will cover the basic theory that will aid the reader understand the main content of the following chapters.

### 2.1 Combustion

Combustion is a concept most of us are in contact with on a daily basis, be it the internal combustion engines of a car for transport, using a gas stove for cooking, or heating up a villa burning wood at a fireplace. The type of combustion handled in this thesis is closely related to the heating of a villa, with the exception of scale and the many quirks and needs of up-scaling such a process. Combustion in chemical terms is an exothermic redox chemical reaction of a fuel (reductant) and an oxidant and can be described in its simplest form using a reaction like below [16]:



In reality it is uncommon to perform large scale combustion of purely hydrocarbons with a pure stream of an oxidant. Instead the fuel is often comprised of a large variety of chemical compounds, moisture and uncombustible material that impact the combustion process [17]. The same goes for the oxidant that is used in the combustion. Most processes use regular air, which contains but 21% O<sub>2</sub>, meaning that a much higher mass flow of air is needed than that of a pure stream of the oxidant, O<sub>2</sub>.

During the combustion process of solid fuels the reductant typically goes through three steps: drying, devolatilization and finally combustion of the volatiles and the remaining char [18]. These three steps have their own requirements for residence time, temperature, as well as availability of oxygen and space. In certain cases the drying and devolatilization steps can be considered simultaneous depending on the combustion conditions and particle sizes [17]. In the drying step the fuels' moisture content is expelled and depending on the initial fraction of moisture this is a step where a lot of potentially useful energy is lost to evaporation, reducing the heating value of the fuel [23]. In the devolatilization step the fuel begins to decompose allowing volatile compounds present in the fuel to be released [17]. Once the fuel has been dried and devolatilized, a husk mostly comprised of ash and the remaining solid carbon, char, remains. The char and the devolatilized gases can then be ignited and burned to complete the combustion. During these steps the fuels' structure will gradually decompose and depending on the type it may continuously fragment and break down into finer pieces where uncombustible material will remain but fly ash

will lifted by the air and leaving volatiles [18].

In this thesis the two main types of fuels that are discussed and handled are: biomass as well as a mixture of municipal and industrial waste; an assortment of other fuels will also be touched upon in later sections. Both of these fuels contain large fractions of moisture and incombustible material (ash) as well as C, H, O, N, S and Cl. All these components influence the combustion environment, but some have their own sets of problems, such as chlorine typically being corrosive and high concentrations leading to the need for more frequent revisions or resistant materials. Ratios, and amounts, of key components such as Cl, S and alkali metals, such as Na and K, are heavily linked to the high temperature corrosion, HTC, and deposition problems and are thus of special interest. Other constituents such as Si and Al which may also influence the depositions. More on this and the effects they have will be discussed in section 2.3.

These key inorganic components may be released to the fluegases in different ways depending on if they are in an oxidizing or reducing environment, in other words in an environment rich or poor in available oxygen. The release of K is closely related to the concentrations of Cl, Si, S and may either, in the presence of Cl, evaporate at temperatures  $>700^{\circ}\text{C}$  as KCl or if reacted to the char structure be oxidized into K carbonates that through further decomposition form KOH. If the available sulphur content is high the K-char structure may instead be sulfated to produce  $\text{K}_2\text{SO}_4$ . If the available silica content is high certain reactions may be inhibited and the K-sulfates or K-carbonates may instead form silicates [19]. The release of Cl from both organic and inorganic fractions form chlorinated hydrocarbons, HCl or in environments high in alkali metals as metal chlorides such as KCl or NaCl at sufficient temperatures [19, 20]. In a reducing environment S is released as species such COS,  $\text{CS}_2$  and  $\text{H}_2\text{S}$ , whereas in oxidizing environments they instead form  $\text{SO}_2$  or  $\text{SO}_3$  [22, 21].

It is also pertinent, besides internal boiler conditions, to adhere to the many external regulations when it comes to large scale combustion. In general there are many gases that have negative impacts on the environment and our health if released and thus have regulations to how much can be released [24]. In particular  $\text{SO}_x$ ,  $\text{NO}_x$  and heavy metal emissions are widely studied for their impacts - and in recent days also  $\text{CO}_2$  - and techniques on how to manage their respective emissions are under constant development. Some of these techniques applied in *Lillesjöverket* are detailed in chapter 3.

## 2.2 Fuel types

As introduced in section 2.1, the previous section on combustion, the main fuels that will be discussed throughout this thesis is MSW and biomass. Alongside these some additional fuels will be touched upon for the purpose of co-firing, which will be introduced further in section 2.6. Since fuels can be quite diverse this section aims to provide some details on those who will be discussed in subsequent chapters.

A first distinction that can be made between fuels are that of natural or artificial fuels, also referred to as primary or secondary fuels. The natural fuels are those that can be found in nature and be used without refinement, such as wood or coal, whilst artificial fuels such as charcoal or petroleum derivatives first have to go through some refinement process [25]. Both natural and artificial fuels are available in both solid, liquid and gaseous forms which all have their own advantages and disadvantages. Some of these have been tabulated below in Table 2.1 and can be dissected further.

Natural Fuels	Artificial Fuels
<b>Solid Fuels</b>	
Wood, Straw, Coal, Peat, Oil Shale	Charcoal, Briquettes, Coke, Pellets, Waste*
<b>Liquid Fuels</b>	
Petroleum	Shale-oil, Alcohols, Coal tar, Petroleum derivatives
<b>Gaseous Fuels</b>	
Natural Gas	Hydrogen gas, Syn gas

**Table 2.1:** Overview of some natural and artificial fuels. (\*) Although not created specifically for the use as a fuel it would for the purpose of this thesis be classified as artificial.

Depending on the usage and distance from which they are harvested to the area they are intended to be used they all have their niches. Gaseous fuels typically contain much lower levels of contaminants and have high levels of the combustible component. Thanks to this gaseous fuels such as natural gas or hydrogen gas typically have high energy densities, but due to their gaseous form the fuels typically have to be liquefied under high pressures to be transported effectively, unless the source and industry are in close proximity where pipelines can be used. Liquid fuels derived from petroleum are generally the most space efficient and easy to transport and store fuels as they can be stored in vats, barrels or filled directly into large tanker ships. The raw product petroleum however contains a lot of contaminants which makes treatment and distillation processes necessary for their use. Solid fuels can typically be used in their natural form, but through refinement or processing into their artificial counterparts one would expect higher energy densities and less environmental impact[17].

In the group of solid fuels, biomass and waste are two sets of fuels which are especially interesting for this thesis and can be divided into several subgroups depending on

composition or degree of refinement or sorting. Coal will also be of particular interest as a reference for future chapters. Both biomass and waste can be grouped under the term 'Biofuels' and can be classified according to the unified bioenergy terminology, UBET, as in Table 2.2[26].

		<b>Woody Biomass</b>	<b>Herbaceous Biomass</b>	<b>Biomass from Fruits and Seeds</b>	<b>Others</b>
		<i>Woodfuels</i>	<i>Agrofuels</i>		
<b>Energy Crop</b>		forest trees plantation trees	grass whole cereal	grain	
<b>By-products*</b>	Direct	thinning logging	crop production byproducts: straw		animal residues horticulture residues landscaping residues
	Indirect	wood processing black liquor	fibre crop- -processing	shells husks food processing	
<b>End use materials</b>	Recovered	used wood	used fibre- -products	used products- -of fruits and- -seeds	<b>Municipal</b> kitchen waste sewage sludge

**Table 2.2:** UBET classification of biofuel sources by different characteristics [26].  
 \* The term "By-products" includes the improperly called solid, liquid and gaseous residues and wastes derived from biomass processing activities.

The MSW used by the reference plant *Lillesjö*, is a combination of industrial waste and 'kitchen waste', as it is referred to in UBET, and is comprised of plastics, paper products, textiles, metals, leftover foodstuff, and from the industrial waste products such as gypsum may also be present. Due to this the MSW varies a lot in composition from country to country depending on each countries sorting and recycling strategies. Typically MSW contains high amounts of chlorine, alkali metals and has high moisture content [27].

Bioenergy as seen in Table 2.2 could be divided up into four categories. Woody biomass is typically the most efficient group due to their lower moisture and nitrogen contents [27]. Herbaceous- and biomass from fruits and seeds typically contain much higher level of minerals and nutrients which in terms of combustion are seen as contaminants and may influence the combustion process negatively. Thus these products usually go through torrefaction, where tars and volatiles are removed, or densification, where moisture and ash contents are decreased, to create pellets or charcoal more suitable for large scale combustion [17].

The last category 'others' includes potential fuels such as animal residues, municipal sewage sludge, and MSW that has been touched upon previously. Animal residues much like biomass from fruits and seeds contain large amounts of contaminants that make them unsuitable for direct firing, but may be an alternative to introduce biogenic material in a fossile process through co-firing. This is especially true for municipal sewage sludge, MSS, which if dried contains very high amounts of S in comparison to MSW [27] that can be implemented as an additive through co-firing.

### 2.3 HTC and depositions

A problem prominent in all boilers is the issue of high temperature corrosion, HTC, and depositions on the tube walls and especially onto superheater tube packages. This problem is especially noticeable in waste and biomass boilers since these fuels contain higher fractions of alkali and halides that form corrosive salts compared to fuels such as coal [29]. In waste and biomass this problem is most commonly met as the K and Cl atoms in the fluegases condense as KCl onto the tube packages. To cope with such problems most waste and biomass boilers reduce their steam data to temperatures as low as 400°C in the case of waste, compared to their coal competitors who may operate at temperatures up to 600 °C [30, 31].

The way the depositions condense onto the surface of the tube packages can be described by a range of mechanisms such as inertial impaction, thermophoresis, condensation and eddy impaction. The initial- or inside depositions are mainly caused by thermophoresis and condensation to the cooler tube surfaces. Outer depositions are results from inertial impaction of larger particles onto the sticky initial layer. The backside depositions are caused by eddy impaction due to the turbulent wake left behind the tubes at high fluegas velocities. The sides are typically a mixture of the three depending on the angle of impaction [32].

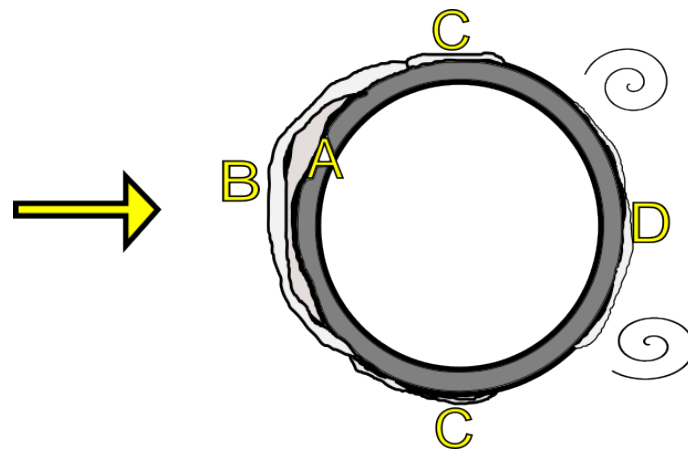


**Figure 2.1:** Schematic illustration of the deposition locations in relation to the fluegas flow. A) Initial (inside) deposition, B) outer deposition, C) side depositions, D) backside (eddy) depositions.

To combat depositions caused by chloride alkali compounds, such as NaCl and KCl, there has been many studies done investigating the effects of sulfation and the beneficial effects of fluegas recirculation, co-firing, or using additives to increase the level of S available in the fluegases [33, 35, 29, 31, 36, 37]. By increasing the S/Cl ratio the KCl available in the fluegases and on tube packages become increasingly susceptible to sulphation to  $K_2SO_4$ , a more benign form of the alkali, much less corrosive to the boiler material that also has a higher melting point, reducing the potential to condense onto the tubes [33]. Ratios of S/Cl less than 2 are susceptible to risks of corrosion, whilst systems operation with ratios above 4 have reduced

risks [36]. The sulphation of KCl occurs in one of two ways, through homogeneously where the reactions take place in the gas phase, or heterogeneous sulphation where the on the surfaces of non-gaseous particles [22]. Sulphation of this manner taking place as S comes in contact with KCl species on tubes may however have a corrosive effect as free chlorine form close to the surface [35].

## 2.4 Waste Fired CHP

In Swedish waste fired CHP plants heat is often considered the prime focus, with electricity as a byproduct, as the district heating system supplies a hefty part of the heating in Swedish households, especially so during the winter portion of the year. In 2013 district heating accounted for 55% of structural heating alone [5]. Much of this heat goes to heating commercial buildings such as offices and stores as well as multifamily residences such as apartments, whilst smaller houses such as villas often opt to use electricity for their heating [38]. With the costs of electricity rising and the availability of district heating improving these numbers are subject to change as more people may turn to district heating as the more economically viable alternative.

Waste fired CHP plants come in many shapes and forms but according to the study for best available techniques regarding waste incineration a waste CHP plant can be described according to the representation in Figure 2.2 [5]. The process starts at the import of fuel to the plant, where the incoming waste either has been treated prior to the arrival or there may exist a treatment facility on site where the fuel is treated prior to usage. For the incineration of waste, treatment includes sorting where recyclables, certain hazardous or problematic components are taken out, and when using industrial waste, the process of turning the waste into smaller workable pieces. Depending on the level of treatment the exiting waste exits as varying qualities of refuse derived fuel, RFD [39]. Most common is course RFD that includes the described steps, but for processes where one want to further increase the efficiency of the fuel there is also fine RFD which is further shredded to sizes less than 100mm or densified RFD which is compressed and turned into briquettes or pellets for increased energy density [39]. The treated waste is then taken to storage or goes directly towards the incineration process, depending on the design of the plant.



## 2.6 Co-combustion technologies

A common strategy for plants operating on fossile fuels trying to reduce carbon emissions and strive towards a more sustainable production of heat and energy is to implement co-combustion technologies [41]. In this study the implementation of co-combustion will be applied more as a means to raise steam temperatures otherwise limited by HTC and deposition problems. Co-combustion can refer to firing with two different fuel types or simply two different qualities of a certain product, such as rice husk and pellets, to achieve a boon in production or emission reduction [42]. For the purpose of this thesis co-combustion is discussed as a potential way of increasing steam data. Detailed in Figure 2.3 below are three techniques used in co-firing [41]. The three technologies differ in the way they introduce the secondary fuel to the combustion and how the heat is transferred to the steam.

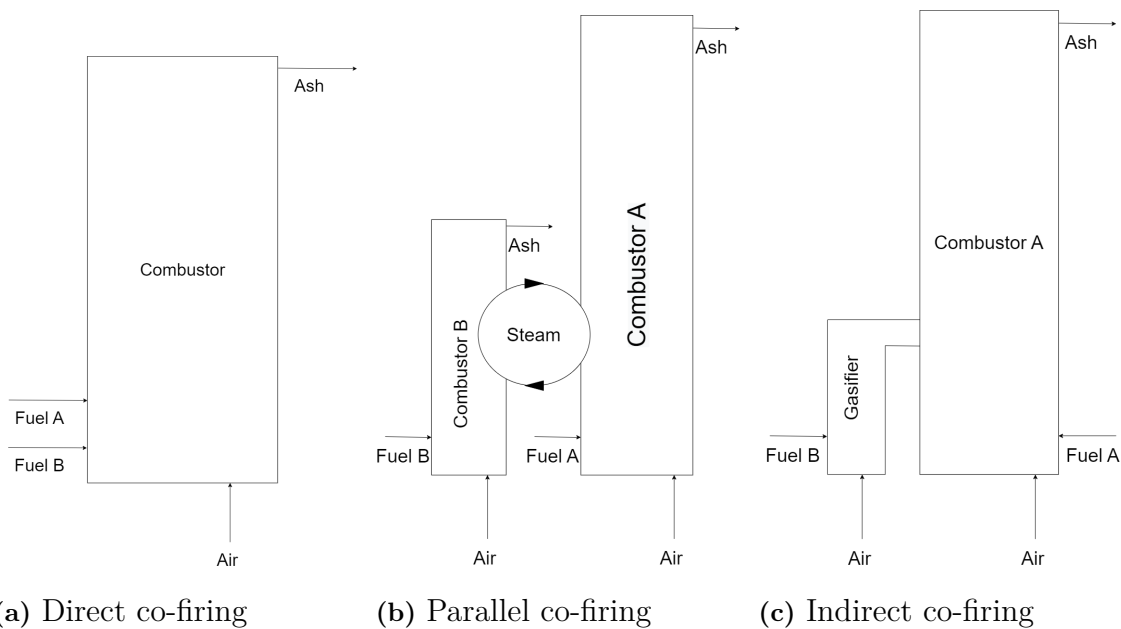


**Figure 2.3:** Three most common technologies for co-firing as described by [41]

Direct co-firing (Figure 2.3a) introduces the primary and secondary fuels into the same combustion unit. This is the most common way of co-firing due to the simplicity and low requirements on new construction and installation and can be introduced post construction as a method of reducing carbon emissions [42]. Introducing a secondary fuel may however impose problems with deposition and corrosion rates but with careful monitoring, trial runs and evaluation these effects can be minimized [43].

The second method, parallel co-firing (Figure 2.3b) introduces the secondary fuel in its own boiler unit. This way of introducing the secondary fuel works in parallel to heat the steam and thus allows the original boiler to remain intact with no major changes having to be implemented. The secondary boiler can then be designed according to the increased output one wants achieve and the specific fuel type. The two units can then have separate or a combined flue gas cleaning system, if the

original one can handle the increased mass flow of fluegases. This method gives the possibility of using two vastly different fuel types, as the second combustion chamber can be designed specifically for the second fuel. It may initially be a more costly alternative than that of direct and indirect co-firing but allows for flexible adjustments.

The third method, indirect co-firing (Figure 2.3c) first gasifies the secondary fuel type in a separate unit and then combusts the working gases and original fuel in the original boiler to generate the steam. This method is slightly more complex and costly to implement than that of direct co-firing but allows for a larger fraction of the secondary fuel to be implemented, as well as allowing solid ashes and incombustible material, to be handled separately which may be of interest with low grade fuels. It also allows for the air to fuel ratios to be separated, which gives an additional degree of freedom when operating the plant, typically helping to reduce certain emission types and depositions inside the boiler [43].

## 2.7 Surface Ionization Detection - SID

A Langmuir-Taylor detector, mainly referred to as a Surface Ionization Detector, SID, is an apparatus used in mass spectroscopy when working with streams of organic or alkali components [44]. Alkali components typically have low ionization energy, IE, which the SID benefits from as the main working principle behind the SID is to have a heated filament with a low work function,  $\phi$ , that melt, dissociate, and desorb incoming particles of low IE that makes contact with the surface [45, 46, 47]. This ionization is then measured as a current and the amount of alkali - or organics - in the measured gas stream can be determined [44, 47].

## 2.8 Fourier-transform infrared spectroscopy - FTIR

FTIR spectroscopy allows for measurements over a broad spectrum and can measure a wide array of gaseous components. The working principle makes use of the fact that many gases absorb IR radiation at specific frequencies [48]. The FTIR unit consists of a blackbody source that generates the emitted IR radiation, and interferometer, a sample gas cell and a detector [49]. The interferometer consists of a beam splitter, a movable and a fixed mirror. The movable mirror is able to translate at various frequencies to create an interference pattern between the slit beams, separating spectral components. The light leaving the interferometer then enters the sample gas cell which has mirrors lining the inside to increase the travel time of the beam and in turn also the sensitivity of the analysis. In this cell the beam is repeatedly redirected through the gaseous media where the gas can absorb certain wavelengths of the IR radiation. The beam leaving the gas cell is enters the detector where a Fast Fourier Transform, FFT is applied to the interferogram produced. This in turn yields the absorbance spectrum which can be used against reference spectra for different species to identify the relative composition in the tested gas [50].



# 3

## A reference plant - Lillesjö

For this thesis there has been the opportunity to work with Lillesjö as a reference plant and in this chapter a description of said plant will be provided to give the reader an deeper understanding of the a reference plant. Information about the plant comes mainly from study visits, the experimental campaign and through discussions with their personnel [11].

The Lillesjö waste-fired CHP plant produces steam at 400 °C and 40 bars producing approximately 36MW of heat and 10MW of electricity. Lillesjö also has a pelletization unit where it produces pellets from spruce and pine using parts of the heat produced, especially during hot months where the need for district heating is low. As the plant operates close to max capacity all year round they also have a cooling unit in case there is an excess of heat produced during hot months that cannot be input to the pelletization.

Waste is delivered to the plant continuously with trucks of both household and industrial waste directly to their bunker. Employing this method of bunker storage allows for a stable influx of fuel to the boiler in the event of delayed imports. Inside said bunker there are claws that can grab upwards 5 tonnes of material and transport it towards hoppers where it is introduced to the boiler, and while idle the claws can move and mix the material contained in the bunker to homogenize the available fuel. By ensuring good mixing one can assure a relatively steady heating value and moisture content of the fuel entering the incineration part of the plant at any given moment. Having a stable flow of a homogeneous fuel into the boiler is essential to ensure that the plant can operate at its designed capacity and also help keep the plants' lifespan as long as possible by avoiding temperature shifts that may lead to unnecessary material stresses and fatigue [51].

### 3.1 Boiler

The reference plant, *Lillesjö*, is designed to consume 14,8 tonnes/h or 355tonnes per day of fuel when operating at full capacity which makes their choice of moving grate a good technology for their size [52]. An example of such a moving grate boiler is shown in Figure 3.1.

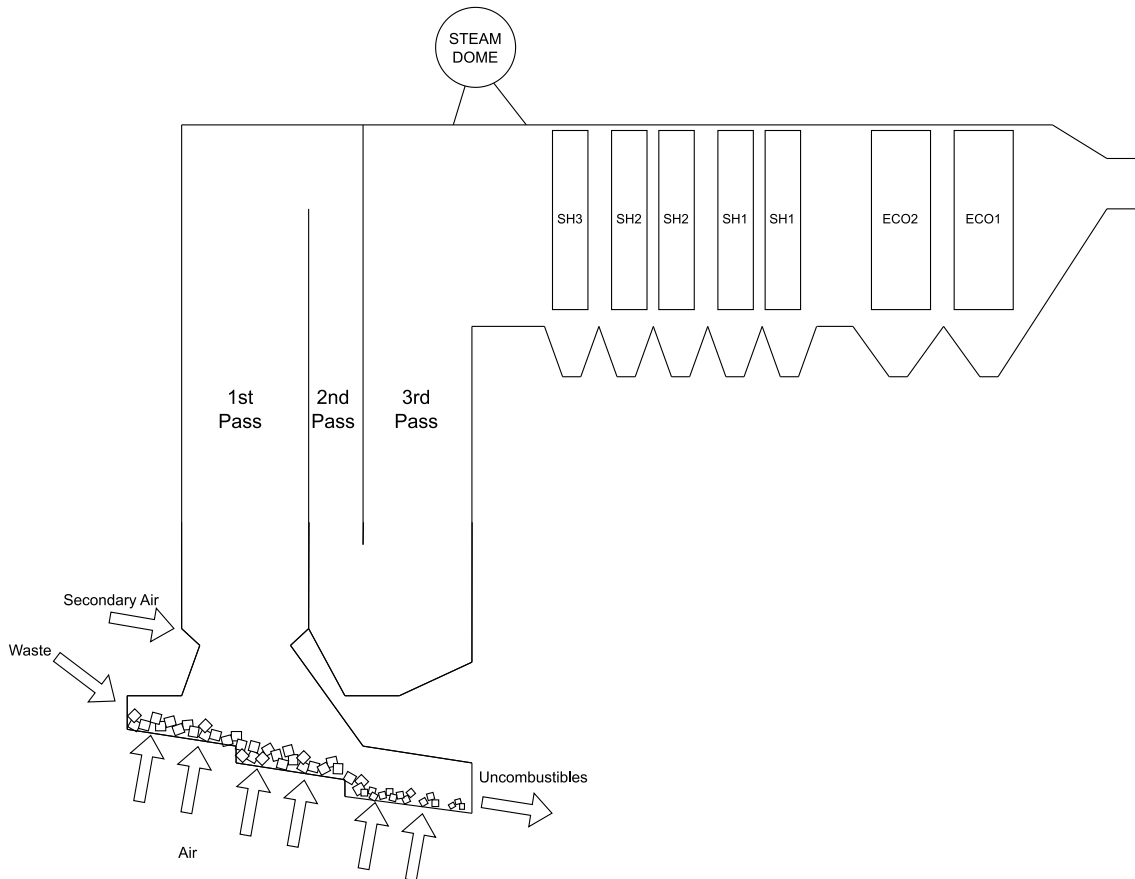


**Figure 3.1:** Representation of the Lillesjö moving grate boiler

As the fuel moves onto the moving grate air is typically introduced at various stages to ensure complete combustion. Air staging also helps reduce the formation of  $\text{NO}_x$  inside the boiler by varying the flow at each respective level which may reduce temperature peaks where  $\text{NO}_x$  are prone to form [17]. As the plant starts up or if the heating value drops there may be a need for assisting burners using oil to support the combustion [5]. The heat generated then travels upwards in the boiler unit via the fluegases where it is gradually transferring its heat to accommodate the heating and evaporation of the condensate and then superheating of the steam.

The design of a moving grate boiler, such as the reference plant *Lillesjö*, typically line the interior of the boiler with tubes, and further along the fluegas path they also include tube packages. In the regions closest to the combustion the temperatures are at their highest and radiative heat transfer dominates. In these regions the tubes are typically covered with refractory wall material to protect and increase the lifespan of the tubes. Further along the first, second and third pass, as the temperature declines protective material is no longer needed and convective heat transfer starts to become the dominating mode of heat transfer. In the reference plant studied the evaporative section of the boiler is designed with three vertical passes to provide enough energy before reaching the superheating and economizing part of the boiler. These areas also have large tube packages obstructing the flow of the fluegases to increase the surface area for heat transfer. As the fluegases reaches

the tube packages the contribution of heat transfer from radiation is significantly lower than in the previous sections as the temperature has gone from above 1000°C to less than 600°C, which means more surface area is needed for the convective heat transfer. The temperatures and pressures generated in plant varies depending on plant, production goals and fuel usage. As mentioned previously for certain fuel types such as waste and biomass where e.g. the chlorine content is high the boiler may need to operate at lower temperatures compared to fossile-operated plants to reduce HTC problems. The *Lillesjö* plant generates steam at 40bar of pressure and 400°C to fulfill their production.

Moreover, as the fluegas passes through the later parts of the boiler, especially when they reach the superheating tube packages particles may condensate onto the tube surfaces and over time accumulate as a thick layer on the tubes [30, 31]. Due to this many plants include soot blowers or a mechanical beater which beats the tube packages at a regular interval to shake down loose particulate matter from the tubes. This helps prolong time between revisions and maintain a good heat transfer surface [53]. This is especially important if the chlorine fraction is high in the particles that condensate onto the tubes as these may be corrosive on the tubes, thus utilizing a soot blower or or mechanical beater may minimize such effects by reducing the amount that may amass [53]. This dust is collected in ducts and processed along with ash and unburnt material from the incineration process. Once the fluegas has passed by the tube packages they enter the fluegas cleaning train which will be covered in part of this chapter.

## 3.2 Fluegas cleaning

Depending on the type of waste that the plant chooses to use, and the level of pretreatment, the requirements for each cleaning unit varies but there are some combinations that are frequently employed. Waste plants that also include clinical and hazardous waste will not be considered since these require other security measures and higher criteria on their emissions. For this section the fluegas cleaning used at *Lillesjö* is described. Presented below is the combination of the units that used to handle the fluegas treatment and ensure that the plant operates under the maximum acceptable emission levels. Certain units can be swapped out, such as the ESP with a bag house filter, depending on the specific composition of the waste being incinerated.

- Electrostatic Precipitator, ESP
- Quencher
- Combiscrubber
- Wet electric filter
- Selective Catalytic Reactor, SCR
- Fluegas condenser, FGC

## Electrostatic Precipitator

The electrostatic precipitator, ESP, is placed as the first fluegas cleaning unit and works to remove particles and fly ash from the fluegases. A representation of the working principle is seen in Figure 3.2. The ESP cleans the fluegases by negatively charging the passing particles as they enter and then attracting them to positively charged plates [40]. In Figure 3.2 the particles pass the middle plates and become negatively charged and pulled towards the positively charged walls as they move through the unit. These units are efficient cleaners of particles and use conservative amounts of electricity. The particles are then collected in an ash silo before being transported away for landfills.

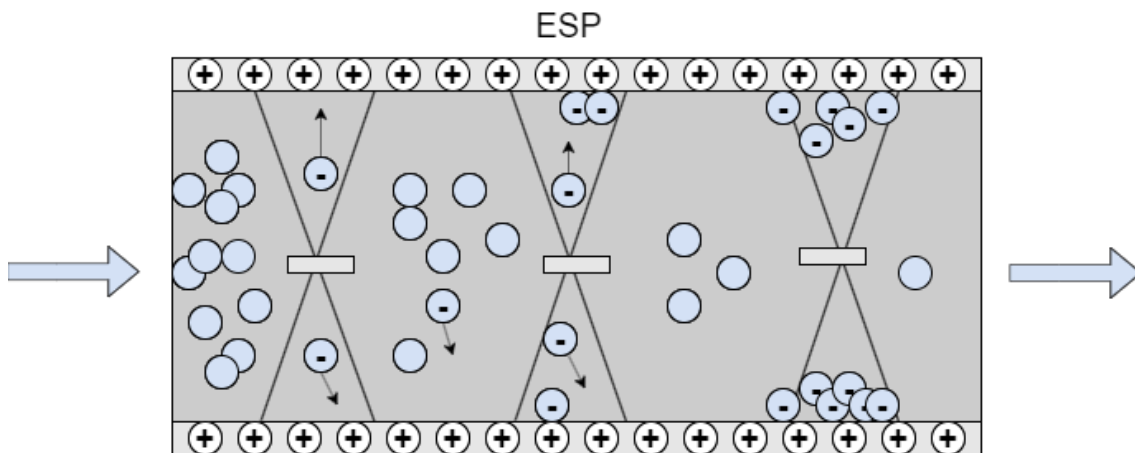


**Figure 3.2:** Representation of how an ESP works, inducing an electric charge on the particles passing through and pulling them from the gas

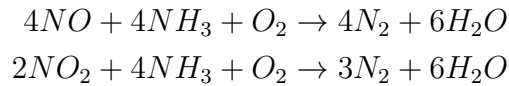
## Wet cleaning process

Once the fluegas has passed through the ESP it enters a series of wet cleaning steps where it first passes through a quencher, a combiscrubber, and lastly a wet electrical filter. As the fluegases enter the quencher they are washed with water and cooled to about 60°C. In this washing step the aim is to wash away HCl and HF, as well as to catch heavy metals such as Hg or Pb and further reduce the fly ash concentration. Due to the direct contact washing with water the fluegases leaving the quencher leaves saturated.

The next step the fluegases enter is the combiscrubber which consists of two units, an acid scrubber and a neutral scrubber. The acid scrubber acts as a second layer to the quencher where any remaining HCl, HF, Hg or particles are removed. In this scrubber it also passes through a mist eliminator, removing water droplets from the fluegases. The fluegases then enter the neutral scrubber where SO<sub>2</sub> is removed, in this step NaOH is added to keep the pH at 6-7, thereby the name 'neutral' scrubber. The wet electrical filter then separates aerosols from heavy metals and H<sub>2</sub>SO<sub>4</sub>, afterwards the fluegases are heated up to 120°C from heat exchanged during the earlier stages of the wet cleaning process.

## Selective Catalytic Reduction unit

The last dedicated cleaning step is the SCR unit where  $\text{NO}_x$  is reacted with  $\text{NH}_3$  in the presence of a catalyst. At Uddevalla this catalyst is three layers of a ceramic material with fine pores. The ammonia is sprayed onto the passing fluegases prior to entering the catalyst where they are reduced into nitrogen gas and water vapour



The catalyst also works dually to destroy dioxins and furans. The amount of  $\text{NH}_3$  added to the flue gases is determined by the fluegas flow and the  $\text{NO}_x$  concentrations. The effectivity of the unit is determined by measuring the  $\text{NH}_3$  slip ( $\text{mg}/\text{nm}^3$ )

## Fluegas condenser

Whilst the main purpose of the FGC is to condense vapour in the fluegases to extract more heat, the FGC reduces the vapour fraction in the emitted fluegases and the condensation may catch particles still left, effectively working as a last filter for particulate matter. The reduced heat may also condense out any aerosols that have not been cleaned out properly.



# 4

## Methods

This chapter covering the method will be divided into three sections, beginning with modelling work done in *Ebsilon Professional* in section 4.1, the experimental work conducted at Lillesjöverket in section 4.2 and a shorter section on fuel classification in section 4.3.

### 4.1 Introductory Ebsilon Modelling

This section will introduce the modelling done using Ebsilon Professional during the thesis, beginning with the base operating cases. The modelling will use *Lillesjö* CHP plant as a reference. Alongside the production of heat and electricity *Lillesjö* also utilizes part of its excess heat during the summer months for the production of pellets, at points there is still remaining heat which is then cooled off. Moreover a fluegas condenser is installed and used mainly during cold months. Due to these distinctions it was decided that two main cases could be constructed. This aids in simplifying the operating conditions and allows for detailed modelling of the two extremes. Two base operating cases for summer operation mode, which deals with excess heat, and the winter operation, which deals with finding additional heat using the flue gas condenser are presented in subsection 4.1.1. Furthermore, when constructing alternative models, where changes to the original plant is made, or a new plant is designed altogether, only the winter will be used as it is assumed changes made to one of the cases will be representative of the changes made to the other case.

The subsequent subsections will focus on presenting the different cases created for potential changes. The most basic case, presented in subsection 4.1.2, introduces the effects of changing the pressures and temperatures of the existing plant. The next case presented in subsection 4.1.3 deals with the addition of a new turbine and increased pressures, utilizing reheat in the boiler to produce additional electricity at the existing plant. The second case, presented in subsection 4.1.4, demonstrates the changes to production and efficiency if an identical plant were to be run using various types of biomass, which paves way for the third case presented in subsection 4.1.5 where the co-combustion of waste and biomass is introduced.

### 4.1.1 Base operation cases

The first cases to be presented are the base operation cases. These are as mentioned divided into two models, for summer and winter operation and can be seen in Figure 4.1 and Figure 4.2. These two models have been constructed in accordance with the data provided by Uddevalla Energi during four days of peak summer and winter respectively, averaged over a five year period.

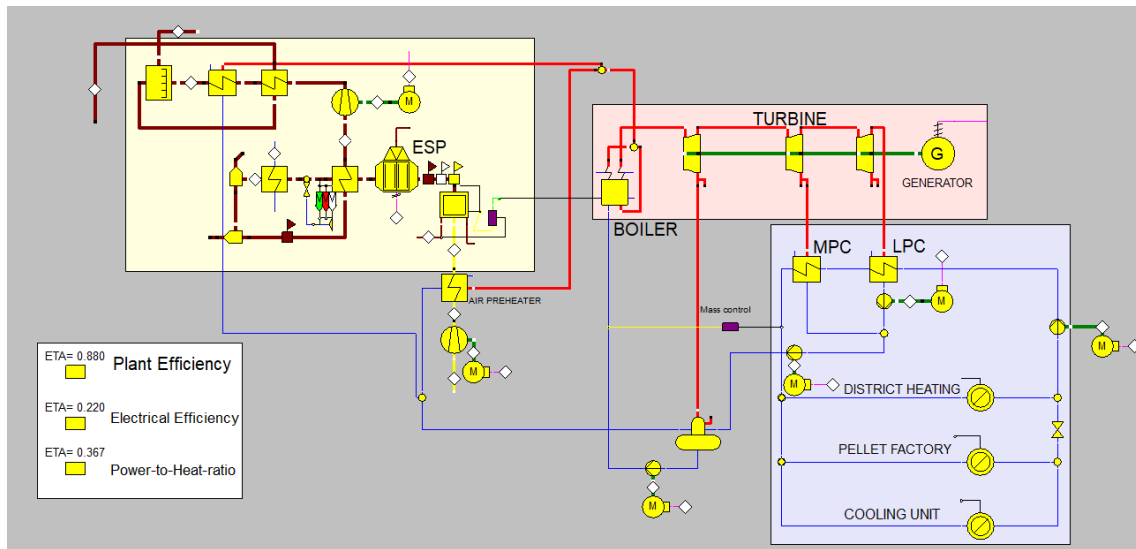


**Figure 4.1:** Epsilon Professional model of the summer operation case.

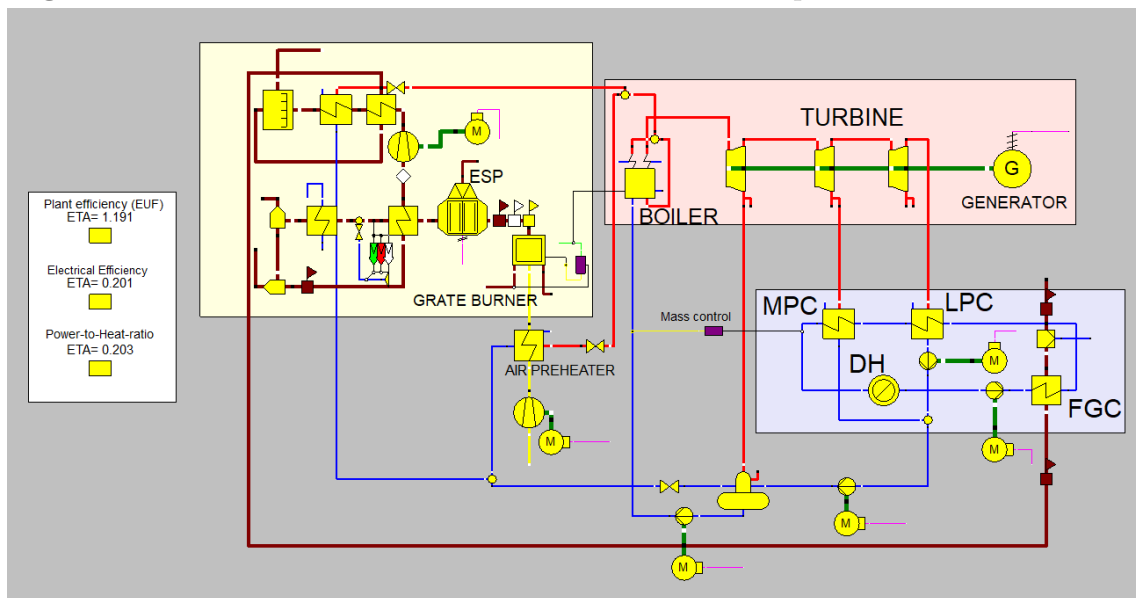


**Figure 4.2:** Epsilon Professional model of the winter operation case.

These models are constructed with three main focus areas, highlighted using the colored rectangles. Visible in both Figure 4.1 and Figure 4.2 is also a fourth area with a white background which displays the models' overall plant efficiency, the electrical efficiency and the power to heat ratio. This helps to compare the model to the reference efficiencies provided by Uddevalla Energi and evaluate changes done.

The yellow area shows the combustion and fluegas cleaning train where the ESP and grate burner has been marked out. The fuel composition is presented in Table 4.1 to demonstrate the small variation in fuel depending on winter and summer operation. These values have been kept constant for the subsequent winter and summer cases for coherency.

	NCV [MJ/kg]	C [wt.%]	H [wt.%]	O [wt.%]	N [wt.%]	S [wt.%]	Cl [wt.%]	H2O [wt.%]	Ash [wt.%]
Winter	10.40	26.8	3.8	13.8	0.5	0.2	0.5	42.5	11.9
Summer	11.02	30.3	4.3	15.6	0.6	0.2	0.6	35.1	13.4

**Table 4.1:** Fuel compositions and net calorific value (NCV) used for the Winter and Summer operational cases

A more detailed description of the components in the fluegas cleaning is presented in chapter 3. In practice the fluegases first enter the ESP, then the three stage quench and scrubber repressed by heat exchangers, gas separators, and liquid injection, portraying the gas-fluid heat transfer in the scrubber. The fluegases then enters the SCR and finally the fluegas condenser. The main distinction between the base models is that the fluegas cleaning ends at the SCR for the summer case, whilst the winter operation the utilizez the FGC where a large fraction water is condensed to allow for more heat to be recovered.

The next two areas show where the steam is generated and utilized to generate electricity and heat for the district heating network. Enclosed by the red rectangle the boiler, turbine and generator are shown. Condensate flows into the steam generator where saturated steam is produced, part of which is diverted towards heating the fluegas cleaning and preheating the air that is used in the combustion. The rest of the steam is reintroduced to the steam generator component to represent the superheating step, where the steam temperature is raised to 400°C. The steam is then led to the turbine which has been designed with three components to represent the available steam extraction pressure levels in the turbine. From the turbine one extraction goes towards a feedwater heater, FWH. The second extraction and the remainder of the steam exit into two condenser units, one of medium pressure and one of low pressure.

These condensers heat the water for the DH system represented in the Blue rectangle, this circle of gradually more heated water can be referred to as the heating cycle. For the winter case all heat is assumed to go towards DH and is thus represented in the model by a singular heat consumer that utilizes all heat available above 40°C. In the summer case two additional units have been implemented, to represent the heat consumed by the pellet factory and the excess heat that is cooled away. Moreover in the winter model the FGC is connected directly to the heating cycle to provide more heat for the DH network. The condensate is then pumped back to higher pressures and led towards the FWH before the cycle is repeated.

Summarized in Table 4.2 are the primary steam, extraction and district heating data for the two models. The extraction pressures vary slightly depending on season but the largest change comes in the heat in the district heating network.

	$P_{primary}$ [bar]	$T_{primary}$ [°C]	$P_{ext,1}$ [bar]	$P_{ext,2}$ [bar]	$P_{end}$ [bar]	$T_{DH,in}$ [°C]	$T_{DH,out}$ [bar]
Winter	40	400	11	0.85	0.39	93.2	52.9
Summer	40	400	9	0.72	0.30	88.8	43.3

**Table 4.2:** Primary steam, extraction and district heating data for Summer and Winter operational cases

For the winter case the addition of the fluegas condenser raises the temperature to 52.9°C before entry into the LP condenser compared to the 43.3°C available in the summer model. This allows for more heat to be extracted in the winter when it is needed most.

### Accessible design

To make the design more accessible and to be able to more accurately access all streams within the boiler the models were re-made with out the use of the built-in component for a boiler (see Figure 4.3). This way the superheater and economizer tube packages can be accessed and interacted with and the steam being diverted to the fluegases more easily controlled. Additional points could potentially be added to the boiler which the original component could not handle, such as radiative losses or heat transfer from particles, which gives this way of designing the boiler potentially more accurate depending on which additions are made.

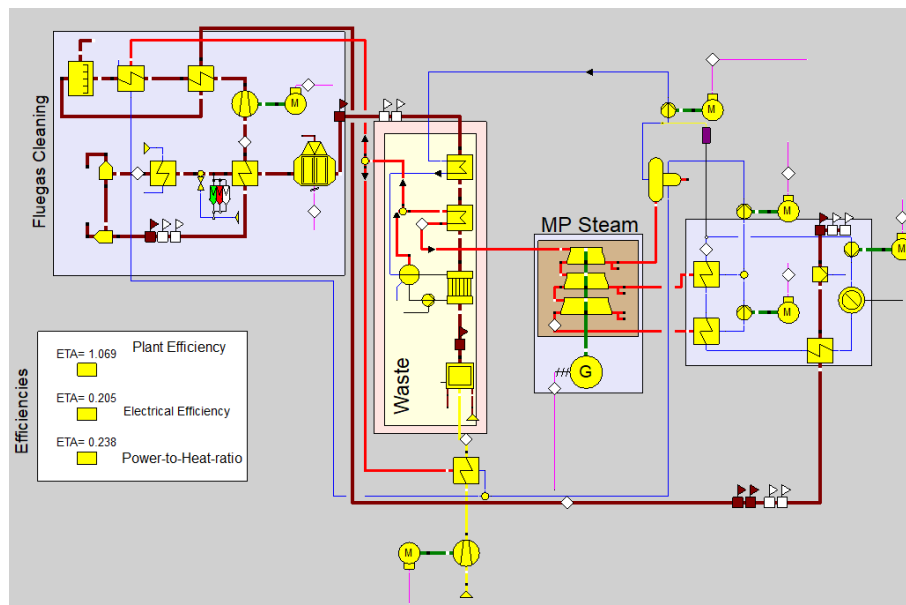


**Figure 4.3:** Epsilon Professional model of the winter operation case, accessible version

### 4.1.2 Temperature-Pressure study

One of the simplest theoretical cases one can examine when looking into potential improvements to a CHP plant is to look at increasing the available steam data. This can be examined using Epsilon Professional's excel addin which can run multiple simulations of different operating conditions whilst not changing the actual model.

Presented in Table 4.3 below are the settings for five different potential cases that will illustrate the effects of changing temperature and pressure either separately or simultaneously in a boiler. The first two will demonstrate the effects of increasing the temperature in increments of 25°C, the third and fourth demonstrates what happens when the pressure is either decreased or increased, whilst the last case will show a combination of both increased temperature and pressure. Other design parameters such as the extraction pressures and outlet temperature from the MPC is kept constant in the cases to illustrate only the effect of changing the steam parameters.

	$P_{primary}$ [bar]	$T_{primary}$ [°C]	$P_{ext,1}$ [bar]	$P_{ext,2}$ [bar]	$P_{end}$ [bar]	$T_{DH,in}$ [°C]
Winter (T+)	40	425	11	0.85	0.39	93.2
Winter (T++)	40	450	11	0.85	0.39	93.2
Winter (P-)	35	400	11	0.85	0.39	93.2
Winter (P+)	50	400	11	0.85	0.39	93.2
Winter (TP+)	50	425	11	0.85	0.39	93.2

**Table 4.3:** Primary steam, extraction and district heating data for Winter operation of Case 0 with lowered and increased steam data

### 4.1.3 Case 1 - Addition of Reheat

A case that does not require major changes to the existing model is to include a reheat cycle and top load turbine to produce more electricity. In practice this is done by first increasing the pressure and routing the generated steam first through an high pressure turbine and then reintroducing it to the boiler for reheating back to the original design temperature, in this case 400°C (see Figure A.30) to then enter the original turbine. Presented in Table 4.4 some example design parameters are shown. For this specific example the primary steam pressure has been raised from 40 bar to 200 bar to provide an extra push to the electricity generation, the pressure of the steam entering the MP turbine is kept at 40 bar and 400°C.

	$P_{prim}$ [bar]	$T_{prim}$ [°C]	$P_{reheat}$ [bar]	$T_{reheat}$ [°C]	$P_{ext,1}$ [bar]	$P_{ext,2}$ [bar]	$P_{end}$ [bar]	$T_{DH}$ [°C]
Winter	200	400	40	400	11	0.85	0.39	93.2

**Table 4.4:** Primary steam, extraction and district heating data for Winter operation of Case 1

#### 4.1.4 Case 2 - Impact of fuel variation

To achieve a good comparison between fuels types and typical operation parameters and outputs for MSW and for cofiring options such as biomass, various types of fuels were tried in the winter model (Figure 4.3). Biomass driven plants typically have other demands on their fluegas cleaning as the biomass typically contains less contaminants and heavy metals than that of MSW. Moreover, biomass typically contain less chlorine and alkali metals such as K and Na which are behind the reduced steam data when incinerating MSW. Due to this biomass plants, and especially if run with processed biomass of high quality such as torrefied wood, can be operated with higher steam data than that of MSW plants and with lower fluegas cleaning constraints. Moreover, biomass can be combined through co-combustion technologies into what was modelled in subsection 4.1.5. Tabulated below in Table 4.5 are a few available alternatives included in this section for co-firing with MSW.

Untreated	Treated	Refined	Miscellaneous
Tree stumps	Refuse wood	Pellets (Generic)	Car tires
Tree stocks	Cardboard	Pellets (White)	Sewage sludge
Logging residues		Pellets (Black)	PTP
Peat			Animal residues

**Table 4.5:** Fuels examined for co-firing with MSW separated into four categories: Untreated, Treated, Refined and Miscellaneous

The fuels presented in Table 4.5 are categorized into four types of fuels: *untreated* fuels that can be utilized directly; *treated* fuels such as refuse wood and cardboard which can be incinerated at the end of their lifecycle; *refined* fuels such as pellets; *miscellaneous* fuels such as sewage sludge, car tires and animal residues. These have been chosen to represent fuels with varying amounts of Cl, S and K.

The pellets used in this section denoted generic, white and black represent different qualities of pellets. White pellets contain very low levels of ash but have higher requirements regarding storage, whilst black pellets have been torrefied, contain higher levels of ash but may withstand water and can thus be stored outside [54]. Paper-tree-plastic, PTP shares many similarities with MSW but has been sorted completely, whereas MSW may still contain other components such as compost. Given time and improved sorting, PTP and MSW should one day be equal in composition.

In Table 4.6 the steam data for each fuel is presented, other parameters such as the pressures for steam extraction and end pressure, as well as temperature in the district heating has been kept constant as in the winter model. The estimated temperatures used are results from section 5.3, whose estimation method is described in section 4.3. The pressures are chosen to keep the steam quality out of the turbine constant through temperature changes.

	$P_{primary}$ [bar]	$T_{primary}$ [°C]
MSW	40	400
Tree stumps	92	520
Tree stocks	95	525
Logging residues	83	505
Peat	89	515
Refuse wood	78	495
Cardboard	89	515
Pellets (G)	98	530
Pellets (W)	92	520
Pellets (B)	98	530
Car tires	68	475
PTP	53	440
Animal residues	78	495

**Table 4.6:** Primary steam data for an array of various fuels estimated in section 4.3 as well as MSW as a reference.

#### 4.1.5 Case 3 - Co-combustion with Biomass

As presented in the theory section, co-combustion is typically implemented in one of three ways; direct, indirect or parallel. For this case both indirect and in parallel models have been constructed to demonstrate the difference in efficiencies, but also to open up for the discussion as to why one is more plausible than the other. Looking in detail at the differences in Figure A.32 and Figure A.31 it can be seen that the parallel model lets the two fluegas streams be separate until the fluegas cleaning, whilst the indirect model first runs the secondary fuel through a gasifier and then combines combusts them in together in the original boiler.

In both models the addition of a top cycle with reheat is added to make use of the fact that co-firing with biomass opens up the opportunity to reach higher temperatures. Through the parallel co-firing the biomass boiler could focus mainly on the HP turbine at higher pressures whilst the original waste system can remain focused on the MP turbine at 400C and 40bar pressure.

For the Parallel cofiring two distinct models have been drawn up, Figure A.32 and Figure A.33, whose main differences are what is kept constant between runs. The first model, Parallel (1), keeps the steam production constant as in the original winter model of 13.6kg/s of steam, this however means that less MSW is being combusted to accomodate the biomass. The second model, Parallel (2), keeps the massflow of MSW constant and lets the steam production vary. Parallel (1) would describe potentially describe a new plant of similar capacity with an increased focus on electricity production, whilst Parallel (2) would describe the extensive retrofitting of the existing plant, where the usage of MSW remains constant, but a new focus on electricity production is added.

For the indirect model seen in Figure A.31 the secondary fuel is first gasified and then combusted alongside MSW. Before the gasifier step the secondary fuel first has to be dried to a maximum of 10% moisture to ensure a high enough carbon content. The cost of this drying is not added in the calculations. Had the secondary fuel instead been added directly the process would instead be direct cofiring, but this reduces the opportunity to influence the incoming gases from the secondary fuel. Another option not considered in this thesis, is having direct co-firing with two separate furnaces, connected at for example the third pass. This way the combustion of the two fuels could be done separately but the same problems would arise as the fluegases reach the superheaters. Moreover, for the indirect co-firing, the working gas could be cleaned between gasifier and the primary boiler, such that only the combustible components are added, removing any unnecessary products.

	$P_{prim}$ [bar]	$T_{prim}$ [°C]	$P_{reheat}$ [bar]	$T_{reheat}$ [°C]	$P_{ext,1}$ [bar]	$P_{ext,2}$ [bar]	$P_{end}$ [bar]	$T_{DH}$ [°C]	$P_{DH}$ [bar]
Indirect	†	‡	40	400	5.5	0.87	0.39	93.7	0.89
Parallel (1)	†	‡	40	400	5.5	0.85	0.39	93.2	0.89
Parallel (2)	†	‡	40	400	5.5	0.85	0.39	93.2	0.89

**Table 4.7:** Primary steam, extraction and district heating data for Winter operation of Case 3 models. (†) 2.25 times the pressures presented in Table 4.6. (‡) same temperatures presented in Table 4.6

The primary pressures set in Table 4.7 are set to ensure that there is no condensation in the high pressure turbine. Higher pressures could potentially be used here, but the pressures provide a safety margin.

## 4.2 Experimental setup - Lillesjöverket

The work conducted at Lillesjöverket was aimed at providing as much additional information about the fluegases and heat transfer as possible to broaden the data provided initially. On site the following items were measured:

- Deposition rate
- Temperature
- Gas Composition
- Aerosols
- Alkali

These measurements were conducted using a set of probes, specialized at different areas of data collection. The first measurement that will be discussed in subsection 4.2.1 is the deposition rate. The second measurement that will be described shortly in subsection 4.2.2 is the temperature readings conducted through out the boiler. Then the gas composition measurements will be detailed in subsection 4.2.3 and aerosol measurements in subsection 4.2.4.

The different entry points for data collection are shown in Figure 4.4 represented by the dots. The different colors represent the availability of the ports. The *Lillesjö* plant had many ports that were available for use, marked out in yellow and orange, but also some ports marked out in blue that could potentially be used but would require more work to access. The orange and blue ports represent positions that would be interesting for future studies in the area. The orange ports in the first and third pass would help provide a better understanding of the combustion environment and could help track dead zones and map the fluegas and temperature distribution through the early parts of the boiler. The blue and orange parts in later part of the boiler would be useful in determining the full temperature development and for further deposition measurements.

In Figure 4.5 the used points have been marked out and given names to help the reader follow which point is being discussed. At the third superheater package a second port was used on the other side of the boiler denoted B1S that was used for certain measurements. Moreover, in Table 4.8 the type and amount of measurements conducted for each port is summarized, and if a measurement was left out at a port this is represented with a hyphen.

	A1	A2	A3	B1	B2	B3	BESP
Deposition rate	-	-	-	IV	-	-	-
Temperature	I	I	I	III	I	I	-
Gas composition	III	I	I	VI	V	IV	II
Aerosols	-	-	-	II	-	-	-
Alkali	I	I	I	I	-	I	I

**Table 4.8:** Summary of measurements conducted in each port, with roman numerals indicating the amount of measurements per position

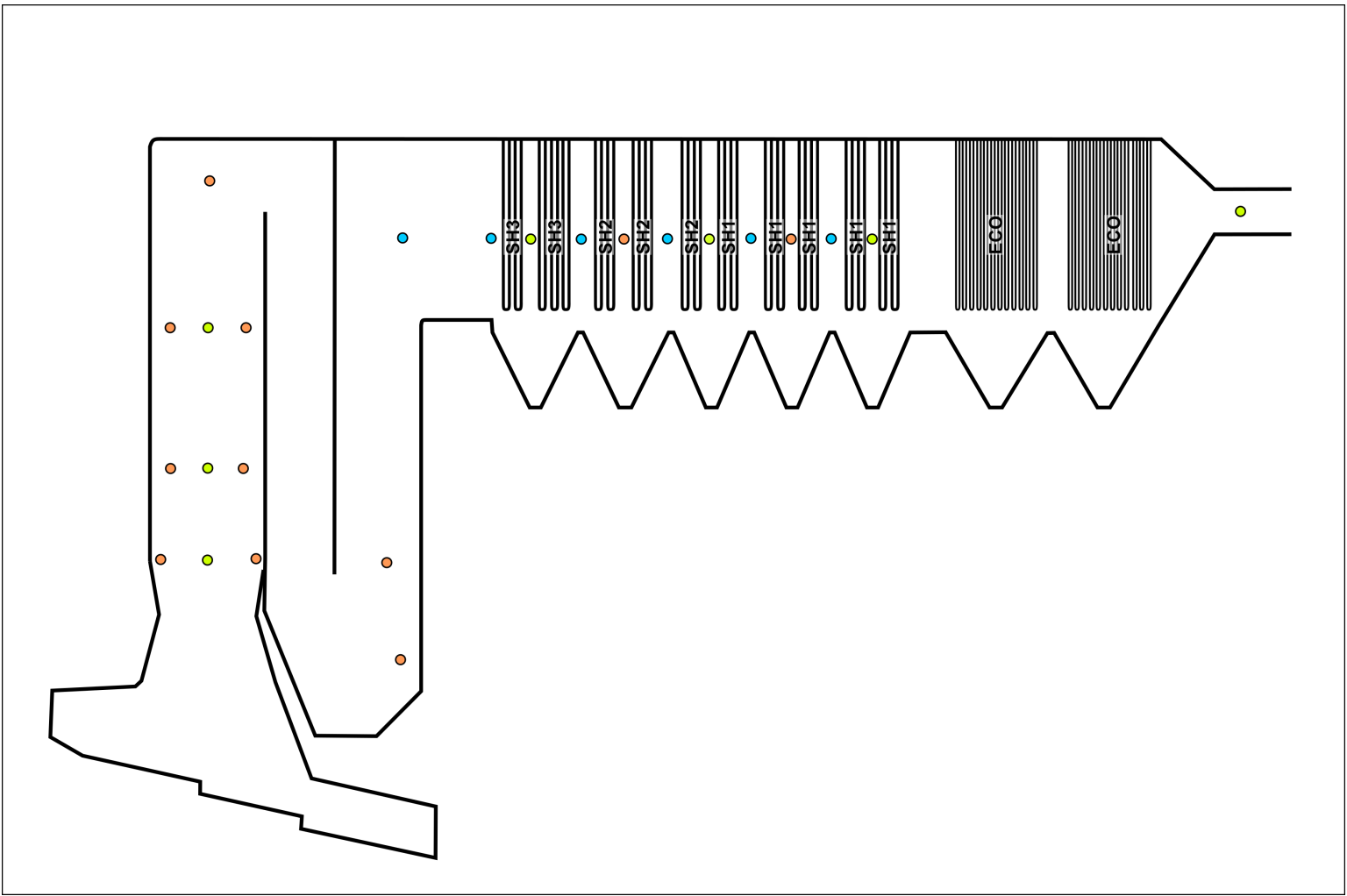


**Figure 4.4:** Schematic representation of the Lillesjö boiler with all available points for measurements marked. Yellow - used points, Orange - ports interesting for future measurements, Blue - semi accessible ports

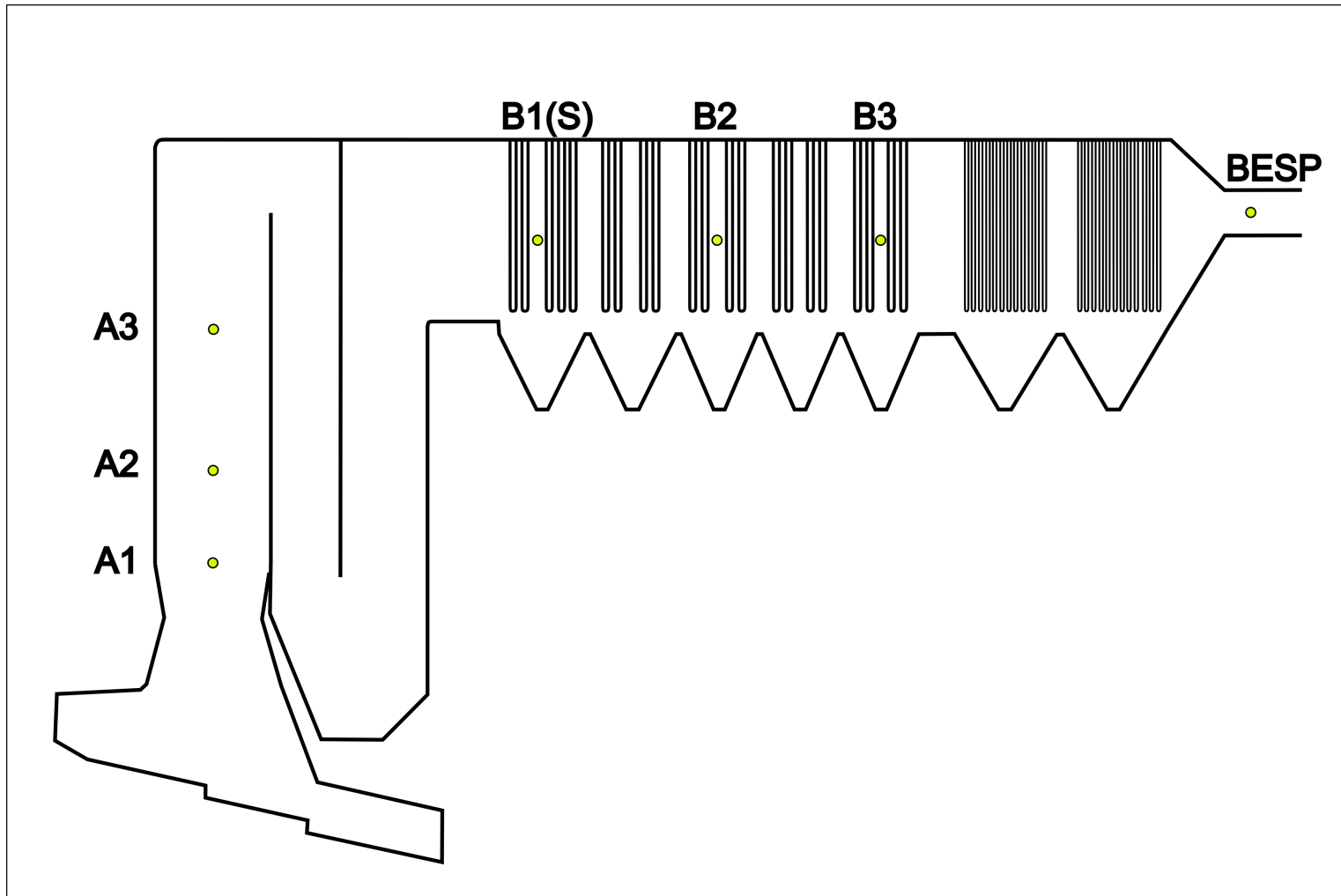


**Figure 4.5:** Schematic representation of the Lillesjö boiler with only the used points marked out in yellow and their respective names. 7.5(S) represents the port 7.5 available on the opposite side of the boiler.

### 4.2.1 Deposition Rate

To determine the deposition rate a heat regulated probe was inserted in port B1 and B1S as most deposition and HTC occur at the superheater tube packages. The probe was regulated using compressed air to maintain the same temperature of the tube packages. The procedure works in such a manner that two rings, of which the weight and dimensions prior to insertion were measured and known, are mounted on the probe and inserted into the boiler. The ports used could be opened to replace cinder blocks inside with ones that had holes big enough to fit the probe. The probe was then left inside for a set amount of time such that a coating of deposition material could build up on the probe. These rings could then removed from the probe and weighed to determine the rate of fouling at the superheaters. The initial weight, depth and exterior diameter of these rings are presented in Table 4.9. The CTH rings are designed specifically to determine the deposition rate and composition, and brought from Chalmers to serve as a baseline. The UKAB ring is made on site from the same type of tubes used within the Lillesjö superheater packages.

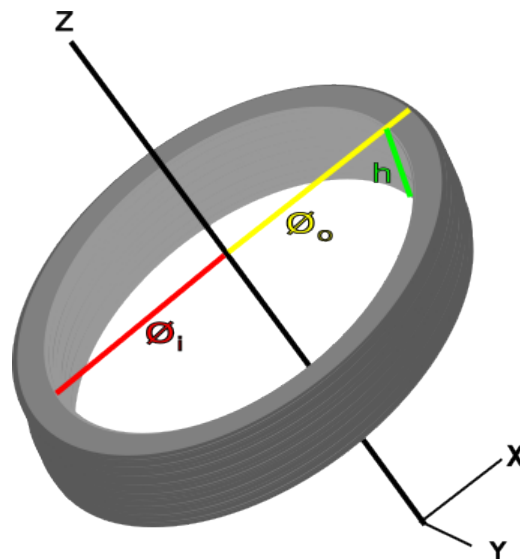


**Figure 4.6:** Schematic of ring dimensions, showing the inner and outer diameters,  $\phi_i$  and  $\phi_o$  respectively, as well as the depth,  $h$ , of the ring.

Ring #	Initial Weight [mg]	Depth (h) [mm]	$\phi_i$ [mm]	$\phi_o$ [mm]	Material Exterior	Material Interior	Position -
UKAB-1	86765.4	14.95	31.0	44.5	-	-	B1
CTH-1	37850.1	15.00	31.0	37.9	Sanicro28	4L7	B1
CTH-2	36566.5	15.00	31.0	37.9	Sanicro28	4L7	B1S
CTH-3	37511.8	15.00	31.0	37.8	Sanicro28	4L7	B1S
CTH-4	37694.1	15.00	31.0	38.0	Sanicro28	4L7	B1S

**Table 4.9:** Initial weight and dimensions of deposition rings prior to usage, as well as the type of material used.

The amount of time for the probe to be inserted can be chosen arbitrarily, but should be chosen to represent the fouling conditions at the plant where the probe is inserted. Typically a longer insertion time, such as a few months would be representative of long term depositions and could be used to study the sulphation of solid KCl stuck on the tubes and how chlorine travels in the deposition. A shorter insertion time would instead be a good way of measuring the initial depositions and what creates the initial crust. Moreover, depending on the plant shorter times would be required where the relative concentrations of Cl, K, P and S are high, as these compounds are likely to condense onto the tube surfaces and stick through thermophoresis, whilst longer time spans may be required in boilers where the concentrations of the aforementioned species are low as such fluegases are more likely to simply stick superficially to the tubes and not condense into a harder crust. Once reasonable lengths of time have been determined at the locations where one wants to conduct measurements and the rings have been inserted for the allotted amount of time the probe can be withdrawn and the rings can be taken off and weighed. Once weighed one can follow Equation 4.1 to find the weights added per unit of time at the specific point in the boiler

$$R_D = \frac{m_d}{A_d \times t} \quad [mg \text{ cm}^{-2} \text{ min}^{-1}] \quad (4.1)$$

where  $m_d$  is the weight of the deposition material,  $A_d$  is the outer area of the ring, or deposition area, and  $t$  is the time the ring was inserted for. The matter accumulated on the rings could then also potentially be removed and analyzed for their composition for more information, but this step was omitted.

### 4.2.2 Temperature

To determine how the temperature is changed throughout the furnace a probe with a thermocouple and water based temperature regulation was inserted into the boiler at all used measurement points except the ESP (see Figure 4.5). Water was used to ensure the probe did not take damage from the heat by applying flow of water such that the effluent temperature would be well below boiling. The thermocouple however protrudes far enough from the surface to be affected by the regulation. The probe was inserted at the different locations until a stable temperature reading could be found and then moved to the next location. For points A1 and A2 where the temperatures are expected to be higher there may be difficulties regulating the temperature and thus shorter measurements are sufficient as to not damage the equipment. These temperature readings are then compared to internal sensors and if they don't deviate their continuous temperature readings can be used for further data analysis.

### 4.2.3 Gas composition

To track changes to the gas composition throughout the boiler a probe using water for heat regulation connected to an FTIR and O2 tracker, was used and inserted in all ports shown in Figure 4.5 for various time intervals. The probe is also fitted

with electrical heating of the inner tube wall to ensure no gases condense inside the probe. Seen in Figure 4.7 the probe is to be connected to a filter, pump and in case one wants measurements on either dry or wet basis a condenser is also connected. Heated hoses are used to connect each individual part. The filter unit operates at  $160^{\circ}\text{C}$  and is comprised of two individual filters, the first catches particles down to  $1\ \mu\text{m}$  and the second particles down to  $0.01\ \mu\text{m}$  that would otherwise be damaging to the gas analysers. Except for the filter unit the pump and the heating hoses connecting each part are heated to  $190^{\circ}\text{C}$ , high enough to ensure no gases condense before the analysers which have an operating temperature of  $190\ ^{\circ}\text{C}$ .

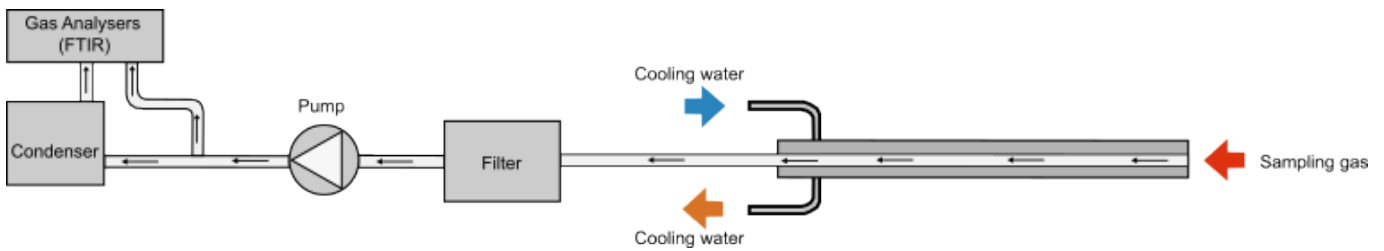


**Figure 4.7:** Schematic representation of the setup used to sample gases and determine composition.

The measurements were conducted with a two different approaches. The first approach was to get long base measurements at each port to what concentrations can be expected at each of the available measuring locations. These measurements were conducted for approximately 30 minutes. The second approach was to do several measurements in quick successions between ports, this was done especially on floor 8 where ports B1, B2 and B3 were readily available and closely adjacent. With this approach the goal is to identify how any peaks and trends travel and change from port to port.

As mentioned the gas analyzers measures the sampled gas composition on either a dry or wet basis in vol. ppm or vol %. Most sampled gases are kept in a wet basis in either vol. ppm or vol% but the measurements conducted using an  $\text{O}_2$  tracker to were done using a dry vol%. Seen from Table 4.8 most of the composition measurements were centered around ports 7.5 and 11.5 following two measuring approaches mentioned previously.

The FTIR, whose working principles are presented in section 2.8, allows for a multitude of compounds to be measured, for this thesis the following are of highest interest;  $\text{NO}$ ,  $\text{NO}_2$ ,  $\text{CO}$ ,  $\text{CO}_2$ ,  $\text{H}_2\text{O}$ ,  $\text{HCl}$ ,  $\text{SO}_2$ . The concentrations of  $\text{NO}_x$  is interesting from an emission point of view, as any modelling done with co-firing of other fuels need to take into account  $\text{NO}_x$  emission limitations. In terms of finding margins in increasing steam data  $\text{HCl}$ ,  $\text{SO}_2$  are especially interesting since the ratio between these will reveal whether it is currently possible or other alternatives should be looked at. For the combustion conditions inside the boiler,  $\text{CO}$  and  $\text{CO}_2$  are of interest to see if there is complete combustion, and  $\text{O}_2$  &  $\text{H}_2\text{O}$  to determine moisture content of the fuel and air to fuel ratios.

#### 4.2.4 Aerosols

Aerosol measurements were collected using a Dekati Low Pressure Impactor (DLPI) where particles are drawn from the boiler into the DLPI, which encloses a set of impaction plates. The DLPI is designed such that larger particles are collected on early levels and the smallest particles at the lowest levels. The DLPI used for this measurement had a set of 13 impaction plates, an after-filter and an additional small vessel for particles from the cyclone. At the impaction plates a thin layer of foil with an adhesive surface is placed that catch the particles that make contact. In Figure 4.8 a schematic representation of the DLPI is presented. The sizes collected at each stage is tabulated in Table 4.10.

Moreover, the inlet of the DLPI is connected to a small probe that can be inserted at locations of interest. A vacuum pump aids in pulling the particles through the impactor at a rate of 10 litres per minute. It can also be noted that to ensure there is no condensation occurring inside the DLPI a heat-band is wrapped around the surface of the apparatus to maintain a temperature of roughly 100°C. Once a certain amount of time has passed the DLPI can be disconnected from the fluegas inflow and disassembled such that each individual piece of foil, the after-filter and the small vessel can be weighed to determine the amount of aerosols at each level and determine a size distribution profile.

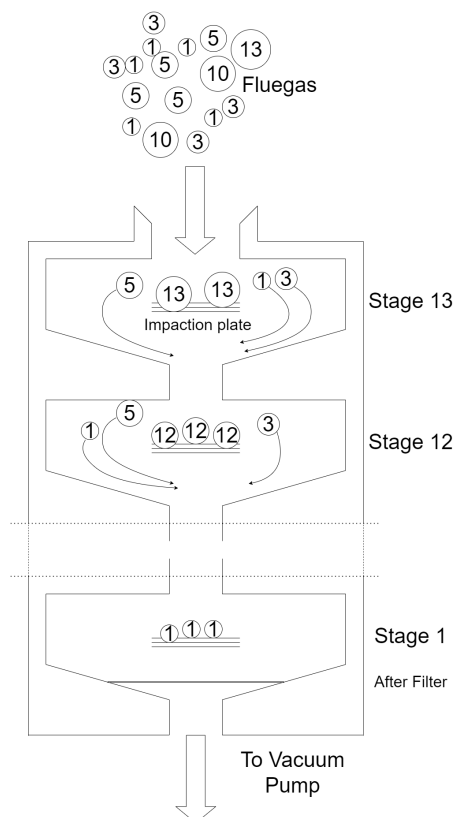


**Figure 4.8:** Schematic representation of a DLPI used to sample and determine a fluegas particle size distribution

Stage	13	12	11	10	9	8	7	6	5	4	3	2	1	Filter
D50% [ $\mu\text{m}$ ]	10	6.8	4.4	2.5	1.6	1.0	0.65	0.40	0.26	0.17	0.108	0.06	0.03	$\leq 0.01$

**Table 4.10:** DLPI stage median particle diameter collection size

### 4.2.5 Alkali

To determine the total alkali concentration, and by extension the systems potential to produce the chloride-alkali salts corrosive for the superheaters, measurements were conducted by a setup detailed in [55] using SID measurements. The SID working principle is presented in section 2.7. The setup consists of three main parts that allow for a total alkali measurement: a calibration system, the SID instrument, and the sampling and dilution system, where the result is given as a potassium equivalent in the units of  $mg/m^3$ . These measurements were conducted at points A1-A3 as well as B1, B3 and BESP (see Figure 4.5). This particular setup has previously been used mainly at temperatures expected to be found around the superheaters, due to this there was a large interest in measuring extensively closer to the combustion environment at A1-A3. However for the purposes of determining the thesis the measurements conducted closest to the superheaters, B1 and B3, were most important as it is in these areas where alkali are expected to condense onto the superheater tubes. In these areas it may also be easiest to get good readings of alkali concentrations since the setup prefers to measure already condensed airborne particles to that of vaporized particles that could potentially also clog up the system.

## 4.3 Fuel classification

For this thesis, the fuels' ability to draw out the chlorine from KCl and HCl by sulfation is of key interest. The MSW will be mapped out thoroughly by experiments and from continuously logged measurements available from the company, other fuels however, such as different kinds of biomass will not be tested directly and thus a way of estimating what steam temperature they may be able to produce is of importance. For this work, a simple method based on the fuels' composition is used to determine which steam data would potentially be applicable for different kinds of renewable, semi-renewable as well as refuse products.

### 4.3.1 Steam temperature estimation

For this estimation it is assumed that typical MSW operates at with steam data of 400C, and on the other side of the spectrum, coal operates at 600C. By tabulating the constituents of the two fuels in a table such as Table 4.11 an array of other possible fuels can be input in between the two. Next one may determine, row by row, which of the two fuels: MSW and Coal the aspiring fuel is closest to. For this certain key parameters containing S, Cl and K, from the fuel composition and the FactSage simulated fluegases are weighted more heavily due to their greater importance and impact in HTC and deposition problems.

Illustrated in Table 4.11 by  $\leftarrow$  and  $\rightarrow$  the fuels are either more similar to MSW or coal respectively and each row is then given a score corresponding to which fuel they are most similar to. For certain available fuel analyses some ash components are not available (marked N/A) and thus the scores are also based on the amount of applicable rows. The roughly estimated temperature is then set according to the following linear estimation,

$$T = 400 + Score \times 200 \quad (4.2)$$

where the lowest possible score corresponds to a fuel matching MSW and the highest possible score corresponds coal in these specific properties. For this calculation the temperatures will also be rounded to the nearest 5°C for simplicity.

The temperatures can then be input into the Epsilon models to investigate how they would impact the electrical efficiencies. This is done in both subsection 4.1.4 where they are burnt on their own, and in subsection 4.1.5 where they are burnt in combination with MSW, either indirectly in one boiler or in two parallel boilers.

	MSW	Fuel A	Fuel B	...	Fuel X	Coal
C	A	→	←	...	→	B
H	A	→	←	...	←	B
O	A	←	→	...	←	B
S	A	←	←	...	→	B
N	A	←	→	...	→	B
Cl	A	←	→	...	→	B
H2O	A	←	←	...	←	B
Ash	A	←	→	...	→	B
Al	A	→	N/A	...	←	B
Ca	A	←	N/A	...	←	B
K	A	←	→	...	→	B
⋮	⋮	⋮	⋮	⋮	⋮	⋮
Zn	A	→	←	...	←	B
Hg	A	←	N/A	...	←	B
KCl	A	←	→	...	→	B
HCl	A	→	←	...	→	B
SO2	A	←	→	...	→	B
CO2	A	←	→	...	←	B
⋮	⋮	⋮	⋮	⋮	⋮	⋮
K2SO4	A	←	←	...	→	B
Score	0	0.21	0.48	...	0.73	1
Temp	400	440	495	...	545	600

**Table 4.11:** Schematic illustrating the method for first estimation of steam temperatures for fuels by comparing compositions. Temperatures rounded to the closest 5°C.

### 4.3.2 FactSage

FactSage was used in two stages for the estimation of steam temperatures. First it was used to determine ratios of post combustion components such as KCl, HCl, SO<sub>2</sub> and CO<sub>2</sub> and then used to find fractions ash melts for each respective fuel type after an initial temperature had been estimated. For these calculations the *Equilib* function in the program was used. Equilib works on the principle that by minimizing Gibbs free energy,  $\Delta G$ , the program will find the most thermodynamically stable components from an input composition and operating conditions. FactSage in of it self is a large database of chemical thermodynamics of a vast array of components that relies on the user to pick the right packages and databases according to the scenario they wish to compute [56].

For the FactSage calculations performed the databases FactPS, FToxid and FTsalt were used for their large collection of solids and solutions for a combustion environment with high levels of sulphur, chlorine and potassium. For the calculations pure gases and pure solids, as well as solution phases where ash melts and slags are

included were considered. For the solution phases the following base-phases were applied FToxid-SLAGA, FTSalt-B1, FTsalt-oP28D, FTsalt-hP22, FTsalt-hP14 in accordance with previous studies by [57, 58]. For the first round of calculations somewhat simplified initial conditions of 1400°C and 1 bar were used to symbolize the combustion environment.

For the next round of calculations the remaining gas phase was recycled whilst any solid and solution phases formed in the first calculations could be removed. The solids and solutions from the first calculations contain the bottom ash and any slag that formed early on and would not transfer over towards the superheaters. The gas phases could then go through the same calculations like before with the same packages and with the same selection of solution phases. This time however the final conditions for the calculation should match the first temperature estimations. Any solution and solid phase material from this step should now symbolize material that condense onto or around the superheater packages.

## Fuel mixes

Furthermore, in the case of direct/indirect cofiring where the fuels are implemented in the same unit the properties of the resulting fuel mixture had to be estimated. Properties such as fluegas flow, fuel requirements, impact on emissions and heating value could be estimated from the fractions of each fuel in the mixture. The resulting mixture could then be put through the method described previously and illustrated in Table 4.11 to estimate which steam temperatures could be plausible if operating on the fuel mixture. Three fuel mixtures were tried in this step to illustrate the effects of mixing fuels to improve the S/Cl ratio, these are shown below:

- 86,50% MSW + 13,50% G. Pellet
- 88,85% MSW + 11,15% MSS
- 75,35% MSW + 13,50% G. Pellet + 11,15% MSS

The ratios were of MSS to MSW were chosen according to a recent inquiry from Uddevalla to implement MSS to their combustion, whilst the addition of pellets was chosen to raise the heating value up to a level where it could be used with different degrees of dried sewage sludge. Adding pellets should, reduce the moisture content by diluting the fuel with a dry component and raise the heating value of the fuel. It would however not implement any additional sulphur. The second mixture, adding MSS can be done in a few different ways since it first has to be dried. Then depending on the moisture content of the added MSS one can expect different results. Fully dried (5-10% moisture content) sewage sludge would have similar effects as the pellets, but also introduce large amounts of added extra sulphur. The third mixture, with both pellets and MSS further reduces the moisture content of the fuel mixture and includes the added sulphur.



# 5

## Results and Discussion

### 5.1 Data collection - Lillesjöverket

In this section the results from the measurement campaign at *Lillesjöverket* is presented and their respective significance and value are discussed. The data is then evaluated and compared to internal continuous data collection during the same time span and to long term data provided by Uddevalla Energi from their process measurements in *Lillesjö* in subsection 5.1.3.1.

#### 5.1.1 Deposition Rate

The deposition rate measurements were conducted on floor 8, where the superheater and economizer tube-packages are situated. These areas are where the deposition and HTC problems occur most noticeably and especially at the superheaters. Thus ports B1 and B1S, on the opposite side of the boiler, were chosen for the measurements. The results of these are tabulated in Table 5.1,

Ring #	Time inserted [min]	Added weight [mg]	Deposition Area [cm <sup>2</sup> ]	Deposition/area [mg cm <sup>-2</sup> ]
UKAB-1	60	202.7	20.9	9.7
CTH-1	60	36.5	17.9	2.1
CTH-2	60	25.0	17.9	1.4
CTH-3	60	28.9	17.8	1.6
CTH-4	345	121.4	17.9	6.8

**Table 5.1:** Deposition rate measurements, in time inserted ( $t$ ), added weight of depositions ( $m_d$ ), the deposition area ( $A_d$ ) and the amount of deposition per area

Comparing the measurements from CTH-1 performed in port B1 to the measurements of CTH-2 and CTH-3 performed in B1S, it can be seen that there may be a difference in deposition rates in the horizontal plane of the boiler. These deposition rates are presented graphically in Table 4.9, and by averaging the measurements conducted for CTH-1,2,3 a deposition rate of approximately  $0.028\text{mg cm}^{-2} \text{min}^{-1}$  is found. Comparing this to the measurement collected on CTH-4 where a deposition rate of  $0.0197\text{mg cm}^{-2} \text{min}^{-1}$  it is clear that the speed of deposition wanes over time. As proposed in section 2.3 the first particles that condense onto the tubes are aided by thermophoresis as there is a big temperature difference between the gaseous phase and the tubes. These initial particles form the interior sticky and

hard layer. However, as more and more particles amass on the tubes heat transfer starts becoming impeded, leaving the surface with a higher temperature. This combined with available sticky surfaces being covered up leads to further condensation to create a porous crust that over time lessens the opportunity for new material to adhere to the tubes.

### Deposition rate measurements

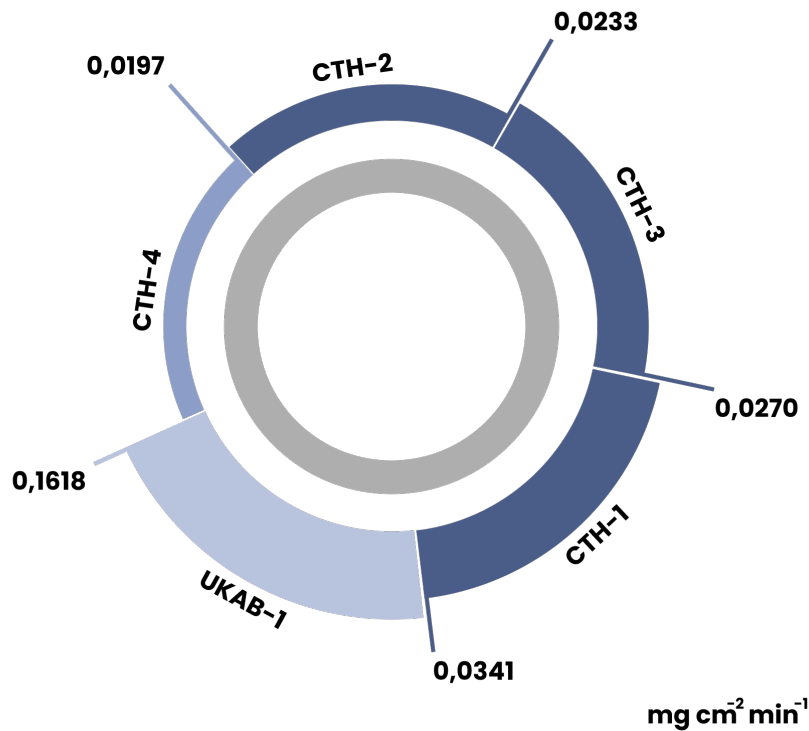


**Figure 5.1:** Graphical representation of the deposition rates,  $R_D$  measured.

In Figure 5.1 the thickness of each colored piece represents the deposition rate,  $R_D$ . The dark blue measurements, CTH-1,2,3 are the Chalmers rings inserted for 60 minutes, the light blue measurement with UKAB-1 was provided by Uddevalla and also inserted for 60 minutes in tandem with ring CTH-1, and the last measurement with ring CTH-4 was a Chalmers ring inserted for 345 minutes.

Another important finding is the difference between the deposition per area between rings UKAB-1 and CTH-1, which were inserted together. Here we see that the material choice drastically impacted the deposition rates, and since the material of UKAB-1 most resembles the material used for the pipes inside the boiler there is certainly a much higher deposition rate inside the furnace than the rings CTH-1,2,3 describe.

For future studies into the deposition rate more measurements at 120, 180, 240 and 300 minutes would be of interest to study the time dependency, but for the scope

of this thesis the measurements conducted is deemed sufficient as it gives a brief insight into the internal environment.

### 5.1.2 Temperature

From the temperature measurements conducted at the *Lillesjö* plant, insight was given into the temperature development at the evaporation stages A1-A3 and the conditioning steps B1-B3 which can be seen in Figure 5.2. The temperature before the ESP was not taken as the measurements taken on our behalf fit well with their sensors and deemed unnecessary.

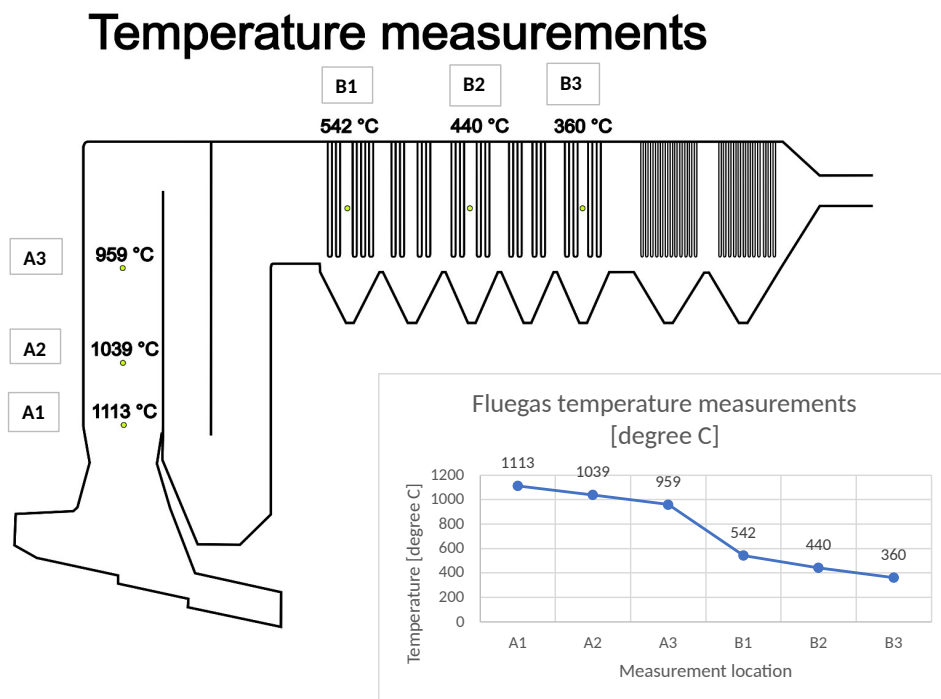


**Figure 5.2:** Temperatures measurements from floor 5 through floor 8.

For future temperature measurements to provide a better view into the temperature conditions inside the boiler more locations should be regarded for measurements. Obtaining measurements in the first, second and third pass of the evaporation section as well as the economizer sections would be of interest to obtain a broader picture into how the temperature is absorbed. Moreover to conduct measurements in both the left, right and centre ports at floor 5 through 7 (A1-A3) would help provide an insight into whether the temperature is distributed evenly on the horizontal plane and potentially identify if there are zones more prone to CO, NO<sub>x</sub> or SO<sub>x</sub> formation. Such measurements could open up discussion on the combustion region and the potential to oversee the different zones where primary and secondary air is added to reduce emissions early on.

### 5.1.3 Gas Composition

A total of 24 measurements were taken of the gas composition in various locations and for varying intervals of time. Presented in Table 5.2 is the order the order of the gas composition measurements of the four days the measurements were performed as well as the averages of each of the interesting species measured. Also included is the average boiler load during the duration of the measurement.

	Port	NO2 [ppm .w]	CO [ppm .w]	H2O [%]	HCl [ppm .w]	SO2 [ppm .w]	O2 [% .d]	CO2 [% .w]	Load [%]
Day 1	B1	170,4	8,6	19,6	286,2	287,7	5,9	10,1	93,9
	B2	194,1	8,5	15,0	57,8	238,9	6,0	10,8	97,1
	B2	171,2	9,3	20,6	438,8	226,9	5,8	10,0	94,9
	B3	169,7	11,4	20,8	429,6	180,6	5,8	10,1	95,1
	B3	179,6	10,0	19,6	417,4	222,2	6,2	9,5	96,0
	B2	172,2	8,5	22,0	458,9	202,9	-	9,8	97,3
	B1	180,4	8,1	19,6	515,1	224,7	5,6	10,3	97,0
	A3	184,0	3,2	20,2	649,1	269,0	5,9	10,6	98,3
Day 2	B1	188,0	8,5	19,3	528,8	169,3	5,8	10,2	95,5
	A1*	197,2	579,9	18,7	1000,4	221,2	5,4	10,6	101,0
Day 3	A1*	172,5	39,9	20,5	611,5	247,2	3,9	10,3	99,3
	A1*	209,4	185,1	20,0	677,1	233,3	3,5	10,3	97,8
	A2	158,6	4,2	19,7	831,1	197,5	5,3	9,6	88,0
Day 4	B1	167,0	8,2	21,0	671,3	226,5	4,9	9,9	88,4
	B2	170,1	8,2	19,6	310,6	212,0	5,6	9,7	91,6
	B1	187,1	7,1	22,0	582,9	222,7	4,3	10,2	96,0
	B1	139,8	9,8	20,4	609,0	210,7	4,3	9,5	91,7
	B2	158,8	9,2	22,5	571,1	191,8	4,3	10,0	94,7
	B1	154,3	7,8	22,7	636,5	211,8	3,7	10,3	95,5
	B2	153,4	10,7	22,4	652,8	232,9	3,9	10,1	101,6
	B3	159,0	10,2	21,4	614,2	244,7	4,1	10,2	100,9
	B3	151,3	10,1	21,4	626,2	249,3	4,3	10,0	101,3
	BESP‡	145,5	9,2	19,1	565,6	196,1	6,8	8,8	102,5
	BESP‡	136,1	8,7	19,0	436,1	177,9	7,3	8,6	96,6

**Table 5.2:** Averaged volumetric concentrations of each respective species for each measurement ordered in the sequence they were performed. (.w) measured on a wet basis, (.d) measured on a dry basis. (‡) due to larger diameter of measuring port air diluted the sample, recalculated values available in Table B.2. (\*) due to pressure fluctuations close to the boundary layer of where combustion ends, short bursts with increased levels of unburnt airborne material drive up the averages.

From the values presented in Table 5.2 and Table B.2 some variations through out the boiler, both in location but also in time are noticeable. One aspect of this is the variability in the fuel that is being combusted. At any given moment the fuel, in this case MSW, consisting of industrial and household waste being introduced to

the boiler may contain larger fractions of either component. The ratio of these can change over the day depending on deliveries, and is also dependent on the speed of the claws that mix and deliver the fuel from the bunker the hoppers that feed it to the boiler. It is also important to remember that both of these fuels enter as inhomogeneous fractions of many components such as plastics, textiles and cardboard, which makes this even more palpable. Moreover, the industrial and household parts of the fuel mix contain slightly different levels of e.g. chlorine and moisture which may explain why the averages may fluctuate noticeably even between measurements conducted in the same ports. An example of this is the four measurements conducted in port B1 during the fourth day of measurements, here the time between each individual measurement is relatively short, but the averages may differ by 10 or more percent.

Trends between ports noticeable from the measurements are shown graphically in Figure 5.3, where the reduced level of  $HCl$  and  $NO_2$  are the most noticeable. The increase in  $O_2$  concentrations also visible here, where the ESP is much higher than the rest due to the air contamination. The initial levels of  $HCl$  measured at A1 average close to 650ppm, and from the graph it can be seen that the levels of gaseous  $HCl$  decrease as the fluegases move further through the boiler, and especially when it reaches ports B1 and B2 where the chlorine is expected to condense onto surfaces. The concentrations of  $NO_2$  also show a similar decrease from 240 ppm averaged at A1 to approximately 0.85% of its original value when it reaches the ESP.

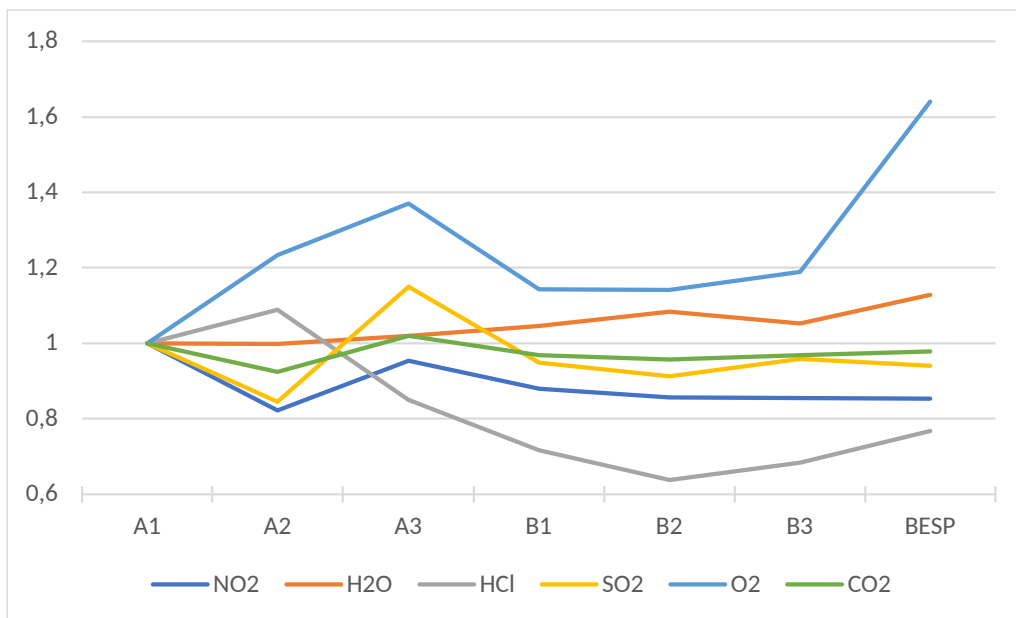


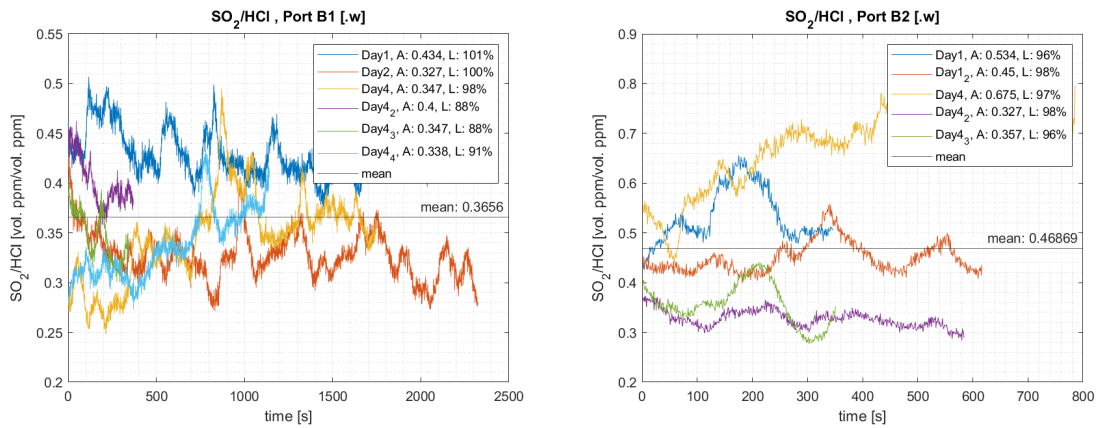
**Figure 5.3:** Changes in average gas concentration between ports, normalized for measurements conducted in ports A1.

The  $CO_2$  and  $SO_2$  concentrations remain quite constant whilst a small increase is seen in the vapour fraction. The  $CO$  concentrations, not shown in Figure 5.3, but presented in Table 5.2, had a large peak when measuring at port A1 which quickly

fell down to stable values at ports A2 and onward. This could be explained as fractions not yet fully combusted since the port of A1 was right next to the end of the combustion area.

Moreover, alongside the alkali metals present in the fly ashes the HCl and SO<sub>2</sub> are assumed react and form chlorides or sulphates respectively, which may condense onto the tubes and should account for the drop seen in fluegas concentrations. From the sulphation of KCl a decrease in SO<sub>2</sub> concentrations should be seen alongside an increase in Cl concentrations, measured as HCl, which may be why the HCl concentrations show an increase between ports B2 and the ESP port.

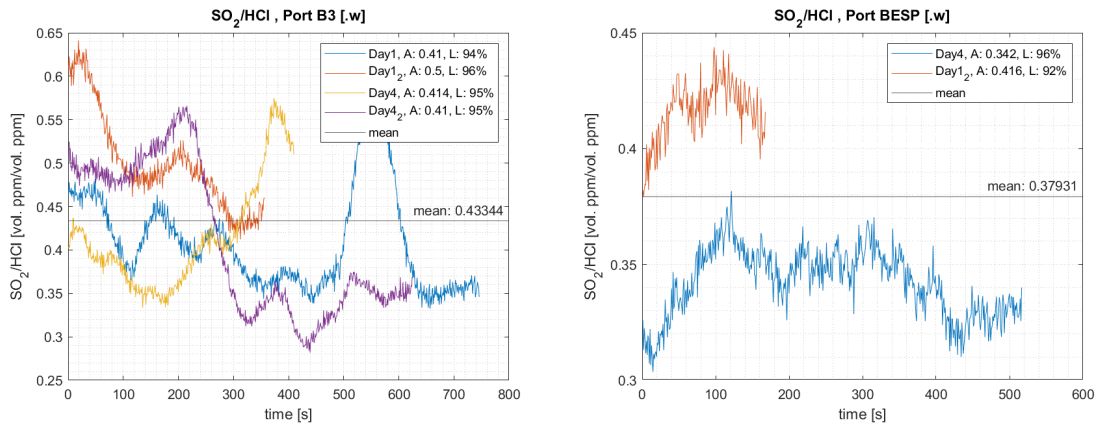
As introduced in section 2.3 ratios of SO<sub>2</sub> to HCl above 2 and especially above 4 would mean that there are opportunities to alter the steam data but as could quickly be seen from Table 5.2, during most measurements the ratio is less than 0.5 and sometimes as low as 0.2 indicating that the boiler is already operating at corrosive conditions and that increases in the steam data could further worsen the HTC and deposition problems related to this ratio. This ratio is also seen in Figure 5.4 and Figure 5.5 where the SO<sub>2</sub> to HCl ratio has been plotted for the measurements taken in ports B1, B2, B3 and BESP respectively. In Figure 5.4a it can be seen that the averages may vary depending on the day the measurement was taken, but the overall average between the ports land around a ratio of 0.36-0.47 S/Cl. It can be seen that there are a few peaks that span 50-100 seconds where the ratios may reach 0.6-0.8. However these events are too short to be able to adjust the temperatures along with the variations in S/Cl accurately. Had they been peaks that spanned 15-60 minutes or longer there would be a potential to track the conditions and regulate ever so slightly, and if spanning hours or days process engineers and operating technicians would perhaps be able to cram out a few extra megawatts each week through the increased steam data. As a complement to the S/Cl ratios found during the measurement campaign more values over a longer time are examined in subsection 5.1.3.1.



(a) port B1 - average 0.366

(b) port B2 - average 0.469

**Figure 5.4:** Relation between  $SO_2/HCl$  in ports B1, B2. Each figure shows the mean ratio for each respective measurement denoted with  $A$  and the boiler load during the duration of the measurement,  $L$ , as well as the overall mean ratio for all measurements in each respective port.



(a) port B3 - average 0.433

(b) port BESP - average 0.379

**Figure 5.5:** Relation between  $SO_2/HCl$  in ports B3 and BESP. Each figure shows the mean ratio for each respective measurement denoted with  $A$  and the boiler load during the duration of the measurement,  $L$ , as well as the overall mean ratio for all measurements in each respective port.

### 5.1.3.1 Comparison to process data

With continued improvements to household recycling the MSW is a fuel that varies over time in its average composition. This is a trend that must be very evident for waste incineration CHP plants as they continuously have to adapt to the fuel they input. Seen from Figure 5.6 the ratio of  $SO_2$  to  $HCl$  has been increasing somewhat steadily over the last four years at the reference plant. As pointed out in subsection 5.1.3 the ratios still are not close to levels that would be needed to increase the steam data, but if the trend continues upwards or with the addition of sulphur

additives or co-combustion with sulphur rich fuels to boost the ratio somewhat it could perhaps be possible to raise the temperature in the future. However, Figure 5.6 also show the day to day swings in the ratio of S/Cl. Even if the average might have been raised slightly over the last couple of years, there are still many days where the ratios are well below 0.5.

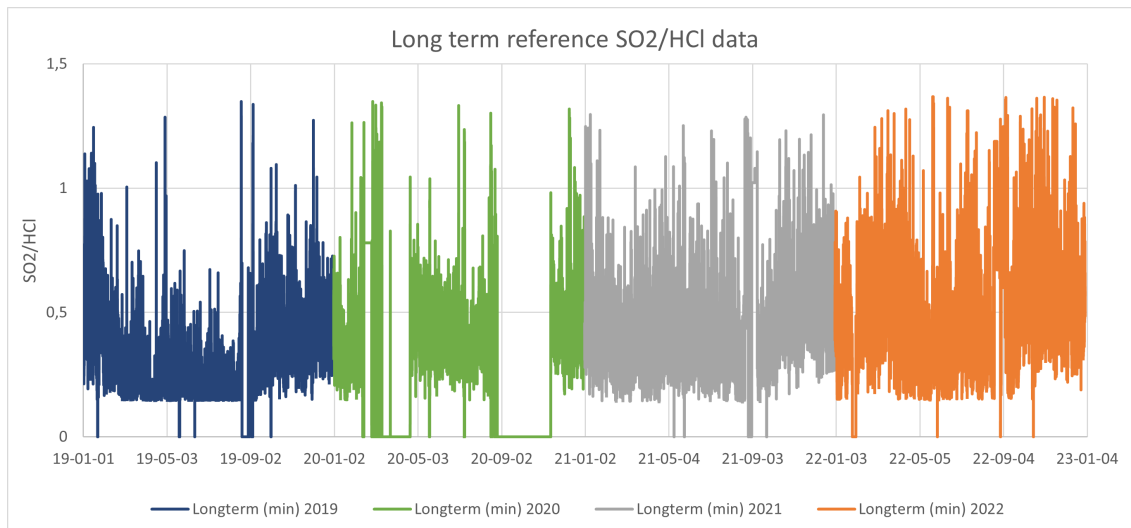


**Figure 5.6:** Ratio of SO<sub>2</sub> to HCl from continuous measurements 2019-2022

From the gas composition measurements many measurements line up nicely such as Figure 5.7a and Figure 5.7d which was the general trend for certain of the species measured. However, for other components such as HCl and H<sub>2</sub>O the experimental measurements often showed higher concentrations than that of the continuous on-site measurements. This becomes even more clear when looking at Table 5.3

Seen in Table 5.3 when measuring the gases CO<sub>2</sub>, HCl, H<sub>2</sub>O, and SO<sub>2</sub> were on average less than 20% greater than their reference counterparts. In the O<sub>2</sub> and CO measurements however the trend was the opposite and we measured lower values than what they found. In respects to combustion it is would be preferable to have lower amounts of CO since the combustion would be seen as more complete. The difference in measurements in O<sub>2</sub> could possibly be explained by the increase in the other components. Us measuring less available oxygen in their system but larger amounts of oxidized components could potentially point towards a more oxidizing environment than the on-site sensors portray.

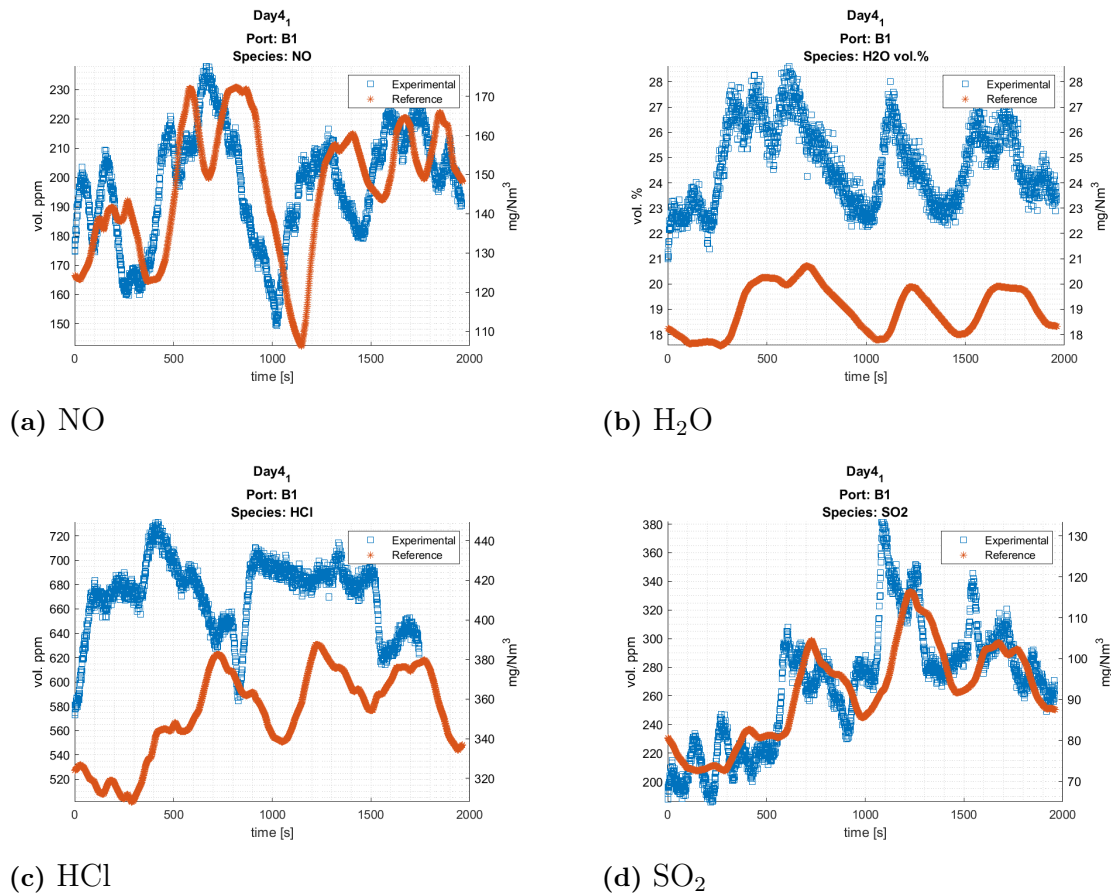


**Figure 5.7:** Compilation of experimental measurements compared with reference measurements from the same time period in vol % and mg/Nm<sup>3</sup>

	NO <sub>2</sub>	CO	H <sub>2</sub> O	HCl	SO <sub>2</sub>	O <sub>2</sub>	CO <sub>2</sub>
Difference [%]	6.7	-41.5	12.4	6.4	18.7	-22.1	10.4

**Table 5.3:** Summary of percentage difference between experimentally measured (CTH) values and reference values (UKAB) in gas composition

### 5.1.4 Aerosols

Two DLPI measurements were done on floor 8 in ports B1 and B1S for a period of 15 minutes. From the two DLPI aerosol measurements conducted Figure 5.8 and Figure 5.9 could be constructed to show the particle size distribution. From these figures it is clear that distribution is centered around stage 6 of the DLPI, corresponding to a mean particle size of  $0.4\mu\text{m}$ .

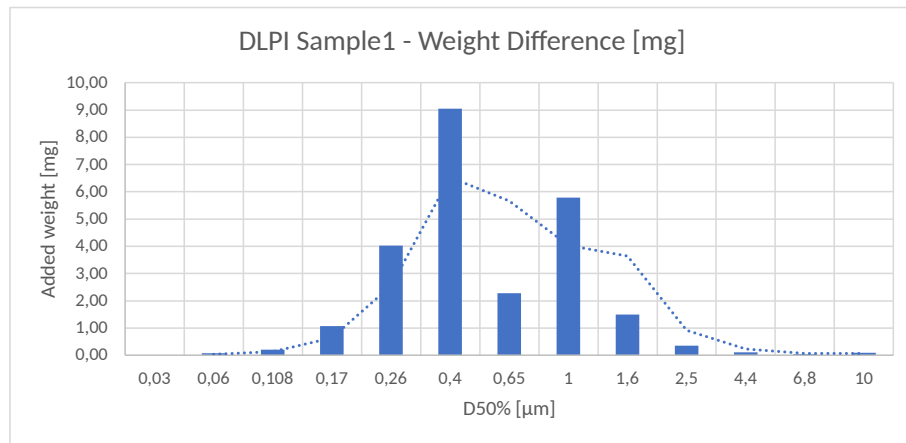


**Figure 5.8:** Trend of particle distribution from first DLPI measurement at port B1 on floor 8.

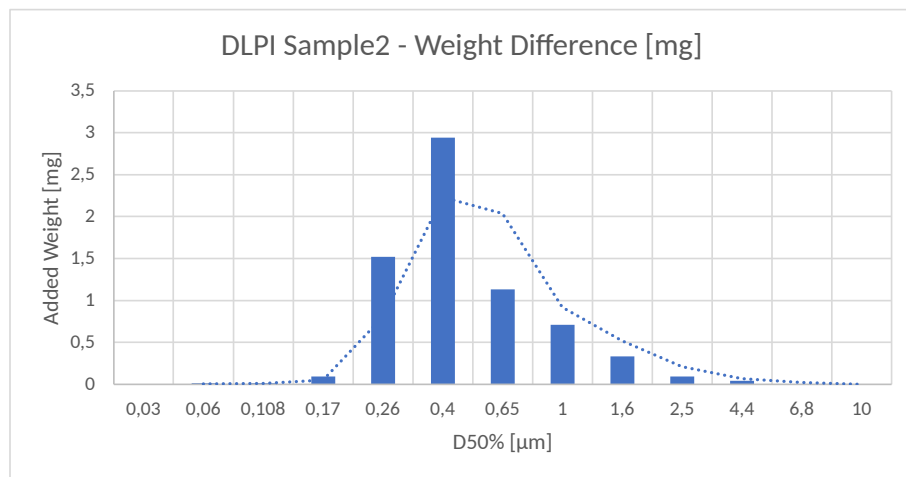


**Figure 5.9:** Trend of particle distribution from second DLPI measurement at port B1S on floor 8.

During the first measurement the DLPI was slightly overfilled with particles which caused some particles to spill over to other steps or get stuck in the ducts when opening the apparatus for weighing (see Figure 5.10). There was an attempt to salvage many of these particles but this may be the reason as for why there is a higher peak at 1 than at 0.65 microns for the first sampling. Besides this discrepancy the trends of the first and second sampling look very similar as there seems to be negligible amounts of particles in stages 1-3 and 11-13 in both measurements and that the rise begins at 0.26 and ends at 1.6 microns.

From the two measurements one can also determine preliminary particle concentrations to  $163,6 \text{ mg}/\text{Nm}^3$  and  $45,8 \text{ mg}/\text{Nm}^3$  at port B1 and B1S respectively. Much like the deposition measurements a trend can be seen here that measurements conducted in position B1S



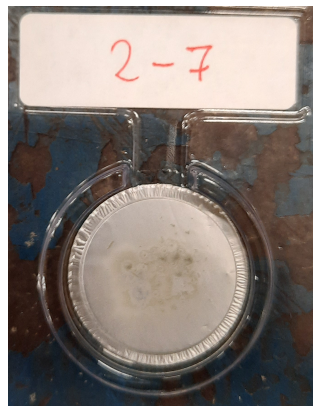
**Figure 5.10:** DLPI component showing excess material spilled over from measurements



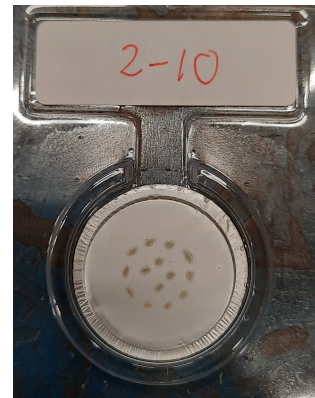
(a) Stage 9 -  $1.60\mu\text{m}$



(b) Stage 10 -  $2.50\mu\text{m}$



(c) Stage 11 -  $4.40\mu\text{m}$



(d) Stage 12 -  $6.80\mu\text{m}$

**Figure 5.11:** DLPI aluminum foil pieces from stages 1, 4, 7 and 10.

### 5.1.5 Alkali

From the alkali measurements using the SID setup the results could be divided up into two areas depending on the floor they were measured on: the *evaporating section* from ports A1-A3 and the *conditioning section* on floor 8, ports B1-BESP. Seen from Table 5.4 the average value for the evaporating section is much lower than that of the conditioning section. The evaporating section also has a much greater span in its results where A1 and A3 measured trace amounts of KCl equivalents, whilst A2 had occasional peaks during the measurements driving the value up. The conditioning section however has a smaller spread in values and an average of 22.4ppm. This presence of alkali metals in the system at levels >1 ppm indicates that the corrosive alkali-chloride salts can form and that the ratios of S/Cl in the system becomes even more important for drawing further conclusions.

	A1	A2	A3	Avg	B1	B3	BESP	Avg
KCl <sub>eq</sub> [ppm]	0,5	19,0	0,9	6,8	4,1	38,1	25,1	22,4
KCl <sub>eq</sub> [mg/Nm <sup>3</sup> ]	1,7	63,4	3,0	22,7	13,7	126,8	83,5	74,7

**Table 5.4:** Results from SID measurements in ppm and mg/Nm<sup>3</sup>, averages for ports A1-A3 and B1-BESP also included.

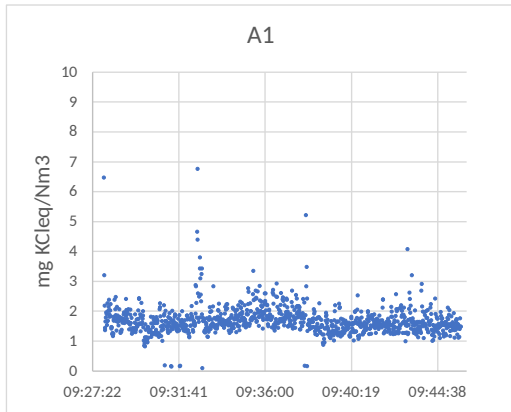
Seen from Figure 5.12 measurements were stable during measurements in port B3 and by the ESP as well as on A1. However, during measurements in A2 (Figure 5.12b) there were noticeable pressure fluctuations which may have influenced the measurement. A3 (Figure 5.12c) also shows a peak but much smaller in nature than on the floor below which resulted in a low average.

A note to be made of the the SID instrument used is that it detects K in forms of KOH, KCl, K<sub>2</sub>SO<sub>4</sub>, and KNO<sub>3</sub>, which all have different signal strengths but gives an output as KCl equivalents. This implies that part of what was absorbed in peaks may be some of the other components, e.g. KNO<sub>3</sub> which has the biggest signal [55]. Thus, as a complement to the measurements an approximation of the theoretical maximum of KCl was made. By combining fly ash analyses from Lillesjö to identify the fraction of K in the ashes, with that of particle count measurements a span of 5-150ppm KCl was approximated. Which if applied to measurement points B1, B3, and BESP seem reasonable, since much of the potential KCl may also be found in the forms such as KOH or K<sub>2</sub>SO<sub>4</sub>. Thus an approximate concentration of 22.4ppm in the conditioning section is plausible, although more measurements with e.g. an in-situ chloride-alkali monitor, IACM, would help to fully determine the levels in both sections of the boiler.

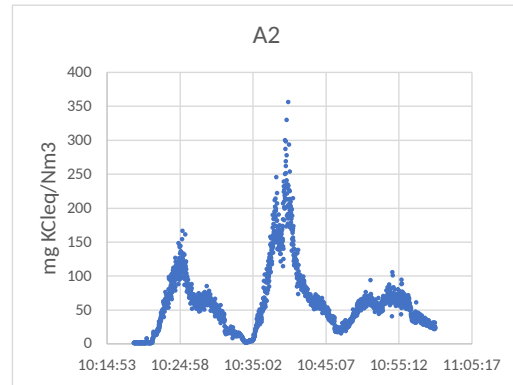
With a value on the K present in the system, represented by KCl<sub>eq</sub>, an approximation of the sulphation could be made with the following equation according to the work of [22].

$$\frac{2n_{K_2SO_4}}{n_{K_{tot}}} \approx \text{degree of sulphation} \quad (5.1)$$

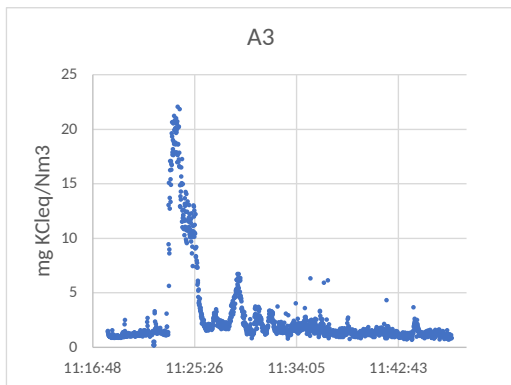
However, since no further studies into the composition of the deposition material or aerosols were conducted, the amount of  $K_2SO_4$  remains unknown. Although, the ratio of S/Cl can still be used as a guideline to which level of sulphation may be present.



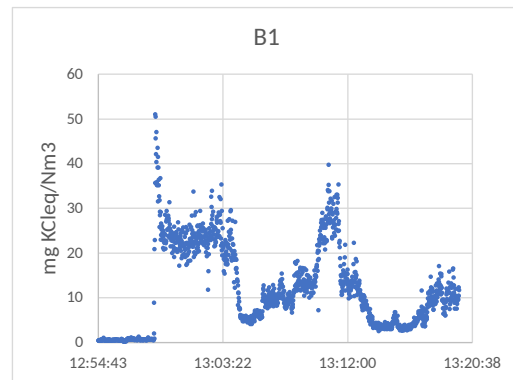
(a) Floor 5 - A1



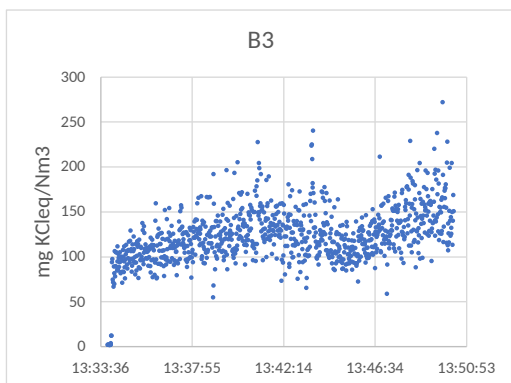
(b) Floor 6 - A2



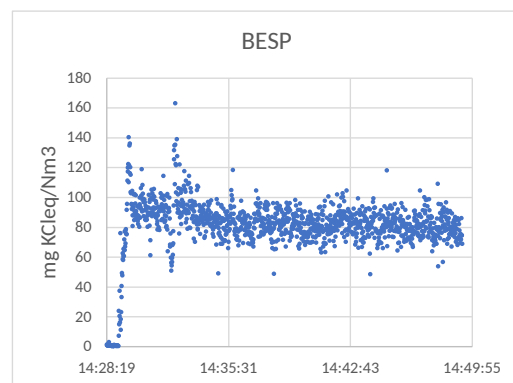
(c) Floor 7 - A3



(d) Floor 8 - B1



(e) Floor 8 - B3



(f) Floor 8 - BESP

**Figure 5.12:** Compilation of SID measurement signal for  $KCl_{eq}$  from floors 5-8

### 5.1.6 Comparison to other MSW plants

From the results found through the experimental campaign in section 5.1 and comparing them to internal measurements from the same period the deviations were small and as such was the case their long term measurements were used for further statistics.

One such statistic, to be able to put the results of this thesis in perspective of other waste plants, was to compare it to the *Best Available Technologies* draft of what is common for MSW plants in regards to flue-gases [62]. Seen from Table 5.5 the fluegases of MSW plants varies quite substantially, partly due to the varying composition of MSW between locations.

Components	Units	Incineration plants for MSW	
		BAT reference	<i>Lillesjö</i>
Dust	mg/Nm <sup>3</sup>	1000-5000	1920
Carbon Monoxide	mg/Nm <sup>3</sup>	5-50	10.6
Inorganic chlorine compounds (as HCl)	mg/Nm <sup>3</sup>	500-2000	580
Sulphur compounds, counted as SO <sub>2</sub>	mg/Nm <sup>3</sup>	200-1000	390
Nitrogen oxides, counted as NO <sub>2</sub>	mg/Nm <sup>3</sup>	150-500	150
CO <sub>2</sub>	%	5-10	6.4
Water steam (H <sub>2</sub> O)	%	10-20	12.8

**Table 5.5:** Overview and comparison of Waste incineration plants from BAT [62] outlying typical parameters common for MSW plants with an 11% O<sub>2</sub> reference value and that of *Lillesjö* recalculated to the same oxygen content.

Compared to these statistics the reference plant, *Lillesjö*, lies somewhere among the lower percentile, making it a good reference for what would be expected elsewhere for most other plants with similar operating conditions. However, for plants which operate at the upper limits or with drastically different ratios of S to Cl the uncertainties may be higher.

As the average S/Cl ratios found in subsection 5.1.3 lay stable at 0.4-0.6, seen in Figure 5.6 and as can be seen from Table 5.5 most MSW plants lie at 0.4-0.5 the plant can be regarded as typical in terms of S/Cl ratios. Moreover, as described by Table 5.5 the best possible ratio would be 1000mg/Nm<sup>3</sup> SO<sub>2</sub> to 500mg/Nm<sup>3</sup> HCl, a ratio S/Cl of 2, which is still rather low for the purposes of increasing steam data. This shows quite clearly that in the typical MSW plant the chances for increasing steam data on the basis of S/Cl ratios are slim without the addition of sulphur additives or the inclusion of sulphur recirculation. Such experiments regarding sulphur recirculation have been conducted at plants such as Måbjerg with very promising results regarding HTC and deposition problems, and thereby also the potential for temperature increases, and by extension, increases to electrical efficiencies [61].

## 5.2 Introductory Modelling cases

This section will present the potential benefits provided by the different modelling cases introduced in section 4.1, as well as a discussion into their respective feasibility and potential for implementation.

### 5.2.1 Base operation cases

As presented in subsection 4.1.1 the base operation cases for summer and winter operation could be distinguished mainly by their usage of the FGC, and whether or not the pellet production and cooling was operational. From the usage of the FGC the amount of amount of liquid left in the fluegases as they exit the chimney change depending on season. Summarized in Table 5.6 is the fluegas compositions as they exit the plant according to the models. The relative ratios of gases remain more or less the same with the exception that the summer model's increased water content pushes down the percentages of the other components.

	N2 [wt.%]	O2 [wt.%]	H2O [wt.%]	CO2 [wt.%]	SO2 [ppm]	HCl [ppm]	NO [ppm]	NO2 [ppm]
Winter	69.0	6.0	6.8	17.0	62	9.6	9.4	1.6
Summer	59.3	5.2	20.0	14.6	53	8.2	8.1	1.4

**Table 5.6:** Fluegas composition post cleaning for Winter and Summer operational cases based on Epsilon models

More interesting aspects with the model is to see how they operate in comparison to the real life plant in terms of parameters such as fuel usage, produced electricity and heat. In Table 5.7 below, a few performance parameters have been summarized along with the efficiencies. At a quick glance the model seems to operate rather differently from the actual plant. However one should remember the simplifications made early on: that the winter model operates using the only the FGC and does not produce pellets nor utilize cooling, whilst the summer model does the opposite. In reality the demand for district heating may fluctuate meaning that the cooling, FGC and pellet unit is typically operated independent of season. Moreover, the plant operators may also choose to bypass the turbine when the demand for heat is high which can heavily influence the ratio of electricity to heat produced over certain periods of time. The model also works using more ideal conditions than would be found in real life with mechanical and thermal energy losses which also contributes to the deviation between actual and model operation parameters.

	$m_{fuel}$ [kg/s]	$m_{DH}$ [kg/s]	$Q_{Fuel}$ [MW]	$Q_{El}$ [MW]	$Q_{DH+P}$ [MW]	$Q_{FGC}$ [MW]	$Q_{Pump}$ [MW]	$\eta$ [-]	$\eta_{el}$ [-]	$\alpha$ [-]
Winter (r)	4.02	167,0	42.2	8.1	36.1	8.8	-	1.059	0.191	0.214
Winter (m)	3.25	125.1	32.3	7.8	27.9	6.8	1.2	1.069	0.205	0.238
Summer (r)	3.74	151.6	41.2	8.8	18.8	0.0	-	0.876	0.214	0.324
Summer (m)	3.17	114.4	32.9	8.5	19.7	0.0	1.3	0.880	0.219	0.366

**Table 5.7:** Results and comparison of base operation modelling (m) in operation parameters and efficiencies with reference values (r) for winter and summer.

Looking on the changes between summer and winter, Table 5.7 shows that the additional heat provided by the fluegas condenser, denoted  $Q_{FGC}$  provides an additional boost to the district heating. As detailed in Table 4.3, the steam is expanded to lower pressures during the summer compared to the winter, allows it extract more energy in the turbine. These two distinctions allow the winter model produce more heat when the demand is at its highest and the summer model to produce more electricity when the demand for heat is at its lowest.

Besides looking at operation parameters, what is of greatest interest for the thesis work is the possibility to increase the performance parameters, and especially the electrical efficiency. Comparatively the models align well with the overall plant efficiency,  $\eta$  in both models. The models are then less accurate in terms of the electrical efficiency,  $\eta_{el}$  and power to heat ratio,  $\alpha$ . However as explained in a previous paragraph there are multiple reasons for these to not align fully, and the most important aspect with the base cases is to create models that represent the plant at the two extremes and perform similarly, such that changes made in the coming cases can be representative and relatable to the real life plant.

## 5.2.2 Temperature-Pressure study

From the temperature-pressure study presented in subsection 4.1.2 the model efficiencies may be seen in Table 5.8 where the impact on the electricity production becomes clear. Here it is seen more clearly between the cases (T+) and (P+) that increasing the pressure is more beneficial when the desire is to increase the electrical efficiency. Moreover a larger set of temperatures and pressures is represented in Figure 5.13 where the increase in pressure and or temperature is plotted against the increase in electrical efficiency.

	$\eta$	$\eta_{el}$	$\alpha$
Winter	1.069	0.205	0.238
Winter (T+)	1.070	0.208	0.242
Winter (T++)	1.070	0.212	0.247
Winter (P-)	1.069	0.199	0.229
Winter (P+)	1.069	0.214	0.251
Winter (TP+)	1.069	0.218	0.255

**Table 5.8:** Results of increasing temperature or pressure on efficiencies

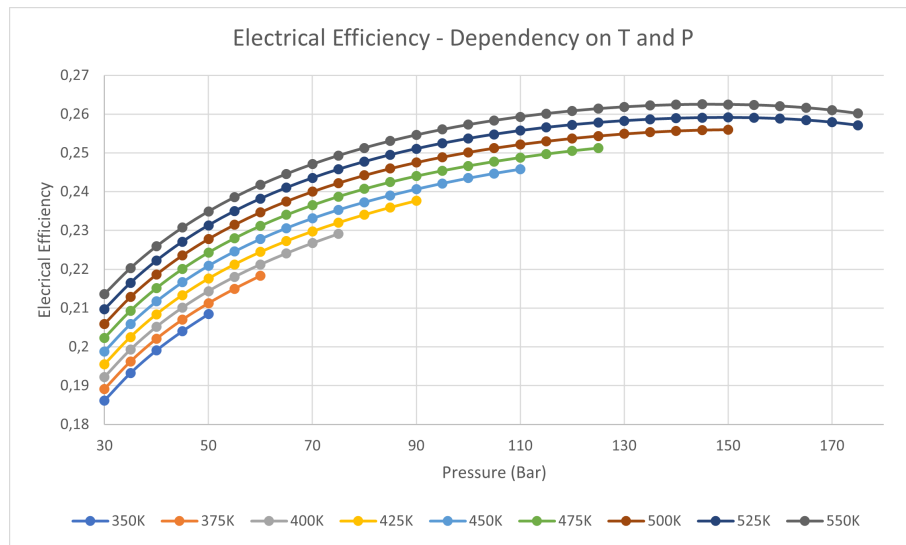


**Figure 5.13:** Plot of electrical efficiencies when altering temperature and pressure in the winter model from 350C and 30bar to 550C and 180bar.

From Table 5.9 and Figure 5.13 it is clearly shown how the pressure and temperature influences the process. A point to be made is that a change in pressure initially has a greater influence on the result than that of changing the temperature which was to be expected as more work can be extracted from the turbine. However, as pressure is increased the steam fraction coming out of the turbine is decreased. Thus if one expands the gas too much without first increasing the enthalpy of the steam, the exiting flow will become too wet. Typical turbines can withstand a certain amount of water droplets in the exiting steam but eventually the turbine blades will start to be damaged due to erosion, and thus reduces the lifetime of the turbine blades [59]. Hence the figure below is based on an exiting steam fraction of 0.85, where some plants may even prefer a higher steam quality of minimum 0.9 or 0.95 exiting the turbine.

From Table 5.9 it can be seen that increasing the temperature and pressures both provide greater relative increases to electricity than they do to the district heating. When both the pressure and temperature are increased, denoted with (TP+), the greatest effect on increasing the electricity production is seen. However, if the operation temperature is restricted by the deposition and HTC rates, as is the case at

*lillesjö*, changes to pressure may be of greater interest.

	$m_{fuel}$ [kg/s]	$m_{DH}$ [kg/s]	$Q_{Fuel}$ [MW]	$Q_{El}$ [MW]	$Q_{DH+P}$ [MW]	$Q_{FGC}$ [MW]	$Q_{Pump}$ [MW]
Winter	3.25	125.1	32.3	7.8	27.9	6.8	1.2
Winter (T+)	3.33	127.2	32.9	8.1	28.4	6.9	1.2
Winter (T++)	3.39	129.2	33.6	8.4	28.8	7.1	1.3
Winter (P-)	3.26	126.4	32.4	7.7	28.2	6.8	1.2
Winter (P+)	3.23	122.7	32.0	8.1	27.3	6.7	1.2
Winter (TP+)	3.30	124.9	32.6	8.3	27.8	6.9	1.2

**Table 5.9:** Influence on operation parameters with changes in T and P.

Again, as presented in section 2.3, changes in temperature may bring problems with corrosion and deposition. For the results presented in Table 5.8 the temperature was raised only by 25 °C as larger changes made to the model could in reality drastically change the HTC and deposition tendencies inside the boiler as presented in section 2.3. Smaller changes in temperature such as 25 or 50 °C may be plausible depending on the internal conditions of a boiler, in section 5.1 those conditions are discussed using data collected from the *Lillesjö* plant. Rather than changing temperature, larger changes in pressure may be simpler to introduce and does not pose the same problems. One such example is brought up when looking into the reheat model in subsection 4.1.3. The results of this is presented and discussed in the next subsection.

### 5.2.3 Case 1 - Addition of Reheat

As seen from the temperature-pressure study an increase in pressure had positive effects on electricity production. Thus, by raising the steam pressure out of the boiler and adding a new high pressure turbine and reheat cycle there is a possibility of extracting more electricity. This approach focuses on increasing the power-to-heat ratio,  $\alpha$ , in the system as this alteration promotes increased electricity generation per unit of energy introduced to the boiler. Whilst keeping the steam production constant it can be seen in Table 5.10 that the implementation of the reheat cycle and turbine increases the fuel requirement by a noticeable amount but that the benefit to electricity production outshines this increase.

	$m_{fuel}$ [kg/s]	$m_{DH}$ [kg/s]	$Q_{Fuel}$ [MW]	$Q_{El}$ [MW]	$Q_{DH}$ [MW]	$Q_{FGC}$ [MW]	$Q_{Pump}$ [MW]
Winter	3.25	125.1	32.3	7.8	27.9	6.8	1.2
Winter + Reheat	3.500	124.3	34.6	10.9	27.7	7.3	1.6

**Table 5.10:** Influence on operation parameters with the addition of a reheat cycle.

The heat available for the district heating remains more or less unchanged when implementing the reheat cycle but the electricity is increased by almost 40 percent

at the cost of a 8 percent increase to fuel usage and 30 percent increase to pumping needs. If looking solely towards increasing the electricity production this is a promising alternative.

Moreover, seen from Table 5.11 the electrical efficiency and power to heat ratios are increased greatly by the increase in steam pressure and the addition of a reheat cycle. One such addition could potentially be added to an existing plant with quite some effort during revision periods or be designed as such from the beginning. However one of the most important aspects of the design is that it would not influence the HTC or deposition tendencies of the plant which makes it a design possible for the reference plant.

	$\eta$	$\eta_{el}$	$\alpha$
Winter	1.069	0.205	0.238
Reheat	1.068	0.268	0.335

**Table 5.11:** Results from the addition of a reheat cycle on efficiencies.

Furthermore, with some more detailed piping and construction the model presented allows for the second ‘top pressure’ turbine to be operated either continuously to or to be bypassed until the demand rises. By operating the extra turbine continuously the overall production of the boiler is increased by a flat amount, but by operating by demand the plant can produce additional energy when the revenues are at their highest rates and also help stabilize the grid by producing extra during hours of peak demand. Remaining in standby is also something sought after by transmission system operators who also compensate such business ventures [60].

## 5.2.4 Case 2 - Impact of fuel variation

To illustrate the impact of fuel choice on the applicable steam data and thereby also the production and efficiencies that can be withdrawn from the winter model a set of fuels were trialed. In Figure 5.14 and Figure 5.15 the impact on production and electrical efficiency are shown. The first column in each figure also shows the base case when operated on MSW. Due to the trialed fuels’ low moisture content there is a reduced usage of the FGC, but thanks to the increased temperature and pressures estimated to be utilizable in subsection 5.3.1 there is a clear increase in the electricity production. The heat available for the district heating network is reduced by an mostly equivalent amount.

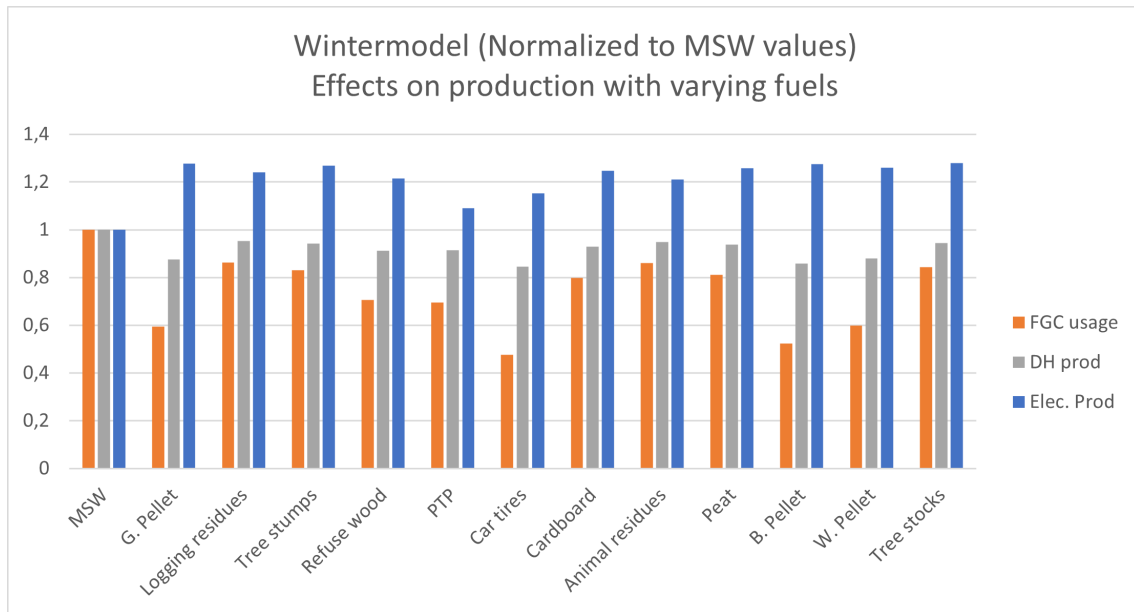


**Figure 5.14:** Effects on the winter model production with varying fuels

In terms of the electrical efficiency plotted in Figure 5.15 one may expect a quite substantial increase depending on the fuel due to the increased steam data. Especially in the wooden products an increase of about 22% of the original value could be expected. For miscellaneous fuels such as PTP and car tires more limited in their steam data more moderate increases can be expected.

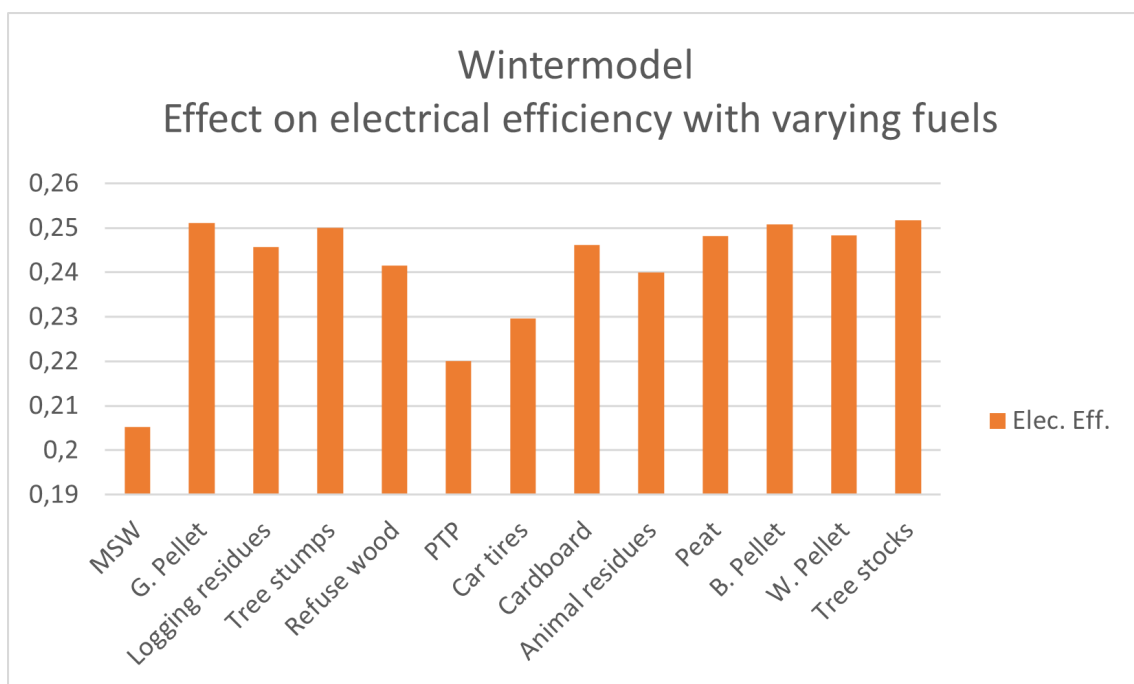


**Figure 5.15:** Effects on the winter model efficiencies with varying fuels

### 5.2.5 Case 3 - Co-combustion with Biomass

The results from the co-combustion models where both co-firing and a top cycle were implemented shown in Figure 5.16 to Figure 5.21. The two models *Indirect* and *Parallel (1)* keep the mass flow of steam in the system constant whilst the model *Parallel (2)* keeps the mass flow of combusted MSW constant. Important to note with these models is the flexibility in the choice of how much steam goes through the reheat and for the case of the parallel models also how much energy is used to heat the steam to the first 400°C. For the results presented below 70% of the steam goes through the high pressure turbine whilst the remaining goes directly towards the ordinary turbine along with the reheat.

#### 5.2.5.1 Indirect co-firing

For the indirect co-firing model there is a substantial increase to the electricity production seen in Figure 5.16 with all of the fuels presented. However, due to their low moisture contents in comparison to MSW a lower effect can be extracted using the FGC. It can be seen that co-firing, even with PTP a fuel very close in composition and applicable steam data, could provide a big boost to the production. The refined fuels such as the generic, white or black pellets show the largest increases due to the high steam temperatures and pressures utilizable.

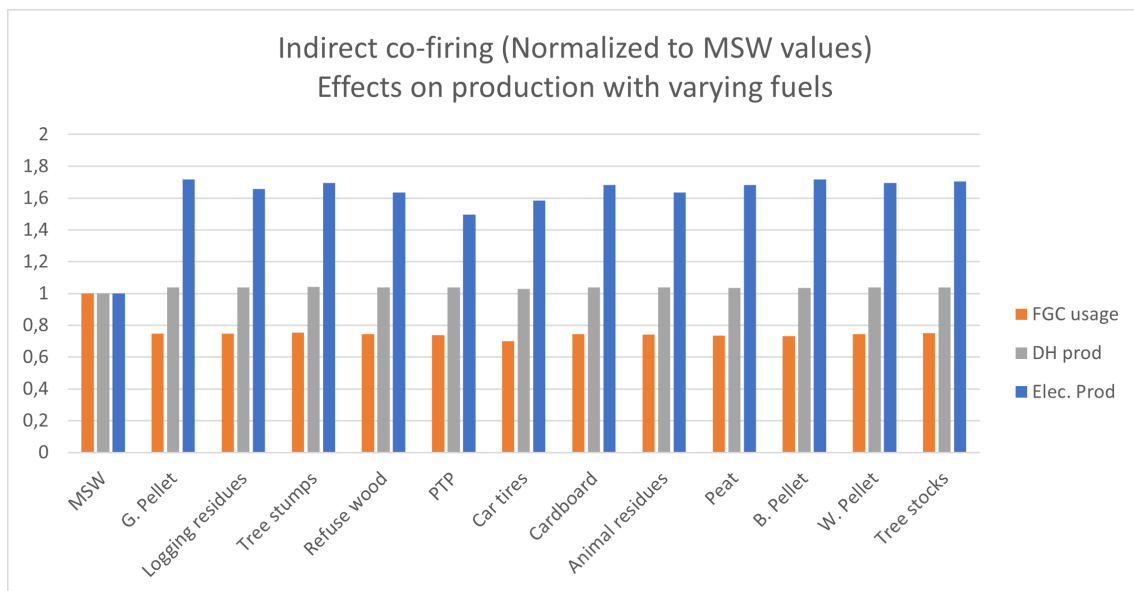


**Figure 5.16:** Effects on the winter model production with varying fuels

The different fuels' impacts specifically on the electrical efficiency seen in Figure 5.17 show the same trends that PTP show the smallest increase, whilst the refined pellets show the largest. All fuels, however, show a substantial increase of 45% or more to the original efficiency.

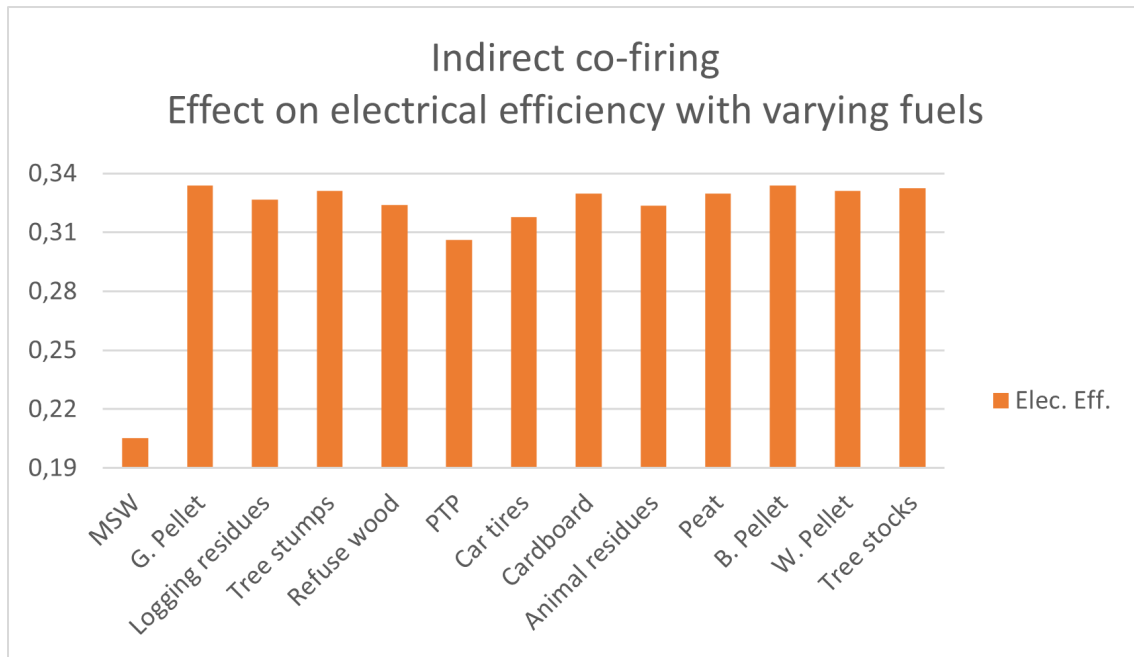


**Figure 5.17:** Effects on the winter model efficiencies with varying fuels

A problem with indirect, and direct co-firing of biomass with MSW is the fact that unless the secondary fuel is rich in sulphur or is able to dilute or capture the chlorine fraction, the previous HTC and deposition problems are still there. And thus, the way the indirect model functions in the present moment an increase in production and efficiency can be seen, but in reality this would also infer an increase in the corrosion and deposition rates that would make it unsustainable. To combat this, a elemental sulphur could be added, or liquids as  $H_2SO_4$  could be sprayed in to increase the S/Cl ratios.

### 5.2.5.2 Parallel co-firing

In the indirect and direct co-firing model the MSW and the supplementary fuel will be present in the same working environment and thus be troublesome in terms of HTC and deposition rates. This problem is avoided in this approach by separating the firing into two parallel units, this way the benefits of the increased steam data can be implemented without the worries connected with temperatures too high for the specified fuel.

Shown in Figure 5.18 the increase in electricity production is increased by atleast 60% whilst the heat production is kept relatively constant. Due to the changed fractions of fuel, the moisture content in the exiting fluegases is lowered and thus a reduced effect can be drawn from the FGC. Looking also at the impact on efficiencies in Figure 5.19 it can be seen that the relative difference between fuels is quite low, but that the changes drive up the electrical efficiencies to approximately 0.32-0.33 compared to the original 0.205. In both Figure 5.18 and Figure 5.19 it can be seen that the Pellets perform the best, this can be traced to section 5.3 where these fuels are estimated to be able to produce the highest temperature steam.

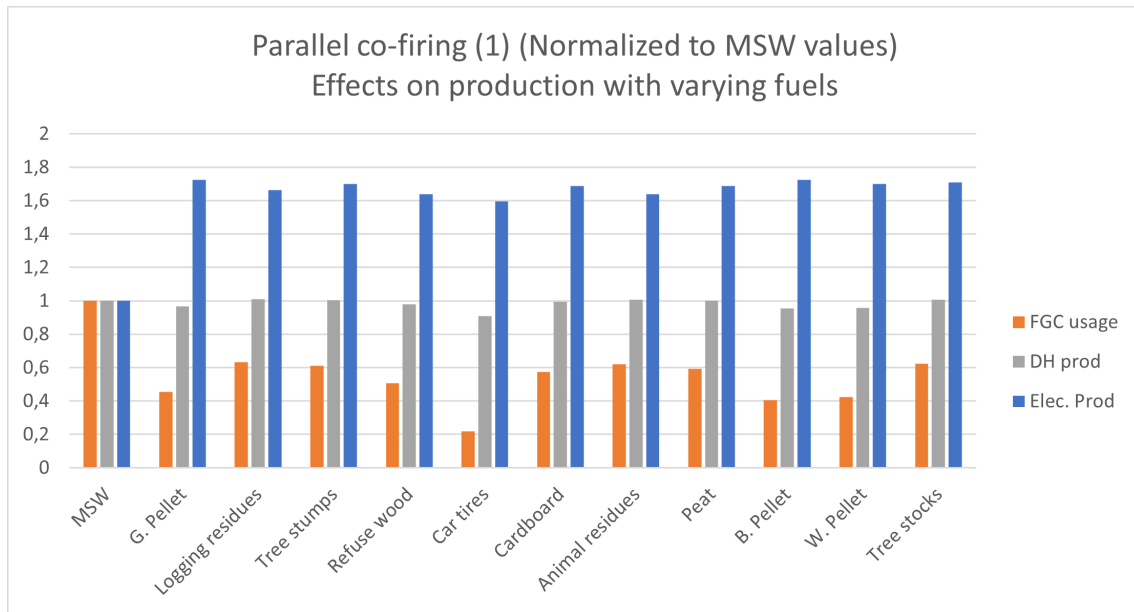


**Figure 5.18:** Effects on the production with varying fuels using parallel co-firing alternative 1

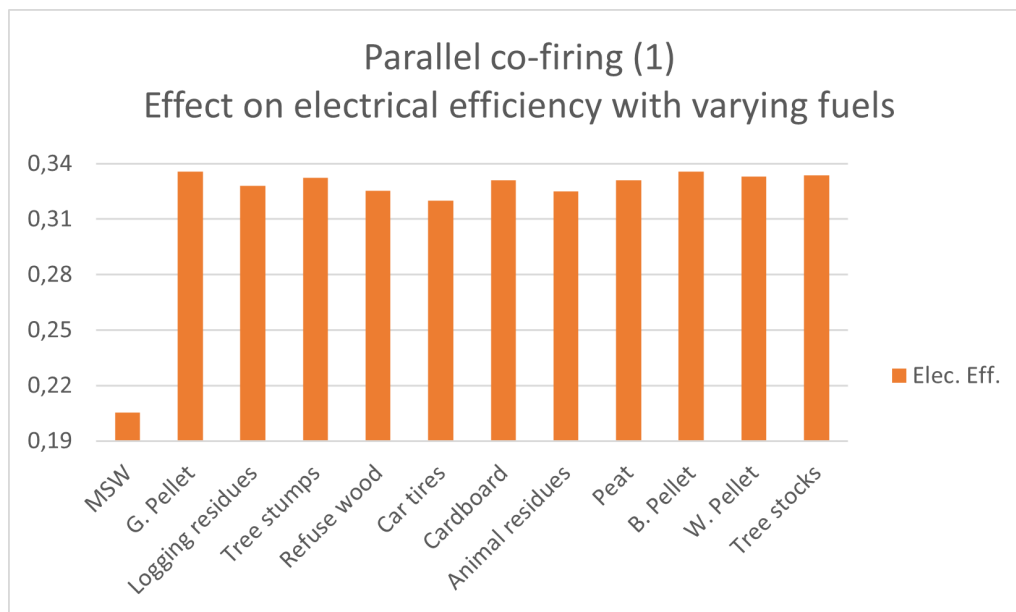


**Figure 5.19:** Effects on the efficiencies with varying fuels using parallel co-firing alternative 1

The second alternative to the parallel co-firing, keeping the intake of MSW constant shows the same trends regarding electrical efficiencies in Figure 5.20. The order of which fuels have the greatest impact on electricity production is however changed in this model. When adding larger fractions, the higher moisture content of logging residues allows the FGC to extract a good amount of extra energy, that the pellets cannot. The efficiencies shown in Figure 5.21 show the same trends, but at the larger scale the efficiencies fall slightly.

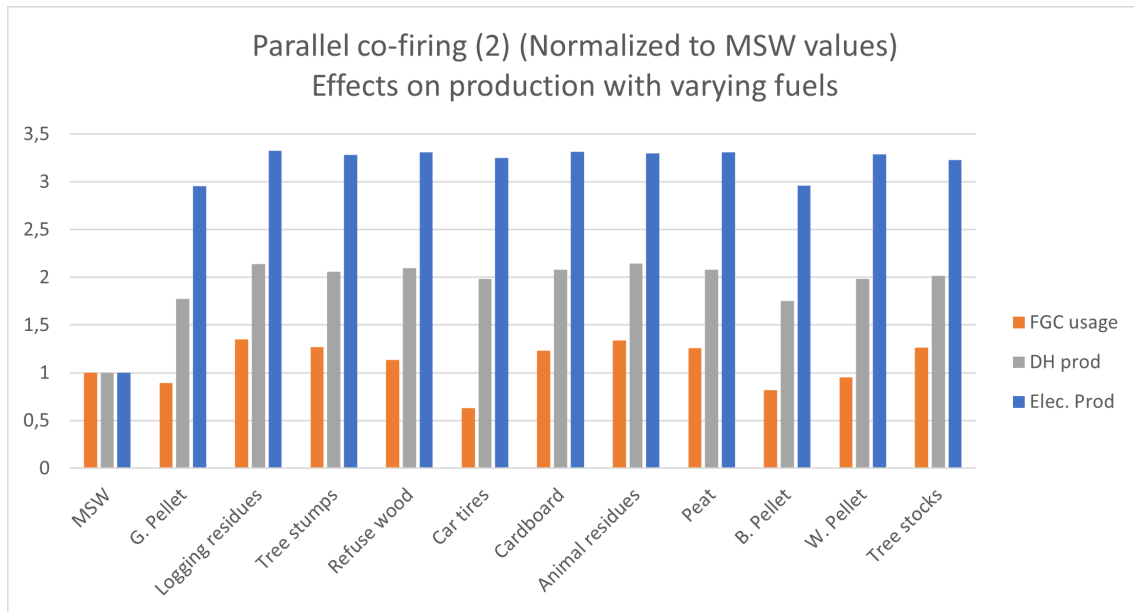


**Figure 5.20:** Effects on the production with varying fuels using parallel co-firing alternative 2

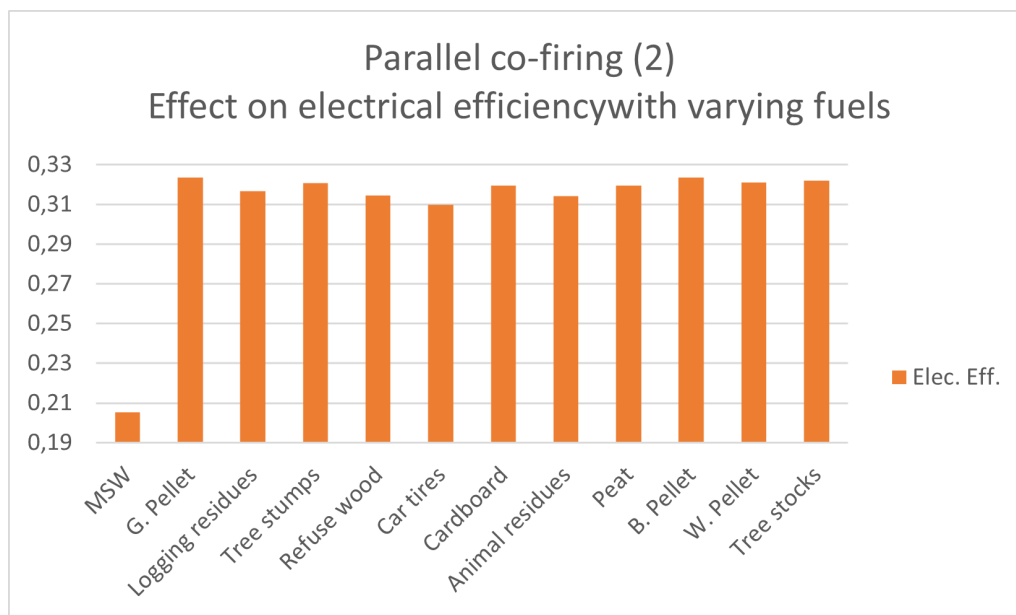


**Figure 5.21:** Effects on the efficiencies with varying fuels using parallel co-firing alternative 2

As could be seen from the results presented, in terms of electrical efficiency the indirect and parallel co-firing were similar, but due to the joint combustion environment in the indirect model the feasibility becomes highly dependent on the sulphur content of the secondary fuel or that of injected additives. Thus in practice only the parallel model could be constructed and run as is, without the need for other or increased need for reagents.

### 5.3 Fuel classification

In this section the results regarding steam temperature estimations and FactSage simulations will be presented, as well as a discussion on the accuracy and reliability of the estimations using ash melts and deposition simulations as a reference on temperature estimates.

#### 5.3.1 Steam temperature estimation

From the temperature estimations, when weighing extra towards the key components S, Cl, K and their reacted components such as  $\text{SO}_2$ ,  $\text{K}_2\text{SO}_4$ ,  $\text{KCl}$  and  $\text{HCl}$ , the following temperatures were estimated to be applicable on the steam data (see Figure 5.22). Indicated in to the left are three potential fuel mixes that could be used in direct co-firing and the their potential increase in steam temperature, whilst to the right there are fuels as combusted individually. As can be seen from the fuel mixtures, adding the MSS which has a high sulphur content has the highest increase. However, due to the method of estimation the fuel mixture is still perceived to be closer to MSW in terms of composition than that of coal and thus yields it a low increase in potential temperature. Compared to combusting pellets by it self in a parallel boiler, the increase in temperature is negligible in the mixtures. However, for direct and indirect co-firing systems these are more like the temperatures one may expect to be able to attain unless more work is done to the S/Cl ratios, whereas the parallel systems may utilize the full increase in temperature in a separate unit.

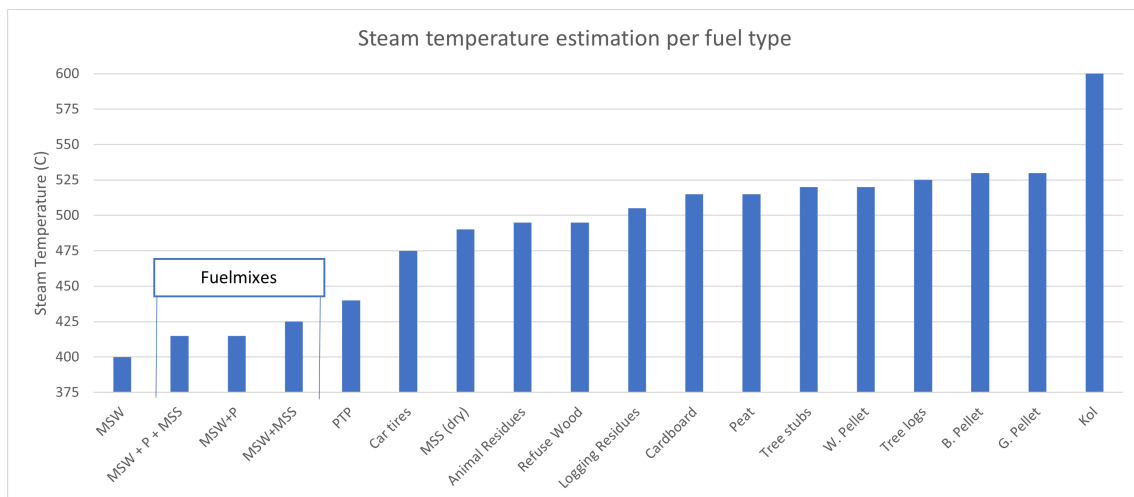
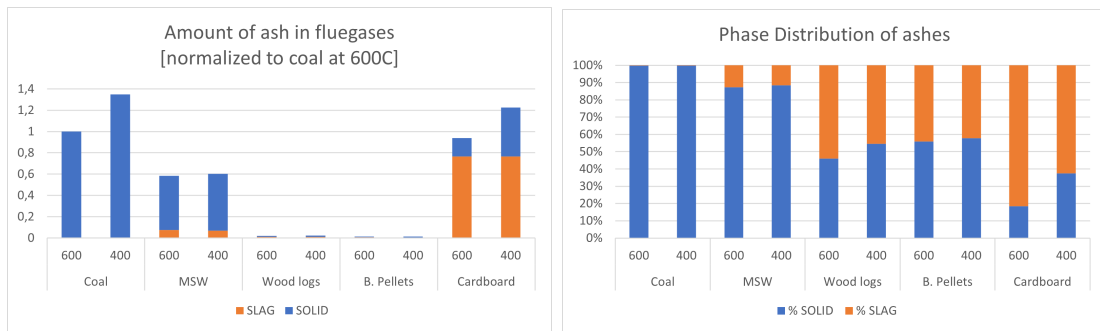


**Figure 5.22:** Estimated temperatures of respective fuels when combusted separately or, if indicated, combusted as an in-going mixture

From the estimations it can be seen that the refined biomass in forms of pellets, be it white, black or the generic types all have properties that would garner the use for high steam temperatures. It is also seen that wood chips from logs or stubs yield high temperatures likewise. On the other side, car tires, PTP and dried MSS yield lower temperatures due to their increase in contaminants and similarities to MSW.

### 5.3.2 FactSage

From the FactSage simulations regarding ash melt fractions Figure 5.23 displays what could be expected in terms of deposition from various fuels. The values have been normalized against the amounts for coal at 600C. As can be seen from Figure 5.23a at equilibrium FactSage expects the ashes to be almost fully solid for coal, whilst MSW, who is typically stickier shows evidence of this as at equilibrium the slag fraction is noticeable. For wood log shavings and torrefied pellets barely any ashes are expected, whilst for cardboard a lot of very slag prominent ash is found. Looking at Figure 5.23b the distribution of solid to slag has been plotted to more clearly show which phase would dominate, and in a sense also how sticky the ashes would be and thereby an indication how much would be deposited.



(a) Ash amounts by fuel type

(b) Phase distribution by fuel type

**Figure 5.23:** FactSage simulations of ash melt tendencies of MSW and Coal as references, to estimate the tendencies of wood logs, pellets and cardboard.

Combining these ashing tendencies with the temperature estimations in Figure 5.22 it may, on the basis of ash chemistry and ashing tendencies, perhaps be possible to further weigh the findings to produce more accurate estimates. From FactSage it can be seen that Pellets have very low ashing tendencies, and could therefore potentially be yielded a higher estimated temperature. Cardboard on the other hand shows a very high ashing tendency with high melt fractions, which shows that although it may be estimated to be able to cope with higher temperatures than MSW, it would potentially be worse in terms of slagging and fouling.

## 5.4 Summary

From the measurement campaign at the *Lillesjö* plant an initial rate of deposition was found (subsection 4.2.1), and the impact of increased time showed that the deposition rate decreases over time. Moreover it was found that there was a decreased tendency for material to stick to the polished rings (CTH) brought to the location, compared to that of the rough outside material used by the tubes on site. The composition of the deposition material was not tested further. The aerosol measurements (subsection 4.2.4) found that the mean particle size of  $0.4 \mu\text{m}$  was most common and a rough estimate on the particle concentration could be drawn. The composition of the aerosols were not tested further either.

The temperature measurements (subsection 4.2.2) conducted were in good agreement with that of their permanent sensors, such was mostly also the case of the gas composition measurements (subsection 4.2.3) conducted and thus it was deemed that alongside our measurements theirs could also be used to draw arguments over longer time periods. Such as that of the S/Cl ratio which over time had increased slightly but had a mean value around 0.5 and large but short variations. Due to this it could be discussed that there were no plausible margins for increasing the steam temperatures based solely on the ratio between these components without some intervention. This could be either through direct sulphur injections, such as elemental sulphur or recirculated sulphuric acid. The SID measurements showed an average concentration of 22.4ppm of alkali in the region around the superheaters, which gave an indication that the alkali-chloride salts would form in the system and a rough estimate to the amount that could potentially form in the system. However, to draw further conclusions regarding the alkali content in the boiler, further measurements with increased accuracy should be performed. These measurements are key in fully being able to determine the need for increased sulphation in the system through the S/Cl ratio, since if there are low levels of alkali in the system to begin with, not a lot of salts will form and the need for sulphation decreases.

From the modelling work other ways of increasing the electrical efficiency were proposed. One such way was discussed in the temperature-pressure study (section 5.2) could be by increasing solely the pressure in the system, which could increase the electrical efficiency somewhat before the steam quality would suffer, and then potentially also the turbine. This was further developed in the first case (subsection 4.1.3) where the introduction of a reheat cycle and top pressure turbine was modelled. In this case an 8 percentage increase in fuel usage predicted an almost 40 percentage increase in electricity production. In such a system the temperatures remained untouched and such there would be no influence on the present HTC or deposition rates, instead only the pressures were increased and by reheating steam expanded first in a high pressure turbine large benefits were seen.

In the following case on the impact of fuel variation (subsection 4.1.4) different fuel alternatives, whom according to the ash and temperature analyses and estimations performed in subsection 5.3.1, could perform at higher temperatures before expe-

riencing similar deposition and HTC problems, were tried out. The study showed that without changes to the existing system there were opportunities to increase the electrical efficiency up to 25% at the cost of some decreased heat for the DH network.

Then combining the work of the temperature-pressure study, the reheat cycle and the impact of fuel variation the third case (subsection 4.1.5) showed how co-combustion of biomass would boost the electricity production and electrical efficiency. In this part of the work, three models were introduced: one indirect co-firing system and two parallel co-firing systems. Both the indirect and parallel models showed great promise in regards to increasing the electrical efficiency, with jumps from 0.205 to as high as 0.338 when utilizing parallel co-firing of pellets alongside MSW.

On the topic of co-firing it was also discussed that indirect or direct co-firing would be possible only with fuels rich in sulphur such MSS or through direct sulphur injections into the system to increase sulphation as to not increase HTC and depositions problems that may caused by heightened temperatures at present S/Cl ratios. For the parallel co-firing system however, this problem is avoided by letting the MSW system work independently of the biomass system. In such a system the original usage and operation could be kept constant for the MSW unit, and the steam temperature could be raised to higher levels in the second, parallel, boiler to increase the electrical efficiency. Furthermore the two boilers could work either in tandem to generate the heat needed for the top cycle and reheat or be provided solely by the parallel boiler, giving the many degrees of freedom in the design and construction of such a plant. Operating with dual boilers could potentially also serve as a safety measure in case of unplanned stops, or to operate only one boiler when one needs to maintenance and such never go to a full stop.

Moreover, from the results presented in section 5.3 on the classification of fuels and estimation of applicable steam temperature per fuel, it was found that through the method of estimation, the three varieties of pellets and wood chips from tree logs could operate at highest temperatures. Alongside the temperature estimations the ash melt tendencies were also examined further in FactSage where it was determined that cardboard, estimated to be able to operate at high temperatures, would yield high levels of melts and thus potentially also depositions. As such the ash melt simulations work as a complement to the temperature estimations to determine if the assumed are potentially valid or if they should be altered.

# 6

## Conclusion

After conducting experiments at the reference plant and by reviewing their long term sensor data it was found that with the present conditions no temperature increases could be made on the basis of available S/Cl margins. Thus a conclusion that could be made for that of MSW incineration plants is that there typically is not expected to be opportunities to increase the steam data drastically based on S/Cl ratios without implementing an inflow of sulphur to the system. This could be done either by sulphur recirculation described in section 2.5, by co-firing with sulphur rich fuels, or by directly inserting sulphur additives.

In terms of modelling work it can be concluded that the two base models constructed can be used to demonstrate the two extremes that *Lillesjö* faces in terms of operation in the Swedish climate, where the winters require as much heat as possible, and summers look for ways to utilize excess heat. The same kind of seasonal demand and constraints could also be expected in other MSW CHP plants, but their strategies towards the issues may be different. Moreover, through further development of the base models alternatives for the design of new plants, or extensive rework of the reference plant were proposed, that would increase the electrical efficiency without influencing the HTC and deposition tendencies. It was concluded in subsection 5.2.3 that by raising pressures and implementing a top cycle with reheat, a raise in the electrical efficiency from 0.205 to 0.268 during the winter months could be expected without changing steam temperatures.

Furthermore, it was concluded in subsection 5.2.5 that by the implementation of a parallel co-firing system, along with a top cycle and reheat, these efficiencies could be raised further to 0.310-0.338 depending on which fuel was utilized in the parallel system. An indirect co-firing system was also investigated, but as the MSW and the secondary fuel would be interacting in the same environment, the high Cl from MSW would still be a trouble unless the secondary fuel was rich in S. Thus it was concluded, that although more complex in its design a parallel co-firing system would be the best fit for MSW incineration plants as both steam pressures and temperatures could be raised, and thereby also the electrical efficiencies, without influencing the original MSW combustion environment and HTC problems.

Moreover, through work conducted with FactSage and fuel- and ash composition a method was proposed in section 4.3 for roughly estimating utilizable steam temperatures per fuels was developed. The method opens up for a quick estimation of fuels that may not have been tested, and by comparing it with simulations of ashing

tendencies from FactSage further arguments could be drawn about the stickiness and thereby potentially also their deposition tendencies could be discussed. These estimations were then used for the biomass case presented in subsection 4.1.4 where it could be seen that solely on the basis of changing fuels an increase in electrical efficiency from 0.205 to 0.25 could be reached. The estimated steam data was also used in producing the results presented in subsection 5.2.5

### 6.1 Future Work

Due to the many ways to approach the issue of increasing the electrical efficiency of a waste CHP plant there are certain approaches that were not included in this thesis. Further work into the areas of fluegas recirculation or sulphur recirculation to increase the available  $\text{SO}_2$  concentration or by the addition of additives such as pure S compounds or sewage sludge rich in S to change the ratio of S/Cl would be of interest to identify if there were options to increase the steam data in plant as it is.

Moreover, further study into the composition of the particle and deposition material collected using x-ray diffraction would be a good complement to the alkali measurements. Moreover, further measurements with an in-situ alkali chloride, IACM, monitor would be of interest for further mapping the alkali levels in the boiler and reinforce the alkali results found.

Further development into the method of estimating temperatures of different fuel types based on ash and fuel composition as well as FactSage simulations could prove useful as a way of more accurately producing estimates. As the method stands it generates rough estimates weighed heavily on S, Cl and K available in the fuel and ashes, with a focus on sulphation. A more accurate method would potentially also look into ratios that describe for example the vitrification and tendencies to produce i.e feldspar or to also look into the phosphorous contents as these can also bind with HCl or KCl and compete with sulphation processes.

# Bibliography

- [1] Gustaver, M. (2020) A Chalmers University of Technology Master's thesis template for L<sup>A</sup>T<sub>E</sub>X. Unpublished.
- [2] "Global Warming of 1.5°C: Special report". IPCC. (n.d.). Retrieved May 3, 2023 from: <https://www.ipcc.ch/sr15/>
- [3] "2021 Swedish Waste Management". Avfall Sverige, 2021. Retrieved May 3, 2023, from [https://www.avfallsverige.se/media/lbdg3vcp/svensk\\_avfallshantering\\_2021\\_en.pdf](https://www.avfallsverige.se/media/lbdg3vcp/svensk_avfallshantering_2021_en.pdf)
- [4] "What is CHP?" Combined Heat and Power (CHP) Partnership. June 1, 2022. EPA, United States Environmental Protection Agency. Retrieved May 3, 2023, from: <https://www.epa.gov/chp/what-chp>
- [5] European comission and common research centre and Cusano,G and Roudier, S and Neuwahl, F and Holbrook, S and Gómez Benavides, J. (2020) Best Available Technologies (BAT) reference document for waste incineration. Publications Office. <https://publications.jrc.ec.europa.eu/repository/handle/JRC118637>
- [6] Fahnestock, J. and Johansson, I. and Hasselqvist, M. and Mirata, M. and Nilsson, C. and Persson, A. and Petterson, A. and Sahlén, J. "Waste Incineration for the Future: Scenario analysis and action plans". 2019. IEA Bioenergy. Retrieved May 3, 2023, from: <https://www.ieabioenergy.com/wp-content/uploads/2019/04/Waste-Energy-for-the-Future-IEA-version.pdf>
- [7] Lejestrand, A. "12 konkreta förslag för en nationell kraft- och fjärrvärmestrategi". Energiföretagen (n.d.). Retrieved May 3, 2023, from: <https://www.energiforetagen.se/fragor-vi-driver/positioner/12-konkreta-forslag-for-en-nationell-kraft--och-fjarrvarmestrategi/>
- [8] Nemanova, V. and Fillman, B. "Bio+". Energimyndigheten. (n.d.). Retrieved May 3, 2023, from: <https://www.energimyndigheten.se/forskning-och-innovation/forskning/bioenergi/bio/>
- [9] "Biomass for Heat and Power: Technology Brief." IEA-ETSAP & IRENA, 2015. Retrieved Jan 5, 2023. [https://www.irena.org/-/media/Files/IRENA/Agency/Publication/2015/IRENA-ETSAP\\_Tech\\_Brief\\_E05\\_Biomass-for-Heat-and-Power.pdf](https://www.irena.org/-/media/Files/IRENA/Agency/Publication/2015/IRENA-ETSAP_Tech_Brief_E05_Biomass-for-Heat-and-Power.pdf)
- [10] Muscat, A. and de Olde, E.M. and de Boer, J.M. and Ripoll-Bosch, R. "The battle for biomass: A systematic review of food-feed-fuel competition". Global Food Security. Vol 25, June 2020, 100330. Retrieved May 3, 2023, from: <https://www.sciencedirect.com/science/article/pii/S2211912418301366>
- [11] Study visit to the plant and personal meeting with process engineers during the experimental campaign in the autumn of 2022.

- [12] Eurostat. "Municipal Waste Statistics". (n.d.) Retrieved May 3, 2023, from: [https://ec.europa.eu/eurostat/statistics-explained/index.php?title=Municipal\\_waste\\_statistics#Municipal\\_waste\\_treatment](https://ec.europa.eu/eurostat/statistics-explained/index.php?title=Municipal_waste_statistics#Municipal_waste_treatment)
- [13] "Latest Eurostat Figures: Municipal Waste Treatment 2020". Cewep. Sep 26 (2022). Retrieved Mar 17, 2023 from: <https://www.cewep.eu/municipal-waste-treatment-2020/>
- [14] Kelly, W.E. "Ground-Water Pollution Near a Landfill." *Journal of the Environmental Engineering Division*, vol 102, p 1189-1199 (1976). Retrieved Jan 5, 2023, from <https://ascelibrary.org/doi/abs/10.1061/JEEGAV.0000564>
- [15] Directive 2010/75/EU of the European Parliament and of the Council. "On industrial emissions (integrated pollution prevention and control). Nov 24, 2010. Retrieved May 3, 2023, from: <https://eur-lex.europa.eu/legal-content/EN/TXT/PDF/?uri=CELEX:02010L0075-20110106>
- [16] Glassman, Irvin, Richard A. Yetter, and Nick G. Glumac. *Combustion*. Academic press, 2014.
- [17] Andersson, Sven and Bengtsson, Per-Erik and Leckner, Bo and Palchonok, Genadij, and Pallarés, David and Thunman, Henrik. "Combustion Engineering". Department of Energy and Environment, CTH. 2020.
- [18] Hupa, M. "Ash-Related Issues in Fluidized-Bed Combustion of Biomasses: Recent Research Highlights". *Energy & Fuels* 2012, 26, 1, 4-14. Accessed Feb 21 (2023) from: <https://pubs.acs.org/doi/10.1021/ef201169k>
- [19] Johansen, J.M. and Jakobsen, J.G and Frandsen, F. and Glarborg, P. "Release of K, Cl, and S during Pyrolysis and Combustion of High-Chlorine Biomass". *Energy and Fuels* 2011, 25, 11, 4961-4971. Accessed Apr 12 (2023) from: <https://pubs.acs.org/doi/10.1021/ef201098n>
- [20] Johansen, J.M. and Aho, M. and Paakkinen, K. and Taipale, R. and Egsgaard, H. and Jakobsen, J.G. and Frandsen, F.J. and Glarborg, P. "Release of K, Cl, and S during combustion and co-combustion with wood of high-chlorine biomass in bench and pilot scale fuel beds". *Proceedings of the Combustion Institute*, vol 34, issue 2, 2013, p. 2363-2372. Accessed Apr 12 (2023) from: <https://www.sciencedirect.com/science/article/pii/S1540748912003173?via%3Dihub>
- [21] Glarborg Peter. "Hidden interactions-Trace species governing combustion and emissions". *Proceedings of the Combustion Institute*, vol 31, issue 1, Jan 2007, p. 77-98. Accessed Apr 12 (2023) from: <https://www.sciencedirect.com/science/article/pii/S1540748906003828>
- [22] Allguren Thomas. "Chemical Interactions between Potassium, Nitrogen, Sulfur and Carbon Monoxide in Suspension-Fired Systems". Thesis for the degree of doctor of philosophy, CTH (2017). Accessed Apr 12 (2023) from: <https://publications.lib.chalmers.se/records/fulltext/251580/251580.pdf>
- [23] Caillat, S. and Vakkilainen, E. "Biomass Combustion Science, Technology and Engineering" Chapter 9 - Large-Scale biomass combustion plants: an overview. *Woodhead Publishing Series in Energy*, pages 189-224. (2013). Accessed Feb 21 (2023) from: <https://www.sciencedirect.com/science/article/pii/B9780857091314500091#f0010>

- 
- [24] "Air pollution". European Environmental Agency. Accessed Feb 21 (2023) from: <https://www.eea.europa.eu/themes/air/intro>
- [25] Ritchie, H. "Primary, secondary, final, and useful energy: Why are there different ways of measuring energy?". Our World in Data. (n.d.). Retrieved May 3, 2023, from: <https://ourworldindata.org/energy-definitions>
- [26] "Unified Bioenergy Terminology, UBET". FAO Forestry department, Dec 2004. Accessed Apr 03 (2023) from: <https://www.fao.org/3/j4504e/j4504e.pdf>
- [27] Strömberg, B. and Herstad Svård, S. "Bränslehandboken 2012". Anläggnings- och förbränningsteknik, Värmeforsk. Apr 2012, Stockholm. ISSN 1653-1248. Retrieved Apr 20 (2023) from: <https://energiforskmedia.blob.core.windows.net/media/17831/braenslehandboken-2012-vaermeforskrappport-1234.pdf>
- [28] Britannica, The Editors of Encyclopaedia. "eutectic". Encyclopedia Britannica, 5 Oct. 2016, <https://www.britannica.com/science/eutectic>. Accessed 15 February 2023.
- [29] Li, X. and Wang, Y. and Allgurén, T. and Andersson, K. and Wendt, J.O.L. "The roles of added chlorine and sulfur on ash deposition mechanisms during solid fuel combustion". Proceedings of the Combustion Institute 38 (2021) 4309-4316, Oct 23 (2020). Retrieved Feb 10 (2023) from: <https://www.sciencedirect.com/science/article/pii/S1540748920306945?via%3Dihub>
- [30] Nuraini, A.A. "Efficiency and Boiler Parameter Effects in Sub critical Boiler with Different Types of sub-bituminous coal". Iranian Journal of Science and Technology 3(11):1. Aug 22 (2018). Retrieved Feb 15 (2023) from: [https://www.researchgate.net/publication/327643514\\_EfficiencyandBoilerParametersEffectsinSub-criticalBoilerwithDifferentTypesofSub](https://www.researchgate.net/publication/327643514_EfficiencyandBoilerParametersEffectsinSub-criticalBoilerwithDifferentTypesofSub)
- [31] Andersson, S. and Dolores Paz, M. and Phother-Simon, J. and Jonsson, T. "High Temperature Corrosion and Dioxin Abatement using Sulfur recirculation in a Waste-to-Energy Plant". Detritus, volume 65 (2019): pages 92-98. Accessed Feb 10 (2023) from: <https://digital.detritusjournal.com/articles/high-temperature-corrosion-and-dioxin-abatement-using-sulfur-recirculation-in-201>
- [32] Fakourian, S. and McAllister, Z. and Fry, A. and Wang, Y. and Li, X. and Wendt, J.O.L. and Dai, J. "Modeling ash deposit growth rates for a wide range of solid fuels in a 100 kW combustor". Fuel Processing Technology 217 (2021) 106777. Accessed Feb 10 (2023) from: <https://www.sciencedirect.com/science/article/pii/S0378382021000564?via%3Dihub>
- [33] Viljanen, J. and Allgurén, T. and Wang, Y. and Li, X. and Toivonen, J. and Andersson, K. and Wendt, J.O.L. "In-situ monitoring of transient gas phase K-Cl-S chemistry in a pilot-scale combustor". Proceedings of the Combustion Institute 38 (2021) 1823-1831. Accessed Feb 10 (2023) from: <https://www.sciencedirect.com/science/article/pii/S1540748920305952?via%3Dihub>
- [34] Li, X. and Wang, Y. and Wendt, J.O.L. "Ash formation and deposition during combustion of pulverized torrefied wood and coal in a 100kW downflow combustor". Proceedings of the Combustion Institute 000 (2022) 1-9. Accessed Feb

- 10 (2023) from: <https://www.sciencedirect.com/science/article/pii/S1540748922001286?via%3Dihub>
- [35] Li, X. and Wang, Y. and Wendt, J.O.L. "Ash formation and deposition during combustion of pulverized torrefied wood and coal in a 100kW downflow combustor". *Proceedings of the Combustion Institute* 000 (2022) 1-9. Accessed Feb 10 (2023) from: <https://www.sciencedirect.com/science/article/pii/S1540748922001286?via%3Dihub>
- [36] Kassman, H. and Normann, F. and Åmand, L.E. "The effects of oxygen and volatile combustibles on the sulphation of gaseous KCl". *Combustion and Flame* 160 (2013) 2231-2241. Accessed Feb 10 (2023) from <https://www.sciencedirect.com/science/article/pii/S0010218013001624?via%3Dihub>
- [37] Dolorez Paz, M. and Phother-Simon, J. and Andersson, S. and Jons-son, T. "High temperature corrosion memory in a waste fired boiler - influence of sulfur". *Waste management* 130 (2021) 30-37. Accessed Feb 10 (2023) from <https://www.sciencedirect.com/science/article/pii/S0956053X21002658?via%3Dihub>
- [38] Energimyndigheten. (2015). *Energiläget 2015*. Energimyn- digheten. [https://www.energimyndigheten.se/contentassets/50a0c7046ce54aa88e0151796950ba0a/energilaget-2015\\_webb.pdf](https://www.energimyndigheten.se/contentassets/50a0c7046ce54aa88e0151796950ba0a/energilaget-2015_webb.pdf)
- [39] Wheeler, P.A. and de Rome, L. "Waste-Pretreatment: A review". R & D technical report, P1-344. Environment Agency. Accessed Feb 21 (2023) from: [https://assets.publishing.service.gov.uk/government/uploads/system/uploads/attachment\\_data/file/290316/sp1-344-tr-e-e.pdf](https://assets.publishing.service.gov.uk/government/uploads/system/uploads/attachment_data/file/290316/sp1-344-tr-e-e.pdf)
- [40] Miller, B.G. "Coal Energy Systems". Chapter 6 - Emissions Control Strategies for Power Plants. Pages 283-392. Academic Press, (2005). Accessed Feb 21 (2023) from: <https://www.sciencedirect.com/science/article/pii/B9780124974517500061>
- [41] Leckner, Bo. "Co-combustion: A summary of technology." *Thermal science* 11.4 (2007): 5-40.
- [42] Li, Kaiyang, and Yimin Zeng. "Corrosion of heat exchanger materials in co-combustion thermal power plants." *Renewable and Sustainable Energy Reviews* 161 (2022): 112328.
- [43] Rohan, F. "Experience of indirect cofiring of biomass and coal". IEA Clean Coal Centre. OCT 2002, ISBN 92-9029-370-9. Re- trieved May 3, 2023, from: [https://www.sustainable-carbon.org/wp-content/uploads/dlm\\_uploads/reports/Combustion/experience-of-indirect-cofiring-of-biomass-and-coal-ccc-64.pdf](https://www.sustainable-carbon.org/wp-content/uploads/dlm_uploads/reports/Combustion/experience-of-indirect-cofiring-of-biomass-and-coal-ccc-64.pdf)
- [44] Hiroshi, Kishi and Toshihiro, Fujii. "A Surface Ionization Detector for Gas Chromatography: Use of a Supersonic Free Jet". 01 Sep (1996). ACS Publi- cations. Retrieved Jan 12, 2023, from: <https://pubs.acs.org/doi/10.1021/ac960028m>
- [45] Taylor, John B. "The reflections of beams of the alkali metals from crystals". General electric company. New York, Jan 15 ( 1930). Retrieved Jan 12 2023, from: <https://journals.aps.org/pr/pdf/10.1103/PhysRev.35.375>

- 
- [46] Kingdon, K.H. and Irving, Langmuir. "Thermionic effects caused by vapours of alkali metals". The Royal Society Publishing. 01 Jan (1925). Retrieved Jan 12, 2023, from: <https://royalsocietypublishing.org/doi/10.1098/rspa.1925.0005>
- [47] Gall, Dan and Viljanen, Jan and Gogolev, Ivan and Allgurén, Thomas and Andersson, Klas. "Alkali Monitoring of Industrial Process Gas by Surface Ionization - Calibration, Assessment, and Comparison to In Situ Laser Diagnostics". *Energy & Fuels* 2021 35 (24), 20160-20171. Retrieved Jan 12, 2023, from: [https://research.chalmers.se/publication/527778/file/527778\\_Fulltext.pdf](https://research.chalmers.se/publication/527778/file/527778_Fulltext.pdf)
- [48] Mohamed, M.A. and Jaafar, J and Ismail, A.F. and Othman, M.H.D. and Rahman, M.A. "Membrane Characterization", Chapter 1 - Fourier Transform Infrared (FTIR) Spectroscopy. pages 3-29, (2007). Universiti Teknologi Malaysia. Retrieved Feb 01, 2023 from: <https://www.sciencedirect.com/science/article/pii/B9780444637765000012>
- [49] Janssens, M. "Flammability Testing of Materials Used in Construction, Transport and Mining", Chapter 2 - Fundamental measurement techniques. pages 22-62, (2006). Southwest Research Institute, USA. Retrieved Feb 01, 2023, from: <https://www.sciencedirect.com/science/article/pii/B9781855739352500028>
- [50] Undavalli, V.K. and Ling, C. and Khandelwal, B. "Aviation Fuels", Chapter 6 - Impact of alternative fuels and properties on elastomer compability. pages 113-132, (2021). Academic Press. Retrieved Feb 01, 2023, from: <https://www.sciencedirect.com/science/article/pii/B9780128183144000017>
- [51] Callister, W.D. "Fundamentals of Material Science and Engineering". John Wiley & Sons, Inc. 5th Edition (2001). Accessed Feb 21 (2023) from: [http://www.ifba.edu.br/professores/iarasantos/QUI%20541\\_Qu%C3%ADmica%20de%20pol%C3%ADmeros/Fundamentals%20of%20Materials%20Science%20and%20Engineering%20-%20William%20D%20Callister%20Jr%20%20047139551X.pdf](http://www.ifba.edu.br/professores/iarasantos/QUI%20541_Qu%C3%ADmica%20de%20pol%C3%ADmeros/Fundamentals%20of%20Materials%20Science%20and%20Engineering%20-%20William%20D%20Callister%20Jr%20%20047139551X.pdf)
- [52] Miljödomstolens DOM M516-08 - naturvardsverket.se. (n.d.). Retrieved October 5, 2022, from <https://www.naturvardsverket.se/contentassets/a6e17ca059af49a5aa8fd122f7884670/miljodomstolen-dom-20090313.pdf>
- [53] "Sootblower and Boiler Cleaning Terminology, Principles and Applications". Babcock & Wilcox. Retrieved Apr 20 (2023) from: <https://www.babcock.com/home/about/resources/learning-center/sootblower-and-boiler-cleaning-terminology-principles-and-applications>
- [54] Strauss, W. and Schmidt, L. "Are Black Pellets Ready to Compete with White Pellets?" *Biomass Magazine*, March 01, 2018. Retrieved March 20, 2023, from: <https://biomassmagazine.com/articles/15072/are-black-pellets-ready-to-compete-with-white-pellets>
- [55] Gogolev, I. "The Release, Distribution and Implication of Alkalis in Chemical Looping Combustion of Biomass" Doctoral thesis at Chalmers University of technology, Gothenburg, Sweden (2022). Retrieved March 15, 2023, from: [https://research.chalmers.se/publication/532029/file/532029\\_Fulltext.pdf](https://research.chalmers.se/publication/532029/file/532029_Fulltext.pdf)

- [56] "FactSage", GTT-Technologies and CRCT. Retrieved March 20, 2023, from: <https://gtt-technologies.de/software/factsage/>
- [57] Link, S. and Yrjas, P. and Lindberg, D. and Trikkel, A. and Mikli, V. "Ash melting behaviour of reed and woody fuels blends" *Fuel*, volume 314, 15 April 2022, 123051. Retrieved March 22 (2023) from: <https://www.sciencedirect.com/science/article/pii/S0016236121029112?via%3Dihub>
- [58] Ma, C. "Aspects of Ash Transformations in Pressurised Entrained-Flow Gasification of Woody Biomass". Doctoral Thesis. Luleå (2017) ISSN 1402-1544. Retrieved March 22 (2023) from: <http://www.diva-portal.org/smash/get/diva2:1087214/FULLTEXT01.pdf>
- [59] Elhadi Ibrahim, M. and Medraj, M. "Water Droplet Erosion of Wind Turbine Blades: Mechanics, Testing, Modeling and Future Perspectives". *Materials* (Basel). 2019 Dec 31;13(1):157. doi:10.3390/ma13010157. PMID: 31906204; PMCID: PMC6982018. Retrieved Apr 20 (2023).
- [60] "Effektreserv", Svenska Kraftnät. Retrieved Apr 14 (2023) from: <https://www.svk.se/aktorsportalen/bidra-med-reserver/om-olika-reserver/effektreserv/>
- [61] Hauris Jespersen, O. and Peder Hansen, N. and Jonsson, T. and Likse, J. and Paz, L. and Phother, J. and Vinter Dahl, K. and Montgomery, M. and Chekol Malede, Y. and Norman, T. and Mikkelsen, L. and Andersson, S. and Aakjær Jensen, S. "Sulphur Recirculation cut corrosion rates". *Energiforsk*. 2018-01-10. Retrieved May 11, 2023, from: <https://energiforsk.se/nyhetsarkiv/arkiverade/sulfur-recirculation-cut-corrosion-rates-kme-714/>
- [62] Neuwahl, F. and Cusano, G. and Gómez Benevides, J. and Holbrook, S. and Roudier, S. "Best Available Techniques (BAT) Reference Document for Waste Incineration". EUR 29971 EN; doi:10.2760/761437. Retrieved Apr 17 (2023)

# A

## Epsilon

This appendix provides the reader with an component list (section A.1) and short explanation for the function for individual components used in constructing the models, as well as additional figures of the models discussed in the main text in section A.2.

### A.1 Component list

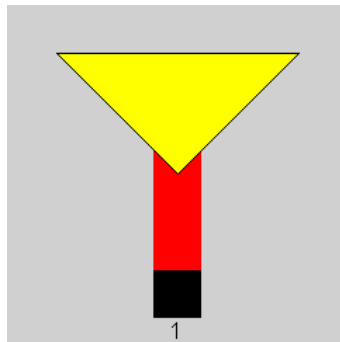


**Figure A.1:** Component 1 - Boundary Input Value: Boundary input where the composition and state of the stream can be specified.

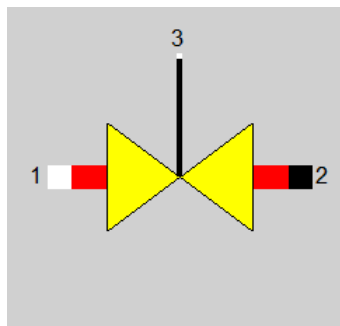


**Figure A.2:** Component 2 - Throttle: Used to model pressure drops in the system, can be specified externally or calculated by the model.

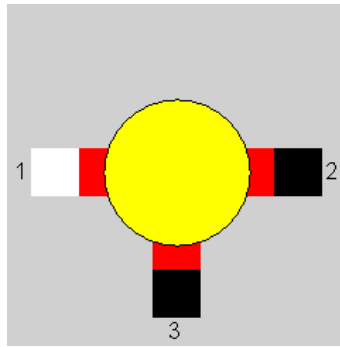


**Figure A.3:** Component 4 - Splitter: Allows streams to be split into two separate streams.

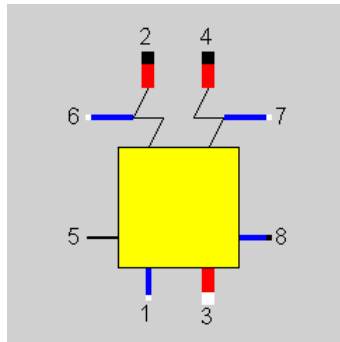


**Figure A.4:** Component 5 - Steam Generator: Component which simulates the economizing, evaporation and economizing of steam in one unit. May also include reheating.

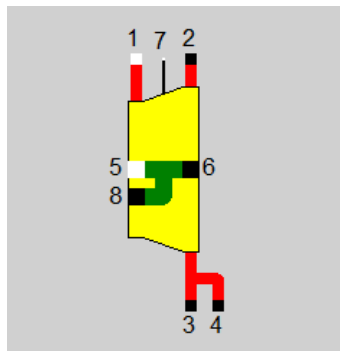


**Figure A.5:** Component 6 - Steam Turbine: Component used to expand streams of pressurised steam, has the option for two extractions in ports 3 and 4, for feed water heating.

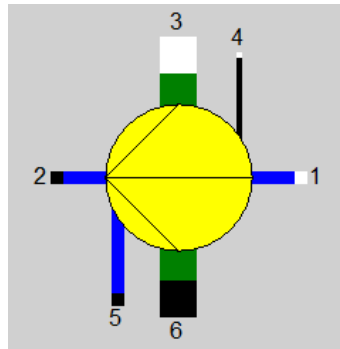


**Figure A.6:** Component 8 - Pump: Component used to simulate pump work in the system increasing or maintaining the pressure.

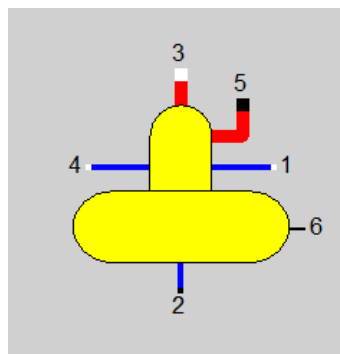


**Figure A.7:** Component 9 - Deaerator / Feedwater Heater: Open heat exchanger used for preheating the feedwater.

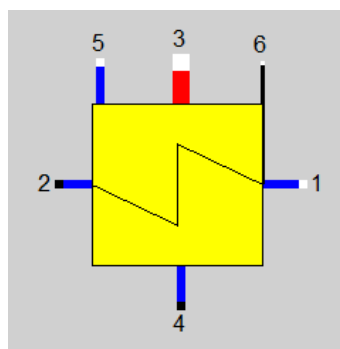


**Figure A.8:** Component 10 - Feedwater Heater: Closed heat exchanger used for preheating the feedwater.

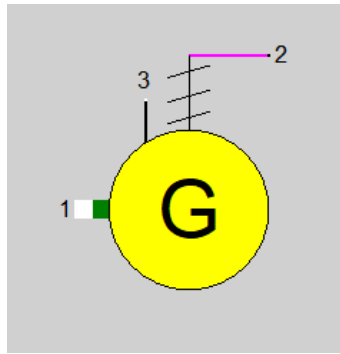


**Figure A.9:** Component 11 - Generator: Component attached to Steam turbine simulating the electricity generation from work extracted by expanding steam.

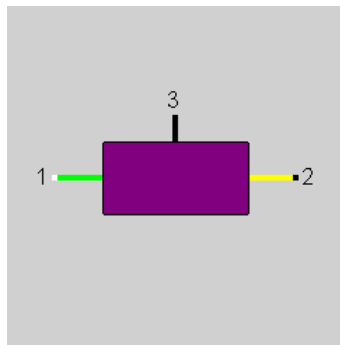


**Figure A.10:** Component 12 - Controller (External): Allows to set control point between to streams based on an external input value

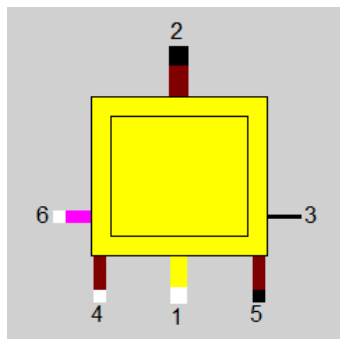


**Figure A.11:** Component 21 - Combustion Chamber: Unit that simulates the combustion of one fuel input in port 4, with the option for a secondary fuel input in port 6. Uses air from port 1, and produces hot fluegases in port 2 for steam generation.

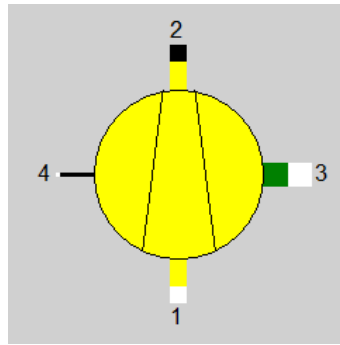


**Figure A.12:** Component 24 - Compressor: Used to simulate the pressurization of primary air inlets.

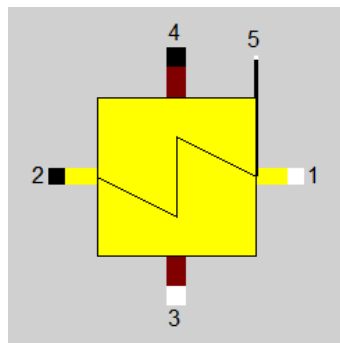


**Figure A.13:** Component 25 - Air Preheater: Used to preheat the air intake to the combustion chamber, preheated using either fluegases or steam in ports 3 and 4.

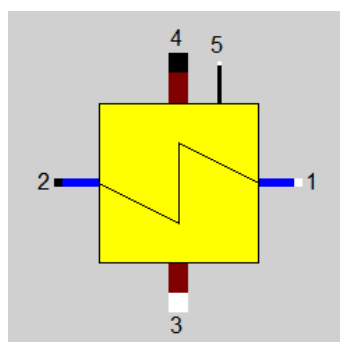


**Figure A.14:** Component 26 - Economizer/Evaporator/Superheater: Heat exchanger unit specialized for fluegas/water and fluegas/steam heat transfer.

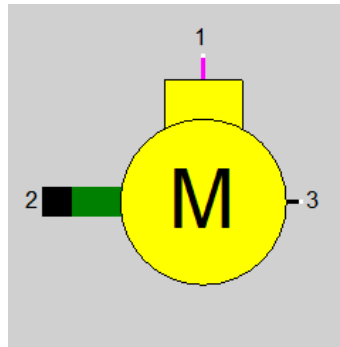


**Figure A.15:** Component 29 - Electric Motor: Provides pump and compressor components with the energy needed, also outputs the electricity demand of these components used for determining efficiencies.

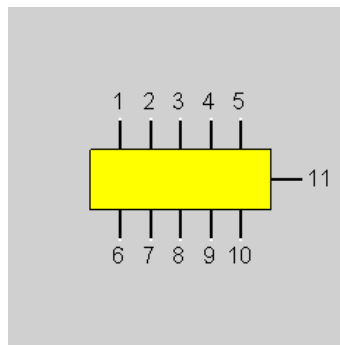


**Figure A.16:** Component 31 - Power Summarizer: component used to summarize logic components indicating pumpwork, electricity demand and generation, as well as heat provided to DH network.

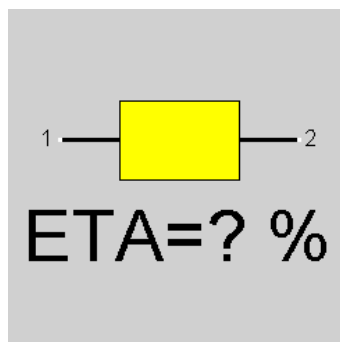


**Figure A.17:** Component 32 - Efficiency meter: Component that determines efficiency based on two given inputs, such as heat provided through fuel and electricity generated.

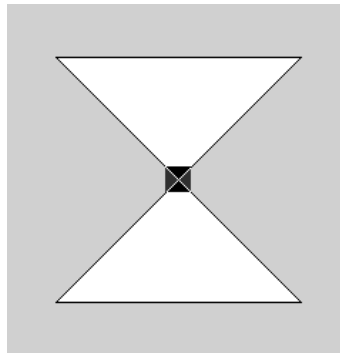


**Figure A.18:** Component 33 - Start Value: similar to component 1, but may be placed anywhere in the system where certain parameters would otherwise be unspecified. Can also set composition of stream.

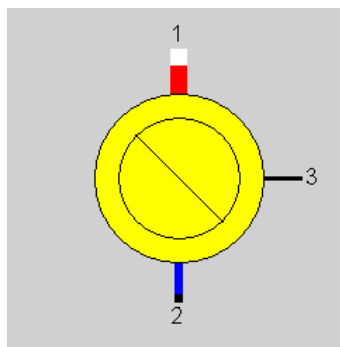


**Figure A.19:** Component 35 - Heat Consumer: Used to simulate outgoing heat flows, such as heat provided to the district heating network, cooling or heat towards the pelletization plant.

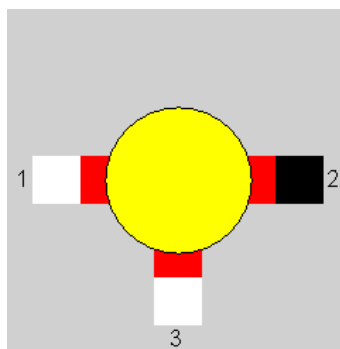


**Figure A.20:** Component 37 - Simple Mixer: Component used to recombine two separate streams into one.

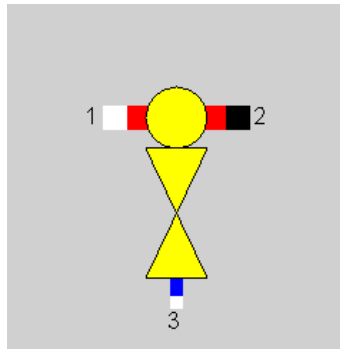


**Figure A.21:** Component 38 - Water Injection: Component used to simulate water being added to the system, used in the fluegas cleaning step where the fluegases are clean by direct contact with water.

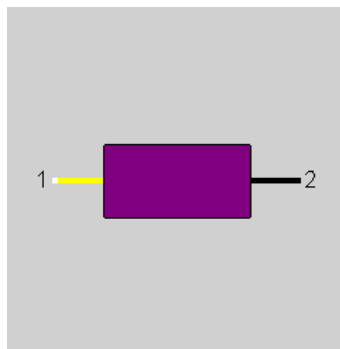


**Figure A.22:** Component 39 - Controller (Internal): Allows to set a control between two streams and an internal input value, such as controlling the temperature of one stream by limiting the mass flow of the other.

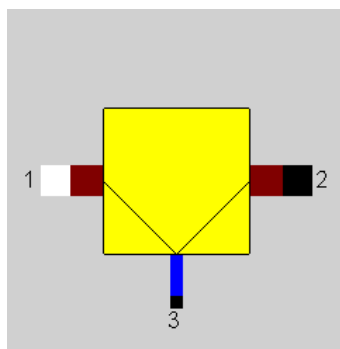


**Figure A.23:** Component 54 - Drain: Component opposite of the water injection, used to drain condensate from fluegas streams post fluegas condensation.

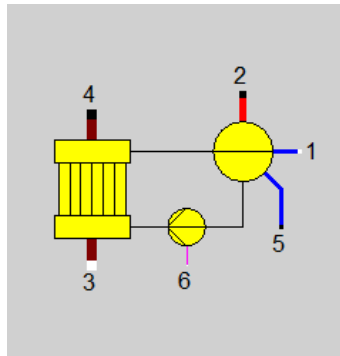


**Figure A.24:** Component 70 - Evaporator with Steam Drum: Component specialized for evaporation of steam and typically works in tandem with component 26.

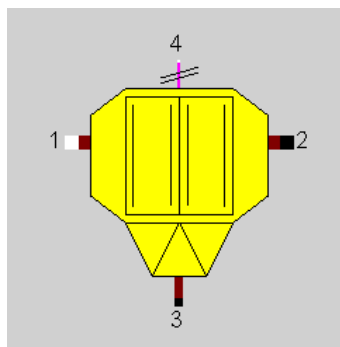


**Figure A.25:** Component 85 - Electrostatic Precipitator: Cleaning unit that removes fly ash and particulate matter.

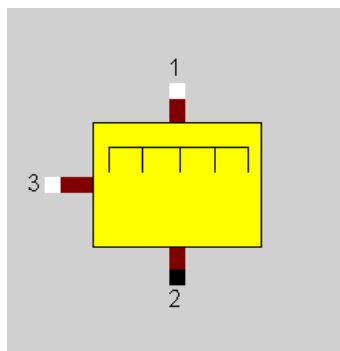


**Figure A.26:** Component 86 - Selective catalytic reduction unit: Unit whose primary assignment is to remove NO<sub>x</sub> from the fluegases.

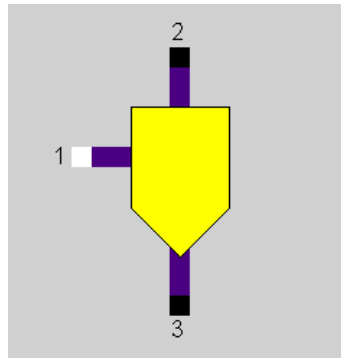


**Figure A.27:** Component 99 - Separator: Used to simulate other fluegas cleaning components. In this case the removal of SO<sub>x</sub> and HF, HCl.

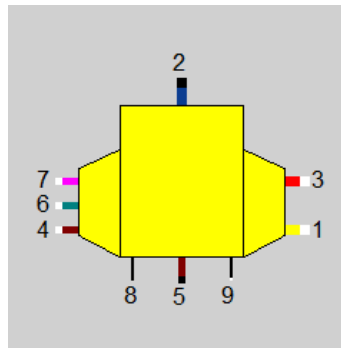


**Figure A.28:** Component 169 - Gasifier: Component that simulates the gasification of the biomass fuels introduced in the indirect co-firing cases after gasification.

## A.2 Models

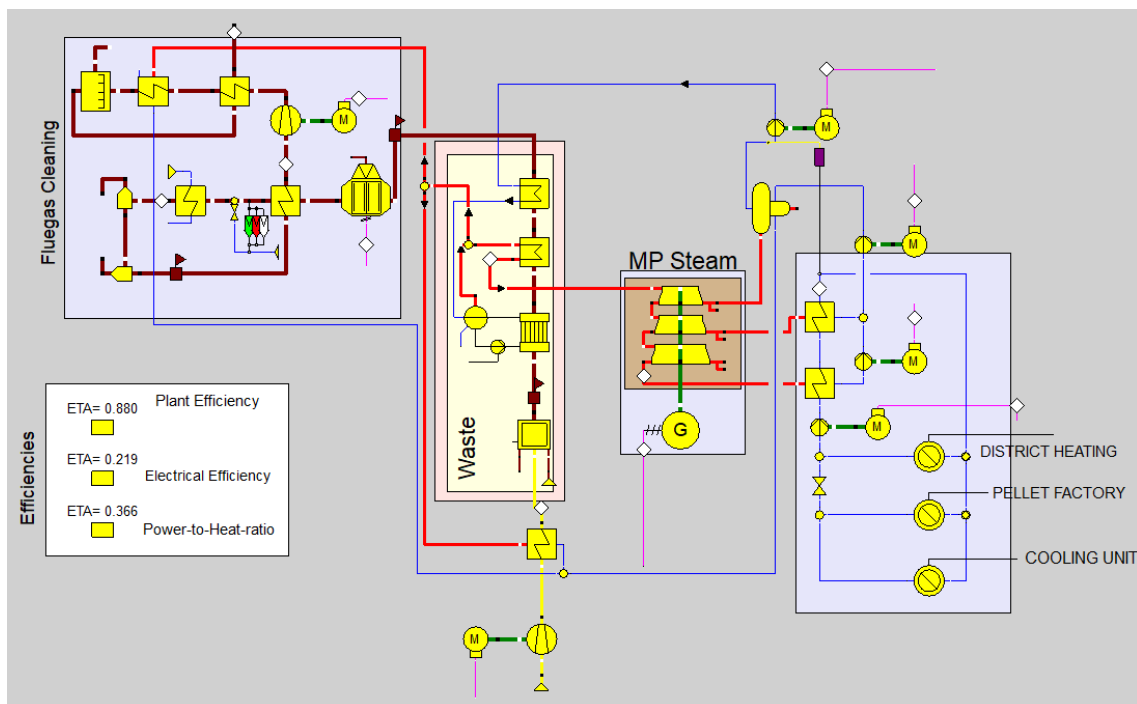


**Figure A.29:** Ebsilon Professional model of the summer model with the accessible redesign.

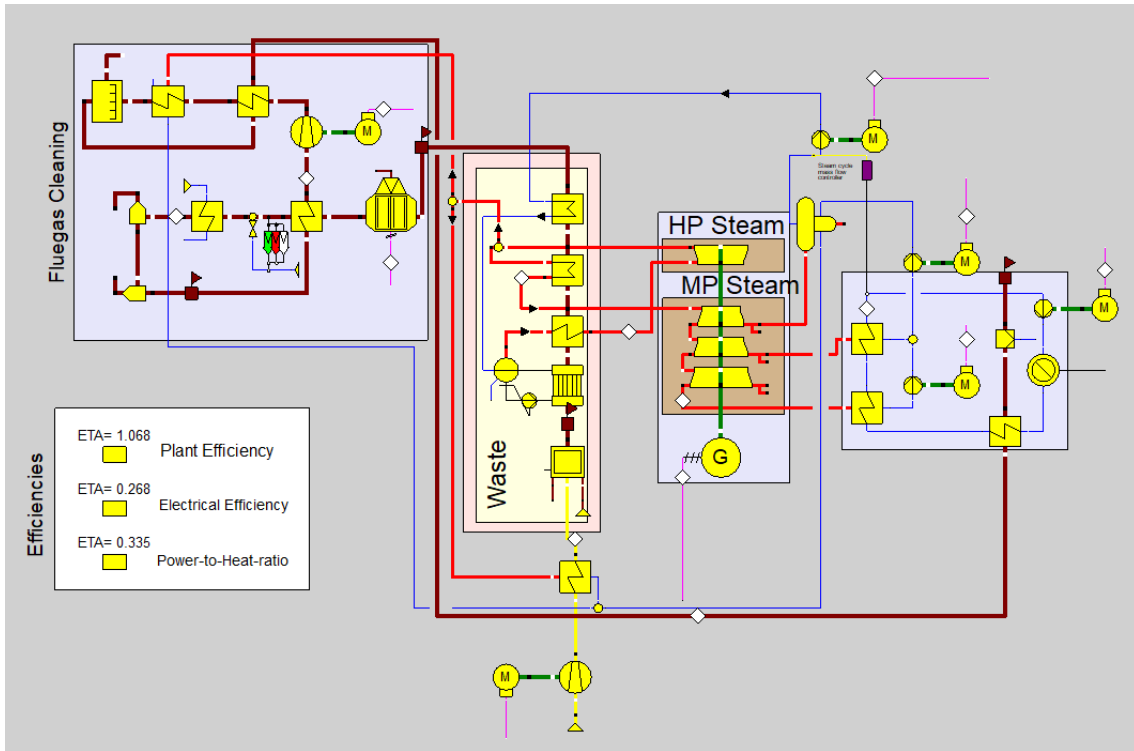


**Figure A.30:** Ebsilon Professional model of the winter operating case with the addition of a reheat cycle and extra turbine.

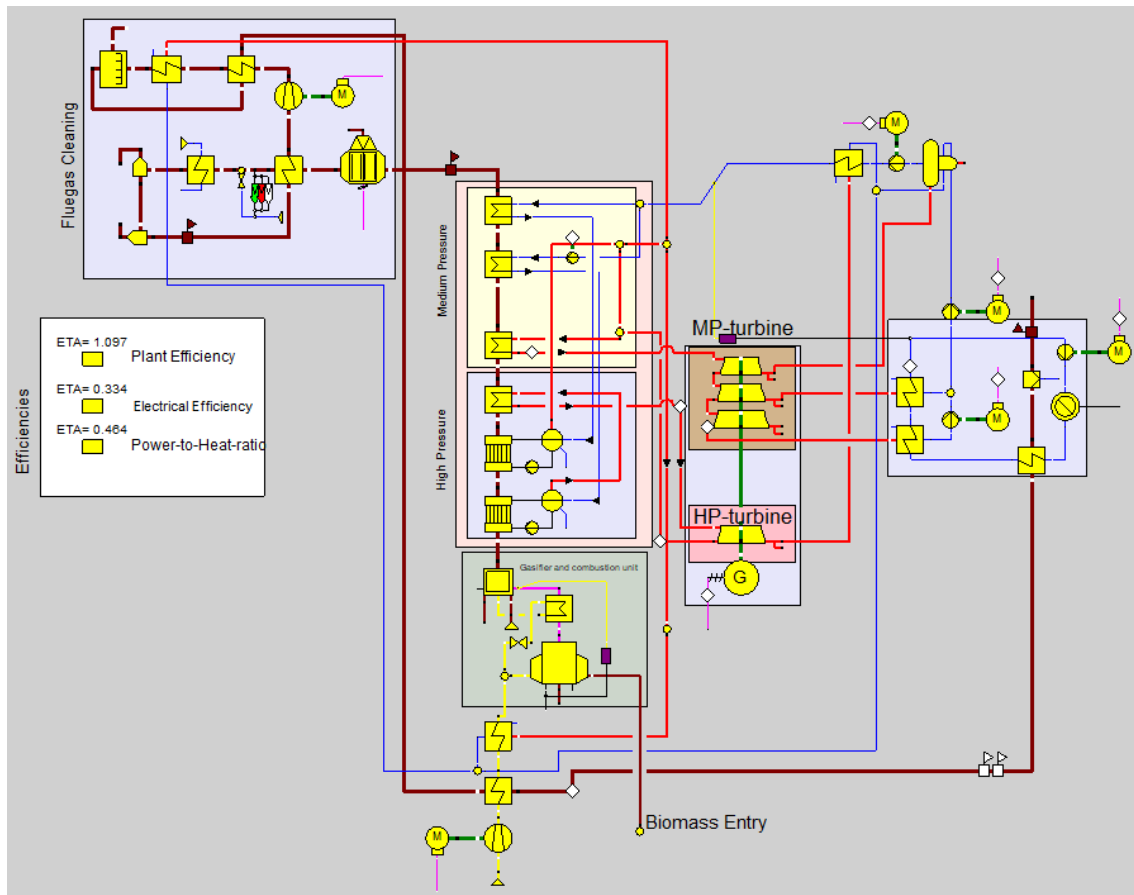


Figure A.31: Epsilon Professional model of an indirect co-firing plant

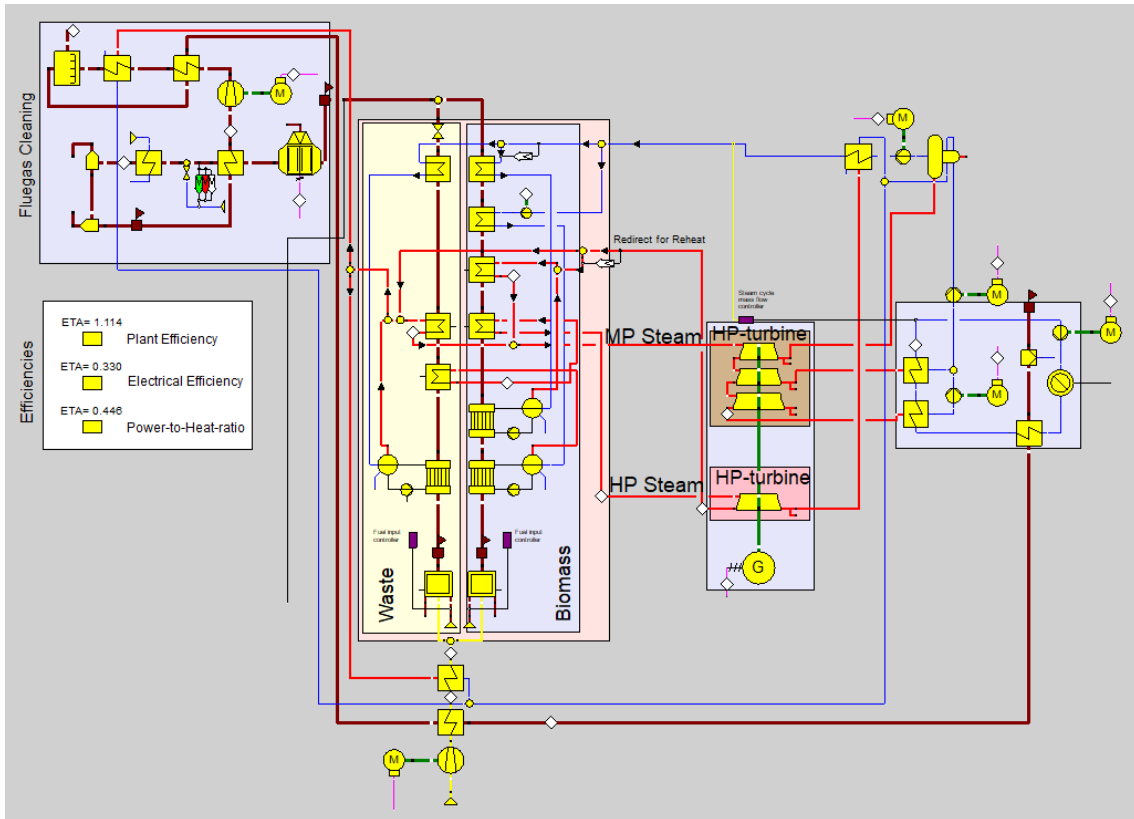


Figure A.32: Ebsilon Professional model of the 1st version of parallel co-firing.

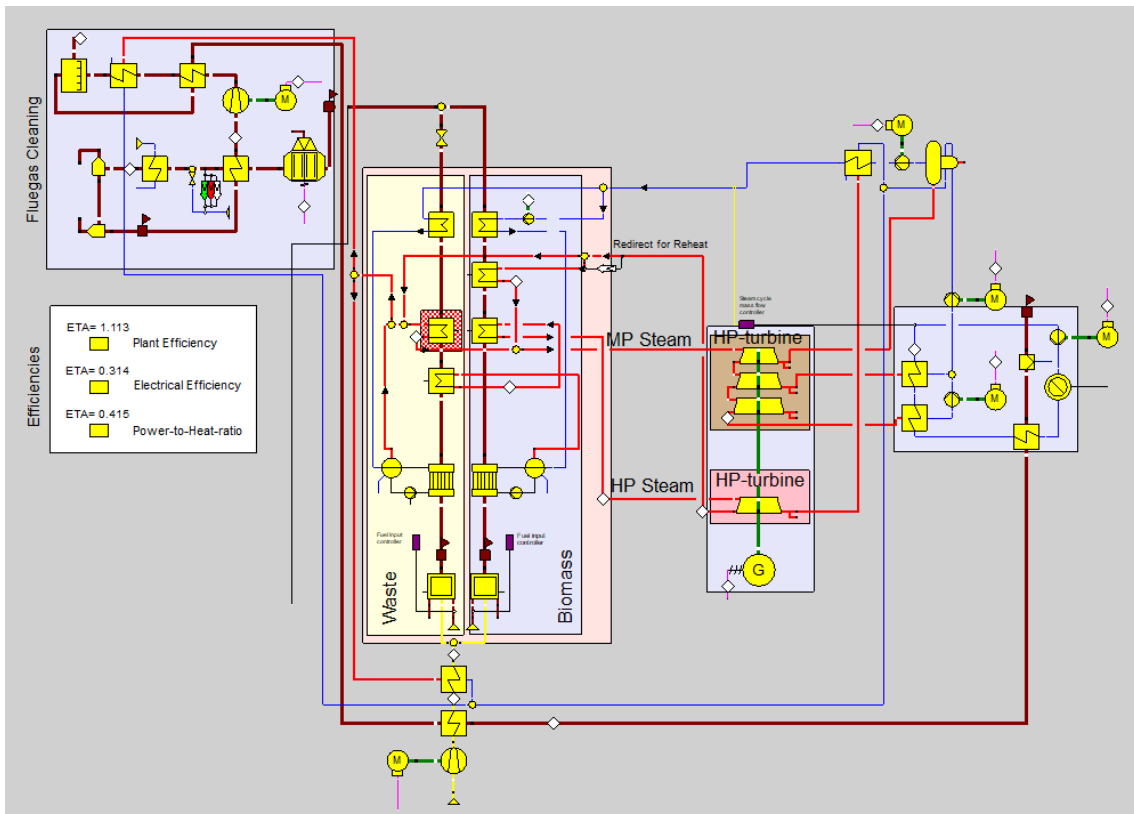


Figure A.33: Ebsilon Professional model of the 2nd version of parallel co-firing.

# B

## Additional Data

Appendix B will include additional data to complement what has been presented in the results. Such as tables, additional figures and raw data used to reach the results and conclusions presented.

### B.1 Experimental Campaign

#### Boiler Load

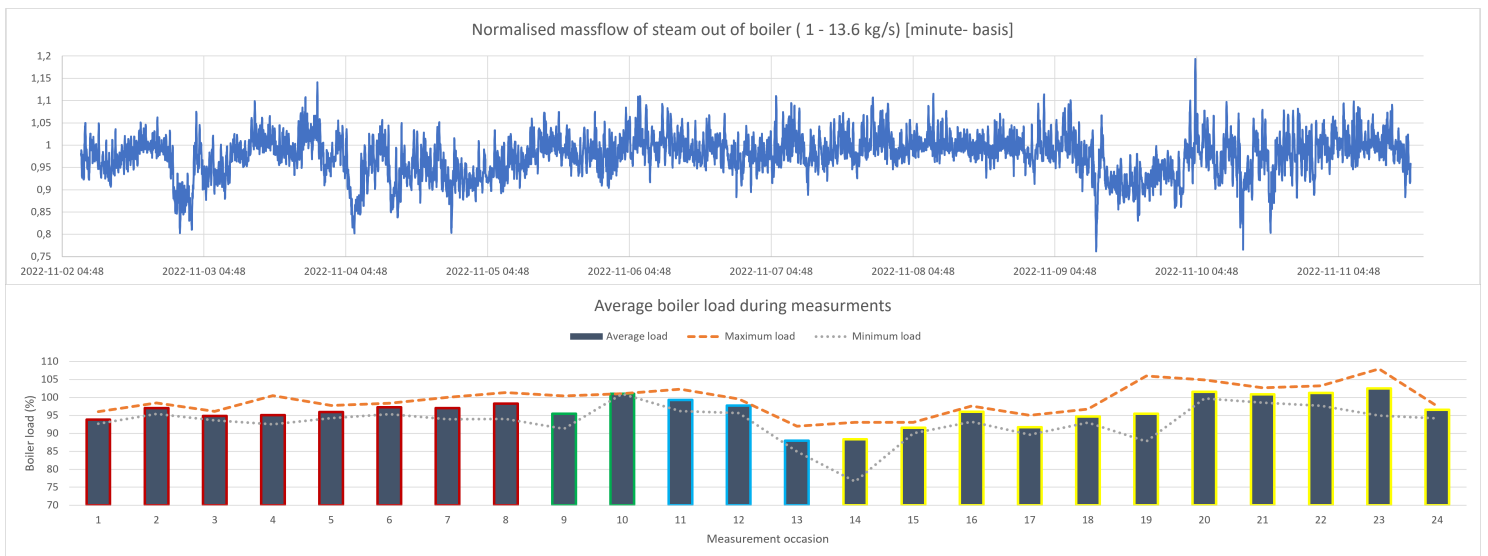


**Figure B.1:** Boiler load during the experimental campaign in terms of steam produced. Top figure showing the entire duration, and the bottom figure showing the load during individual gas measurement occasions.

## Deposition Rate

ring	Before use			After use			Added weight
	weighing 1	weighing 2	mean	weighing 1	weighing 2	mean	
CTH-1	37850,16	37850,00	37850,08	37886,59	37886,62	37886,61	36,52
CTH-2	36566,49	36566,43	36566,46	36591,38	36591,54	36591,46	25,00
CTH-3	37511,87	37511,74	37511,81	37540,93	37540,38	37540,66	28,85
CTH-4	37694,11	37693,98	37694,05	37815,45	37815,48	37815,47	121,42
UKAB-1	86765,38	86765,50	86765,44	86968,05	86968,55	86968,3	202,86

**Table B.1:** Weighing protocol for the deposition rings, in milligrams (mg).

## Gas composition

	Port	NO [ppm]	CO [ppm]	H <sub>2</sub> O [vol. %]	HCl [ppm]	SO <sub>2</sub> [ppm]	CO <sub>2</sub> [vol. %]	Load [%]
Day 2	ESP	171,9	10,90	22,61	668,0	234,1	10,39	102,51
		183,4	10,13	22,00	505,2	206,2	9,91	96,58

**Table B.2:** Recalculated concentrations of each respective species for measurements conducted before the ESP to compensated for increased air dilution.

## Aerosols

level	before use	after use	difference
1	15,13	15,13	0,00
2	15,26	15,33	0,07
3	15,00	15,21	0,21
4	15,00	16,07	1,07
5	15,06	19,08	4,02
6	15,07	24,12	9,05
7	15,19	17,46	2,27
8	15,10	20,88	5,78
9	15,06	16,55	1,49
10	15,06	15,41	0,35
11	15,18	15,28	0,10
12	15,02	15,06	0,04
13	15,08	15,17	0,09
F	81,77	81,94	0,17

**Table B.3:** DLPI particle measurement: Sample 1 - port 7.5. Weighed three times, measurements in milligrams (mg).

---

level	before use	after use	difference
1	15,21	15,21	0,00
2	15,33	15,34	0,01
3	15,25	15,26	0,01
4	15,17	15,26	0,09
5	15,14	16,66	1,52
6	15,19	18,13	2,94
7	15,04	16,17	1,13
8	15,17	15,88	0,71
9	15,03	15,36	033
10	15,10	15,19	0,09
11	15,28	15,32	0,04
12	15,09	15,09	0,00
13	15,02	15,02	0,00
F	81,31	81,32	0,01

**Table B.4:** DLPI particle measurement: Sample 2 - port 7.5S. Weighed three times, measurements in milligrams (mg).

## B.2 FactSage & Temperature Estimations

### Temperature Estimations

Below a figure showing the effects of three different temperature estimations are shown, the used method weights S, Cl, HCl, KCl and SO<sub>2</sub> with a factor of 2, Al, K, Si, Na, H<sub>2</sub>O and total ash with 1, and then reduces the weight of other components to 0.25 for ash components and 0.5 for fuel components such as C, H, O or N. The secondary method weights more softly with all uninteresting components weighted as 0.25. The non weighted method all components are scored as 1.

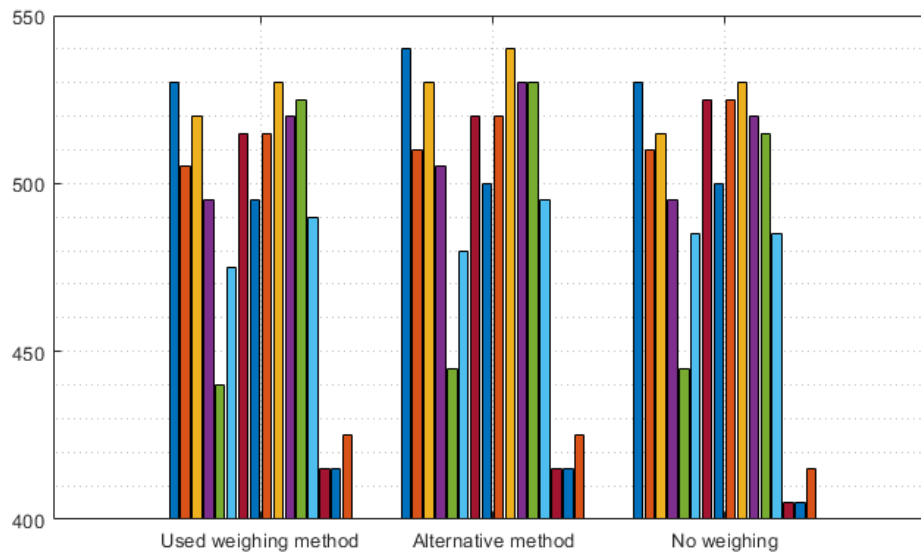


**Figure B.2:** Differences in temperatures estimated per fuel depending on method of weighting. Alternative weighting using a softer 0.25 weight on several components instead of 0.5 that is used in the current method.

DEPARTMENT OF SOME SPACE, EARTH AND ENVIRONMENT  
CHALMERS UNIVERSITY OF TECHNOLOGY  
Gothenburg, Sweden  
[www.chalmers.se](http://www.chalmers.se)



**CHALMERS**  
UNIVERSITY OF TECHNOLOGY